UNIVERSIDADE FEDERAL DE PERNAMBUCO
CENTRO DE TECNOLOGIA E GEOCIÊNCIAS
DEPARTAMENTO DE GEOLOGIA
PROGRAMA DE PÓS-GRADUAÇÃO EM GEOCIÊNCIAS

JOSÉ CAVALCANTE DE OLIVEIRA FILHO

PROCESSOS DE TRANSPORTE, HIDRODINÂMICA E RETENÇÃO DE MATERIAL PARTICULADO SUSPENSO EM ESTUÁRIOS DE RIA COM PEQUENAS BACIAS HIDROGRÁFICAS

Recife
2021

JOSÉ CAVALCANTE DE OLIVEIRA FILHO

PROCESSOS DE TRANSPORTE, HIDRODINÂMICA E RETENÇÃO DE MATERIAL PARTICULADO SUSPENSO EM ESTUÁRIOS DE RIA COM PEQUENAS BACIAS HIDROGRÁFICAS

Tese apresentada ao Programa de Pós-Graduação em Geociências da Universidade Federal de Pernambuco, como requisito parcial para a obtenção do título de Doutor em Geociências.

Área de concentração: Geologia Sedimentar e Ambiental.

Orientador: Prof. Dr. Valdir do Amaral Vaz Manso.

Coorientador: Prof. Dr. Aldo Sottolichio.

Coorientador: Prof. Dr. Carlos Augusto França Schettini.

Recife

2021

Catalogação na fonte
Bibliotecária Margareth Malta, CRB-4 / 1198

O48p Oliveira Filho, José Cavalcante de.
Processos de transporte, hidrodinâmica e retenção de material particulado suspenso em estuários de ria com pequenas bacias hidrográficas / José Cavalcante de Oliveira Filho. – 2021.
109 f., il., grafs., tabs.

Orientador: Prof. Dr. Valdir do Amaral Vaz Manso.
Coorientador: Prof. Dr. Alto Sottolichio.
Coorientador: Prof. Dr. Carlos Augusto França Schettini.
Tese (Doutorado) – Universidade Federal de Pernambuco. CTG. Programa de Pós-Graduação em Geociências, 2021.
Inclui Referências e Apêndice.
Parte do texto em inglês.

1. Geociências. 2. Circulação estuarina. 3. Marés. 4. Transporte sedimentar. I. Manso, Valdir do Amaral Vaz (Orientadora). II. Sottolichio, Alto (Coorientador). III. Schettini, Carlos Augusto (Coorientador). IV. Título.

UFPE

551 CDD (22. ed.) BCTG/2021-191

JOSÉ CAVALCANTE DE OLIVEIRA FILHO

PROCESSOS DE TRANSPORTE, HIDRODINÂMICA E RETENÇÃO DE MATERIAL PARTICULADO SUSPENSO EM ESTUÁRIOS DE RIA COM PEQUENAS BACIAS HIDROGRÁFICAS

Tese apresentada ao Programa de Pós-Graduação em Geociências da Universidade Federal de Pernambuco, Centro de Tecnologia e Geociências como requisito parcial para a obtenção do título de Doutor em Geociências. Área de Concentração: Geologia Sedimentar e Ambiental.

Aprovada em: 16/07/2021

BANCA EXAMINADORA

Participação por videoconferência
Prof. Dr. Carlos Augusto França Schettini (Coorientador)
Universidade Federal do Rio Grande

Participação por videoconferência
Prof. Dr. Roberto Lima Barcellos (Examinador Interno)
Universidade Federal de Pernambuco

Participação por videoconferência
Prof.Dr. Elírio Ernestino Toldo Júnior (Examinador Externo)
Universidade Federal do Rio Grande do Sul

Participação por videoconferência
Prof.Dr. Carlos Eduardo Peres Teixeira (Examinador Externo)
Universidade Federal do Ceará

Participação por videoconferência
Prof. Dr. Nils Edvin Asp Neto (Examinador Externo)
Universidade Federal do Pará

AGRADECIMENTOS

O autor agradece a todas as pessoas que contribuíram de forma direta e indireta para a elaboração dessa pesquisa. Inicialmente, não poderia deixar de mostrar minha gratidão a minha família, José e Elizabete, pais; Érica, Elaine e Emeline, irmãs, por todo suporte de sempre e apoio incondicional à minha carreira. Ainda, agradeço a minha mulher, Raynne, e Marina, filha, por ser minha fonte de felicidade todos os dias e por toda parceria e companheirismo. Agradeço também aos companheiros de pós-graduação da Universidade Federal de Pernambuco, tanto do Departamento de Oceanografia, quanto do de Geociências. Especificamente, agradeço ao amigo Ernesto pela parceria de sempre e divisão de escritório, além de todo conhecimento trocado. Além dele, agradeço ao KrishnaMurti, secretário da pós-graduação em Geociências por toda ajuda no desenrolar das burocracias ao longo dessa jornada. Agradeço ao meu orientador, Guto Schettini, por todo conhecimento transmitido e pela paciência para transmiti-lo. Agradeço também a ele todas as oportunidades abertas a minha pessoa e incentivo diário na elaboração deste documento. Não posso deixar de lembrar e agradecer a todos os colegas de estadia na França, durante o Doutorado Sanduíche: Paulo Victor, PV, pela parceria e divisão de perrengues, além da ajuda imensurável com o Telemac. Por fim, agradeço a pessoa do professor Aldo Sottolichio por todo conhecimento passado e por ter tornado o período sanduíche uma experiência muito proveitosa para mim. Agradeço também ao Nicolas Huybrechts pela ajuda com o Telemac e a todo pessoal do laboratório EPOC, da Universidade de Bordeaux, em especial ao Vincent Marieu e aos colegas do Doutorado.

RESUMO

O transporte e a distribuição do Material Particulado em Suspensão (MPS) na zona costeira são influenciados por processos hidrodinâmicos, meteorológicos e oceanográficos (marés, descarga fluvial, ventos etc.), em escalas temporais de segundos a anos. Os rios e estuários são bastante estudados, pois são as principais fontes de sedimento para a zona costeira, funcionando como um filtro natural entre o continente e o oceano. Além da problemática relacionada à erosão ou assoreamento que ocorre na zona costeira e em estuários, em canais portuários, é importante entender a dinâmica do sedimento em suspensão para fins de análise de distribuição de poluentes e possíveis sumidouros e fontes de substâncias contaminadas. A presente tese tem como objetivo investigar a dinâmica e distribuição do MPS entre o sistema estuarino de Itapessoca e Itamaracá (SEII) e a plataforma interna adjacente, focando nos processos de importação de material da plataforma, através de dados observacionais e modelagem numérica, para identificar as fontes alóctones de material para dentro do estuário. A primeira parte da tese mostra que existe um padrão residual de circulação entra as ilhas de Itamaracá e Itapessoca e a morfologia de fundo da seção transversal da Barra de Catuama define uma importação duas vezes maior de água e MPS para dentro do sistema. Um filtro passa-baixa do tipo *Butterworth* evidenciou a circulação gravitacional como sendo a principal forçante da circulação submareal. Além disso, o modelo hidrodinâmico 3D do sistema SEII mostrou que o padrão de correntes do sistema tende a importar MPS de maneira residual da plataforma. Esse resultado é corroborado pela propagação da maré no sistema, que mostrou a presença de dois pontos nodais ou nulos (sem variação de maré), onde as correntes diminuem sua magnitude. Por fim, a partir dos resultados do modelo 3D, foram realizados experimentos com trajetória de partículas *off-line.* Os resultados mostraram que a fonte do MPS é alóctone com origem na deriva litorânea da plataforma ou estuários vizinhos. Da mesma maneira, os resultados utilizados no terceiro artigo da coletânea desta pesquisa mostra a trajetória de partículas, utilizando um modelo numérico lagrangeano. Após simulações em 4 combinações de cenários distintos: i) maré; ii) maré + descarga fluvial; iii) maré+descarga fluvial+vento e iv) maré+vento, foi possível identificar o preenchimento do estuário ocorre da plataforma para dentro. Uma combinação de vento, descarga fluvial e maré, juntamente a vento e maré,

mostraram que as partículas provenientes da plataforma e do estuário do rio Capibaribe (adjacente) influenciam na presença de MPS dentro dos canais da ilha de Itapessoca.

Palavras-chave: circulação estuarina; marés; transporte sedimentar.

ABSTRACT

Transport and distribution of Suspended Particulate Matter (SPM) in the coastal zone and estuaries are influenced by a bunch of different sedimentological, hydrological and oceanographic processes in timescales from seconds to decades (e.g. tides, river inflow, wind). Rivers and estuaries are broadly assessed because they are the main source of sediments supply for the coastal zone, acting as a natural filter. Besides the problematic related to the coastal erosion and shallowing processes of channels and ports, it is important to understand sediment dynamics in order to predict and assess pollutant or waterborne material dynamics. This thesis aims to investigate the suspended sediment dynamics in a ria type coastal estuarine system, by using observational and modelled data. The first part of the thesis shows that there is a residual circular velocity pattern around the islands and one inlet import twice the amount of volume. A Butterworth low-pass filter showed the classical gravitational circulation pattern for the cross sections, showing the predominance of the estuarine circulation process. A hydrodynamic 3D model of SEII showed importation patterns from the shelf added to a clockwise circulation around Itamaracá Island northwards. This result is supported by the tide propagation in the system which identified two nodal points in the system which can explain in part the importation aspects and where currents are null. From the 3D model results, offline particle tracking experiments were performed in order to assess the origin and fate of particles (here treated as SPM). Results showed that SPM main sources into the estuary are the longitudinal shelf transport. Results from the last chapter corroborated previous results from the 3D hydrodynamic model. After four different scenarios were tested: tide, tide and freshwater inflow, tide + freshwater + wind, and tide + wind, it was possible to determine the filling mechanisms of the estuary. A combination of tide + wind and tide+wind+freshwater spotted accumulation in the Itapessoca channels and the origin is related to Capibaribe river estuary and the adjacent shelf.

Keywords: estuarine circulation; tides; sediment transport.

SUMÁRIO

1 INTRODUÇÃO 9
1.1 OBJETIVOS 11
1.1.1 Objetivo Geral 11
1.1.2 Objetivos Específicos 11
1.2 Hipóteses e JUSTIFICATIVAS 11
2 METODOLOGIA 14
3 RESULTADOS 15
3.1 ARTIGO 1 - Circulation and suspended sediment transport in a sediment starving ria: the Itapessoca Estuary, Northeast Brazil 15
3.2 ARTIGO 2 - Residual circulation in a semi-enclosed tropical embayment with complex geometry 33
3.3 ARTIGO 3 – TROCAS ESTUÁRIO-PLATAFORMA EM UM SISTEMA DE RIA COM GEOMETRIA COMPLEXA 58
4 CONSIDERAÇÕES FINAIS 85
REFERÊNCIAS 86
APÊNDICE A - OBSERVATIONS OF LOCAL AND LATERAL FLOW IN HIGHLY ENERGETIC, BAR-BUILT ESTUARY 96

1 INTRODUÇÃO

As regiões costeiras e estuários desempenham importante papel econômico no seu uso e ocupação, servindo como via de transporte de mercadorias e pessoas. Além disso, possuem um essencial papel ecológico, pois servem como habitat natural de várias espécies de peixes, aves e mamíferos (Miranda *et al.*, 2017; Miranda, Kjerfve e Castro, 2002). Os estuários são reconhecidos como eficientes armadilhas de sedimento fluvial e marinho por causa de suas intrínsecas condições hidrodinâmicas. Em um contexto geológico, são definidos como a porção mais próxima ao mar de um vale de rio inundado que recebe o aporte de material fluvial e marinho, e contém fácies influenciadas por marés, ondas e processos fluviais (Dalrymple et al., 1992; Dalrymple e Choi, 2007)

As ondas, os ventos, as marés e a descarga fluvial são as principais forçantes que controlam o transporte de sedimento entre o continente e o oceano (Prandle, 2009). Grande parte do Material Particulado em Suspensão (MPS) que chega à zona costeira pelos rios fica retido nos estuários ou então é exportado para a plataforma continental adjacente(Dyer, 1995). Este material é composto, basicamente, por silte e argila com partículas inferiores a 80 μm (Eisma, 1991). Assim, o material particulado em suspensão determina a qualidade da água e, portanto, a produtividade primária, os ciclos biogeoquímicos e a distribuição de poluentes (Brown *et al.*, 2015).

Uma das grandes dificuldades de se monitorar a variabilidade espaço-temporal do material em suspensão, na água, é a dificuldade de obtenção do dado de forma direta, pois é uma tarefa laboral que requer mais de um técnico em atividade, além de equipamentos. No entanto, o desenvolvimento tecnológico, nas últimas décadas, vem permitindo a coleta de dados indiretos mais robustos e em maiores escalas temporais (Zaleski e Schettini, 2006). Esses dados obtidos servem para implementar modelos numéricos mais precisos e exatos que, por sua vez, podem geram estimativas e previsões para tomada de decisão em contexto socioambiental (e.g. políticas públicas ambientais, e o monitoramento e estimativa de qualidade de água e sedimento).

Os estuários são a principal rota pela qual o sedimento proveniente da erosão continental é transportado dos rios em direção ao mar. Rio abaixo, a distribuição do tamanho das partículas se altera em um contínuo ciclo de deposição, erosão e

transporte (Dyer, 1995). O material de granulometria mais grosseira se mantém retido ao longo das planícies fluviais, enquanto as frações mais finas são transportadas em direção ao estuário. Lá, os processos estuarinos agem criando um filtro natural de sedimento (Mehta, 1986)

Recentemente, os pesquisadores expandiram a teoria clássica e identificaram mais mecanismos que impactam a dinâmica sedimentar e o aprisionamento sedimentar no estuário. Geyer (1993b) mostrou que a estratificação vertical reforça a retenção sedimentar agindo de maneira a reduzir a difusividade turbulenta. Além disso, assimetrias no cisalhamento vertical de velocidade, turbulência e rugosidade de fundo podem, similarmente, afetar o padrão de transporte sedimentar (Jay & Musiak, 1994; Allen *et.* Al; Scully & Friedrichs, 2007)

Da mesma maneira, Wolanski (1995) acrescentou a importância dos estuários com presença de manguezal no transporte de sedimento. Foi mostrado que a vegetação altera o prisma de maré e intensifica os processos de floculação e bombeamento de maré. A presença de vegetação nas zonas intermareais dos estuários é intensificada em estuários tropicais que estão sujeitos a variação sazonal da descarga fluvial e intensa evapotranspiração.

Investigações nos estuários e na plataforma continental do Nordeste Brasileiro têm mostrado que os padrões de circulação e fluxos residuais de material particulado em suspensão possuem características não convencionais com estuários de climas úmidos e temperados, pois estão sujeitos à sazonalidade (e.g. Medeiros & kjerfve, 2005. Schettini *et al*., 2013., Oliveira-Filho, 2015., Schettini *et al,* 2016. Valle-levinson & Schettini, 2016). A zona costeira dessa região brasileira, em particular, representa uma das poucas áreas do mundo onde uma margem aberta e passiva é quase completamente coberta por sedimentos biogênicos carbonáticos (Summerhayes et al., 1975). De acordo com os autores, quanto maior for o aporte da descarga fluvial, menor a quantidade de sedimento carbonático presente. Medeiros & Kjerfve (2005) mostraram que existe um fluxo residual de sal e sedimento em direção ao mar no Canal de Santa Cruz do estuário de Itamaracá, PE, Brazil e o principal mecanismo físico é o bombeamento de maré.

Ainda no setor NE do Brasil, os platôs sedimentares são interseccionados por inúmeras falhas Holocênicas (Medeiros et al, 1993; Knoppers, 1999; Lessa et al., 2018), o que gerou uma série de estuários com estruturas de graben ao longo das planícies costeiras. Tal processo deu origem ao estuário de ria de Itamaracá e

Itapessoca, PE, além dos estuários do rio Mamanguape e Paraíba (Lima et al., 2016; Rossetti et al., 2011). Um estuário de ria pode ser definindo como um vale de rio inundado formado por subsidência tectônica do continente, um aumento do nível relativo do mar ou a combinação de ambos (Evans & Prego, 2003). A topografia é semelhante a um vale de rio. São relativamente profundas, estreitas e com canais bem definidos. O substrato deste tipo de estuário, portanto tende a ser de fundo rochoso e o aporte sedimentar tende e vir do oceano, pois as bacias de drenagem, geralmente, são pouco extensas.

1.1 OBJETIVOS

1.1.1 Objetivo Geral

O Objetivo geral dessa tese é identificar as trocas de sedimento em suspensão entre estuários pequenos e com bacias hidrográficas reduzidas e a plataforma continental adjacente e entre estuários vizinhos.

1.1.2 Objetivos Específicos

Especificamente, espera-se obter a distribuição espaço temporal da circulação estuarina, além da propagação da onda de maré e o transporte de material particulado em suspensão em quatro cenários diferentes simulados pelo modelo hidrodinâmico Telemac 3D. Por fim, espera-se identificar as zonas de acúmulo de partículas sedimentares dentro do estuário com a utilização de rastreamento virtual de partículas.

1.2 HIPÓTESES E JUSTIFICATIVAS

O Sistema Estuarino de Itamaracá e Itapessoca, PE, Brasil (SEII) foi escolhido como área de investigação dessa análise, pois é um sistema estuarino tropical, formado por duas ilhas e pequenos rios litorâneos que encontram o oceano por duas conexões principais, a Barra de Catuama e o Cabo Orange, além de uma vasta área de manguezal. Há ainda a presença de grandes depósitos de sedimento finos nas zonas intermareais do estuário e cinco pequenos rios que desaguam no local.

Tendo em vista que os estuários tropicais pequenos são definidos por apresentarem baixa produção sedimentar fluvial, a presença de depósitos lamosos

neste local é paradoxal, se a principal fonte é quase nula ao longo do ano. Associado a isso, a plataforma continental adjacente apresenta uma deficiência de aporte sedimentar dos rios. Nesse contexto, criam-se, então, algumas questões que motivam a presente investigação: quais os processos responsáveis pela importação do Material Particulado em Suspensão, uma vez que a baixa descarga fluvial média dos rios é não condiz com a quantidade de sedimento depositado nos estuários? Quais os mecanismos físicos, meteorológicos e geológicos que transportam as partículas que “alimentam” estes estuários? A origem do sedimento local é alóctone ou autóctone? As correntes residuais são as responsáveis pelo aprisionamento de material dentro estuário?

Figura 1. Mapa da plataforma continental de Pernambuco com a área selecionada para a investigação, evidenciando as entradas estuarinas do rio Capibaribe e do SEII em condições secas e chuvosas.

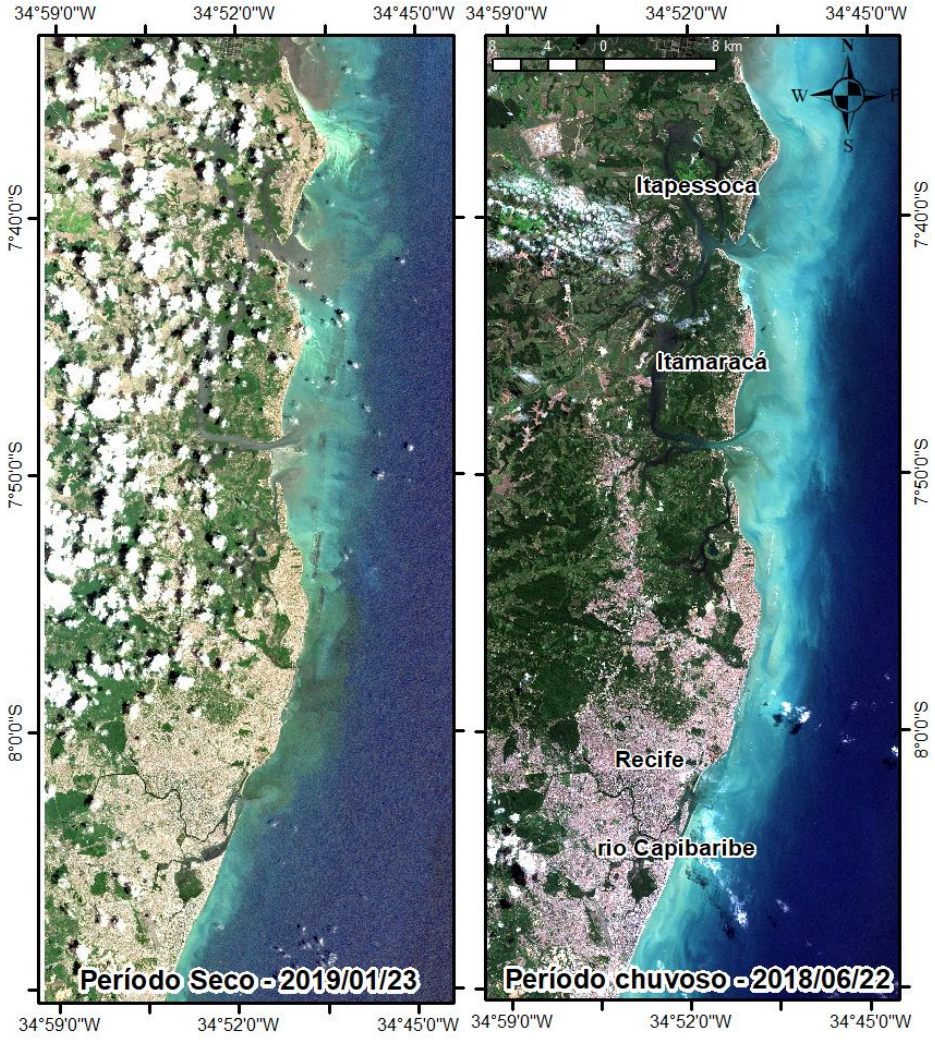

Fonte: The author (2021).

Uma das hipóteses para explicar a origem do sedimento alóctone no ambiente é a corrente de deriva litorânea da região NE do Brasil assim como foi citado por Knoppers et al., (1999). O sedimento em suspensão teria origem principalmente pela erosão da formação barreiras do litoral. A segunda hipótese é que o sedimento é retido da plataforma e teria origem nos rios adjacentes como os mecanismos de importação atuando para trazer o sedimento da plataforma interna adjacente.

2 METODOLOGIA

A metodologia dessa investigação foi composta pela análise de dados observacionais e resultados das simulações numéricas do modelo TELEMAC 3D. Primeiramente, os dados foram obtidos em uma campanha oceanográfica nos canais de Itapessoca e Catuama durante a estação chuvosa do ano de 2013 e se estendeu de 15 a 30 de julho. Dados de velocidade foram obtidos localmente com dois PACDs (Perfiladores Acústicos por Efeito Doppler) da marca Nortek, modelo aquadopp profiler de 1000 khz. Além disso, o campo de velocidade foi obtido em duas seções transversais, através da coleta de dados por PACD RDI workhorse da marca Teledyne de 1200 khz de freqüência. Finalmente, foram coletados dados hidrográficos através da sonda multiparamétrica Rinko Profiller JFE *advantech Technologies.*

Os dados observados foram utilizados para calibrar e validar o modelo hidrodinâmico TELEMAC 3D da plataforma continental de Pernambucon incluindo o SEII, a plataforma interna adjacente e o estuário do rio Capibaribe. Esses dados foram analisados em termos submareais por um filtro passa-baixa do tipo Buterworth com um período de corte de 30 horas. O modelo numérico e os cenários simulados são descritos com mais detalhes no capítulo 2 deste documento.

Com os resultados do modelo triangular, não estruturado 3D, foi criado um grid retangular e os dados hidrodinâmicos foram interpolados para camada de superfície e fundo. Esses dados foram escritos em uma variável NetCDF em conformidade com o input do modelo numérico lagrangeano OpenDrift, que simula de maneira off-line e requer um input de outra fonte numérica. Após isso, 4 cenários foram simulados, incluindo 9 diferentes origens.

3 RESULTADOS

Esta seção apresenta uma série de artigos elaborados para explicar a variabilidade espaço-temporal da circulação estuarina e do transporte sedimentar entre estuários pequenos tropicais com baixo aporte de água fluvial, com o objetivo de investigar o acúmulo de sedimento e o processo de preenchimento das bacias estuarinas. O primeiro artigo trata da circulação residual no estuário e dos valores de concentração de sedimento em suspensão, bem como sua distribuição e variabilidade temporal. O segundo utiliza os resultados do primeiro para calibrar, validar e desenvolver um modelo numérico hidrodinâmico 3D (Telemac 3D) para a plataforma interna rasa do estado de Pernambuco, Brasil. Por fim, os resultados da modelagem hidrodinâmica do segundo artigo foram usados para rodar o modelo de rastreamento offline de partículas OpenDrift, a fim de analisar as trocas sedimentares e o destino final das partículas que são transportadas com origem no estuário do rio Capibaribe e na plataforma continental interna adjacente ao Sistema Estuarino de Itamaracá-Itapessoca.

3.1 ARTIGO 1 - CIRCULATION AND SUSPENDED SEDIMENT TRANSPORT IN A SEDIMENT STARVING RIA: THE ITAPESSOCA ESTUARY, NORTHEAST BRAZIL

Running title: Circulation of the Itapessoca Estuary

Artigo submetido para o jornal OCR – Ocean and Coastal Research

Status atual: aceito com major revisions. Revisão submetida.

Author 1: José C. de Oliveira Filho, ORCID: 0000-0002-4785-2986

Graduate-Program in Geosciences, Federal University of Pernambuco. Av. Prof. Moraes Rego, 1235 Recife, PE, Brazil. CEP 50670-901

Author 2: Carlos A. F. Schettini, ORCID: 0000-0003-4286-3691

Institute of Oceanography, Federal University of Rio Grande. Av. Itália, km 8, Rio Grande, RS, Brazil. CEP 96000-000.

Corresponding author

ABSTRACT

The Itapessoca estuary is part of the Itamaracá-Itapessoca Estuarine System, a ria type estuary located at the Brazilian Northeast shore, in the State of Pernambuco. Here we present an assessment on the estuarine circulation, suspended sediment dynamics and its main transport mechanisms. We carried out a field survey where water level, currents, salinity, temperature and suspended sediment concentration (SSC) were recorded at 10-minute intervals during two complete semi-diurnal tidal cycles under spring tide condition. The field survey was conducted in September (2012), which is a transitional period between wet and dry seasons. Water level displayed symmetrical ebb-flood phases; however, currents were ebb-dominated. Freshwater contribution was negligible, and the mean salinity ws ~35 g/kg, which is slightly lower than the adjacent shelf values (36.5 g/kg). The SSC transport was driven by the ebb-dominated tidal currents, with highest values of ~30 mg/l occurring during the peak current during the ebb. The source of the suspended sediment was the erosion from the bottom, and the concentration was much lower than other similar estuaries (e.g. Caravelas). This observation suggests this system is a 'sediment starving system' in the sense that it presents low concentration of suspended sediment.

Keywords: estuarine circulation; tides; sediment transport.

INTRODUCTION

Estuarine environments play a key role in the mass transfer in the continent-ocean interface (Sweet *et a*l, 1971; Valle-Levinson, 2010). They act as a filter being efficient traps for sediments and other continent born materials (Schubel and Kennedy, 1984). The inflow of nutrient supplied waters makes estuaries highly biological productive environments. Due their strategic localization, they favour economic development such as harbour activity, fostering industrial development. This led to some of the largest cities in the world growing on estuarine margins.

The sharp longitudinal gradient of salinity is one of the main characteristics of estuaries. This physical feature produces the longitudinal density gradient which drives the estuarine circulation. A lighter upper layer flows seawards above a denser

layer which flows landwards (Cameron & Pritchard, 1963; Geyer & MacCready, 2014). Morphology and winds may also play roles on the circulation, resulting in complex patterns of circulation, mixing and transport of materials. The several forcings on the hydrodynamics act in a wide span of time and space scales, what make the assessment of distribution and transport of properties a challenging task (Kjerfve *et al.,*1982; Valle-Levinson, 2010). Although these circulation patterns, will drive the sediment and other scalars budget (Dyer, 1995; Uncles, 2002).

There is a rich diversity of estuarine environments along the Brazilian shore, subjected to a variety of physical settings from 33° south to 4° north. At south, the climate is subtropical, and the tidal regime is under micro tides regime. At north, in contrast, the climate is tropical, and the tidal regime is macro tidal type. Between them, along the Northeast shores, occur patches of tropical and semi-arid climates with tidal regime ranging from micro to mesotidal. The semi-arid climate is severe enough to produce conditions of hipersalinity and inverse estuarine circulation (Schettini et al., 2016; Valle-Levinson and Schettini, 2016). With exception of the São Luis (Maranhão) and Todos os Santos (Bahia) bays, estuaries along this shore are relatively small, making them more prone to man induced changes (Schettini et al., 2017). Because the semi-arid climate, most systems present a relatively small freshwater inflow, even with considerable large drainage basins, e.g., the Capibaribe River estuary (Schettini et al., 2017). Some systems present very small drainage basins with shape of drought river valleys, e.g., the Caravelas estuary (Schettini & Miranda, 2010). These systems may be classified as rias according to the physiographic classification of Fairbridge (1980).

There are two Rias in the Pernambuco State: the estuary of Formoso River (Silva et al., 2004) and the Itamaracá-Itapessoca Estuarine System (IIES) (Medeiros & Kjerfve, 2005). Both are smaller than the Galician Rias, known as prototypes of this type of system. Both present very small drainage basin and a drought river valley surrounded by relatively high relief. The small drainage basin means reduced freshwater inflow and continent born sediments. Another feature of these systems is their proportionally larger inter tidal areas occupied by mangroves, indicating active sediment trapping (Burchard et al., 2018; Schettini et al., 2020). These are tide dominated systems, and taking into account the limited sediment production, it may be possible thata substantial fraction of the sediments trapped on the mangroves is imported from the shelf. In order to improve the understanding the estuarine

dynamics in rias, sediment starving estuaries, we present here an assessment on the circulation and sediment transport in the Itapessoca estuary.

STUDY AREA

Itapessoca estuary is a drought river valley unfilled by sediments (e.g., Fairbridge, 1980), interconnected with the Santa Cruz Channel/Itamaracá Island (Medeiros & Kjerfve, 1993; 2005 – Figure 1). The system is formed by two channels ~8 km long and 300 m wide, at the flanks of Itapessoca Island. The channels are connected through a narrow and shallow channel at the northern part. The mainstream debouching there is the Itapessoca Creek, with a drainage basin of 125 km^2 from 1024 km^{2}which is the total watershed area. The land use on the drainage basin is manly sugar cane crops and there is also an industrial complex (CPRH, 2003).

Figure 2.1. Localization of the Itapessoca Estuary, in the context of South America and Pernambuco State. The Itamaracá-Itapessoca estuarine system. A high-resolution satellite image (from Google Earth) of the Itapessoca estuary with the indication of mangrove

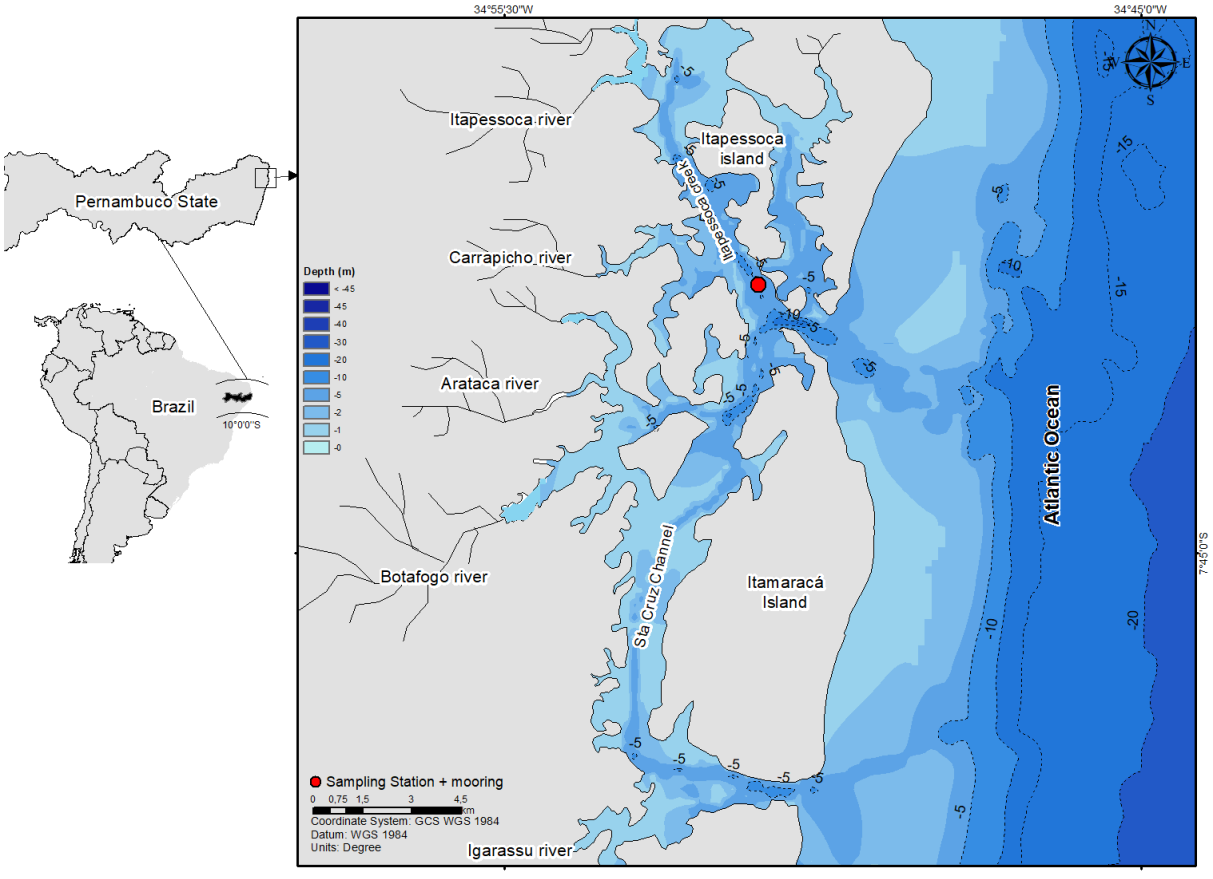

Source: The author.(2021)

Regional climate of Brazilian Northeast region is semi-arid (Kopen's Aw, tropical savannah), however along the east shore occurs a stripe (~ 100 km wide) named Zona da Mata (Bush Zone), where the climate is tropical wet (Kopen's Am, tropical monsoon). The mean annual temperature is 25.5 °C, ranging from 23.9 and 26.6 °C in August and February. At the countryside the annual precipitation rate is ~600 mm/year, with 5/6 dry months. At shore, precipitation rate can exceed 2,000 mm/year, with rains concentrated in May-July months, although rains occur all year long, while in the country the precipitation is nearly null during the dry months. There are sharp changes on the precipitation regime along the Zona da Mata caused by orography (Pereira, 2013). To characterize the IIES drainage basin climatology we adopted the values provided by Francisco et al. (2017) for the Caaporã Town, ~20 km north. The mean annual precipitation and evapo-transpiration rates are 1,917 and 1,508 mm/year, with a strong seasonal modulation. The rainy period is from May to July, and the dry period is from October to December (Figure 2A).

Figure 2.2. (A) Monthly precipitation and evapo-transpiration rates for the Caaporã Town situated 20 km north form the IIES. (B) Monthly mean and median river flow of Tracunhaém river which flows along the western border of the IIES drainage basin.

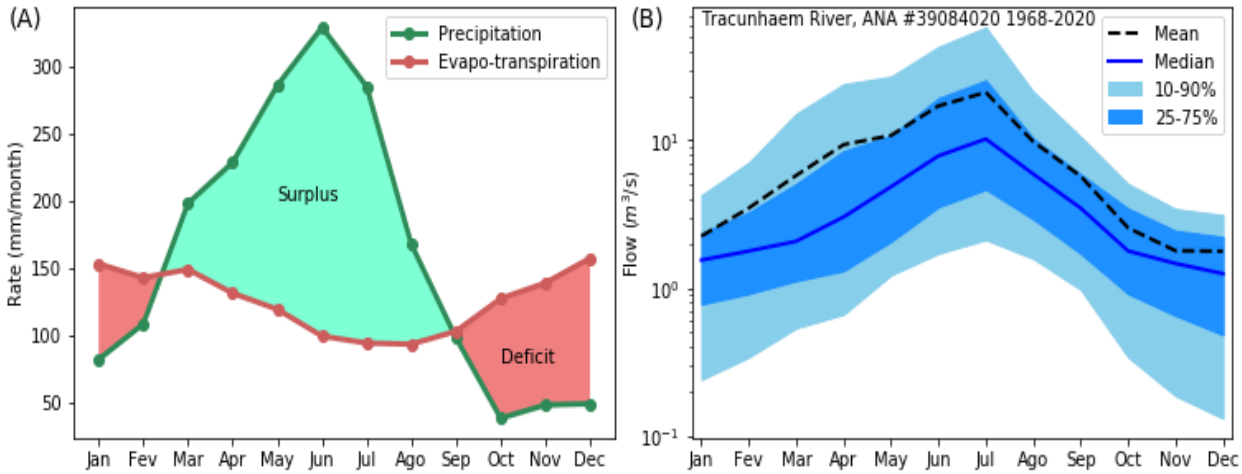

Source: The author (2021).

There is no river flow measurement in the IIES drainage basin although it has been estimated by Medeiros et al., 1993). The Figure 3B shows the monthly climatology of river flow for the Tracunhaém River. This river borders the western side of the IIES drainage basin (gauged area = 1,230 km^2) and reflects the behavior

of the IIES streams. The river flow follows strictly the balance between precipitation and evapo-transpiration. The maximum monthly mean occurs in July at the end of the rainy period, and the minimum occurs in December at the end of the dry period. The maximum mean value is ~ 20 m^3/s, and the minimum is < 2 m^3/s. However, the Tracunhaém drainage basin extends towards the country where the climate changes to semi-arid and a higher flow may be expected towards the coast in proportion to the drainage area. Estimates of the freshwater inflow to the IIES during the dry period is null and ~50 m^3/s during the wet period (Medeiros and Kjerfve, 1993).

The adjacent inner shelf is narrow (~ 40 km) with the shelf break at 60, 65 m deep (Barcellos et al., 2020). The high salinity (> 36.5 g/kg) and high temperature (> 26 ºC) Tropical Water dominates all year long, with little contribution of continental runoff (< 5%)(Domingues et al., 2017). The regional winds are controlled by the South Atlantic High, blowing from east on summer and from southeast on winter. Along shelf currents are driven mainly by northward winds most of the time, reversing southwards during summer (Dec/Feb) (Schettini et al., 2017). Regional tides are purely semi-diurnal and range between 0.7 and 2.3 m under neap and spring tide conditions and explain ~99% of the water level variance at daily timescale (Schettini et al., 2017).

MATERIAL AND METHODS

Field Observations

The field survey was carried out on 28-Sep to 1-Oct 2012, to gather hydrodynamic and suspended sediment concentration data. An acoustic Doppler current profiler (ADCP), three conductivity-temperature data loggers (CTs) and an optical backscatter turbidity-meter (OBS) were moored at the thalweg of the Itapessoca estuary at 9 m deep and ~0,5 km from the channel mouth (Figure 1). The period of data acquisition comprised two complete semi-diurnal tidal cycles (25 hours).

Water level, current velocity/direction and acoustic backscatter (ABS) were recorded with the ADCP by Nortek A/S, model Aquadopp Profiler of 1,000 kHz. The ADCP recorded vertical profiles with 0.35 m of bin size, with the first bin ~0.9 m above the bottom. Each profile was assembled from an average of 180 s at 2 Hz, at

10-minute intervals. CTs and OBS recorded at 10-minute intervals, performing bursts of 30 s at 1 Hz. The CTs and OBS were by JFE Advantech. The CTs were positioned at bottom, mid-depth and at surface. The OBS was positioned at the bottom. Currents were decomposed to the principal axis component. We use the convention of negative values for the seaward's currents and positive values for the landwards currents.

Suspended Sediment Concentration

Suspended sediment concentration (SSC) was derived from the OBS and from the acoustic backscatter (ABS) recorded by the ADCP. Both OBS and ABS are reliable proxies for the estimation of SSC (Schettini et al., 2010). OBS is measured usually in formazin turbidity unity (FTU), and ABS is in decibels (dB). The relationship between OBS and SSC is direct and linear for low SSC conditions (e.g., <500 mg/L, Winterwerp and van Kesteren, 2004). The relationship between ABS and suspended sediment is direct and non-linear (Deines, 1999).

To convert the ABS to SSC we adopted the procedure described in Zaleski and Schettini (2006), which is a two-step method. First we must obtain a relationship between SSC and OBS, as we adapted the Equation 1 by Pereira et al., (2010).

$$SSC(OBS) = 1.03 \times OBS - 1.05 \quad (1)$$

With coefficient of determination r^2 = 0.99. Despite being a calibration for another estuary, both systems are relatively similar. Both present small drainage basin and are tide-dominated, and the SSC is relatively low (<< 1.000 mg/L), draining the same Barreiras geological formation, so we may expect similar sediment characteristics, such as mineralogy assembly and color. Thus, we may use the OBS data recorded at the bottom simultaneously with the ABS to assess the relationship between them.

First the acoustic intensity recorded by the ADCP in 'counts' must be converted to acoustic power in dB, discount the basal noise of the instrument, and made the correction for the water absorption and conical acoustic beam spreading, using:

$$\text{ABS} = K_c(E - E_{BN}) + 20\log_{10}(z) + 2\alpha_w(z) + TS \quad (2)$$

(Deines, 1990; Lohrmann, 2001; Gartner, 2004). The first term of right side of Equation 2 is the conversion from counts to dB. The Ee instrument recorded echo intensity (counts);$E_{BN}$is the instrument basal noise, or the value of echo intensity recorded when the instrument is in the air; $K_c$is a factor of conversion from counts to dB. The second term of the right side of the Equation 2 accounts for the effect of acoustic spreading along the vertical distance from the instrument z. The third term account for the acoustic absorption of the water, being $\alpha_W$the water absorption coefficient which depends of water density. The last term accounts for the suspended acoustic reflectors target strength, usually unknown and not considered. The relationship between the SSC and the ABS from the bottom surface cell (0.25 cm from sea level) of the vertical profile is presented in the Figure 2.3. The SSC can be estimated by the ABS by

$$SSC = 0.022e^{0.115\text{ABS}} \quad (3)$$

with determination coefficient of $r^2 = 0.51$ (Figure 3).

Figure 2.3. Relationship between the acoustic backscaterr (ABS, dB) and suspended sediment concentration (SSC, mg/L) from the moored data.

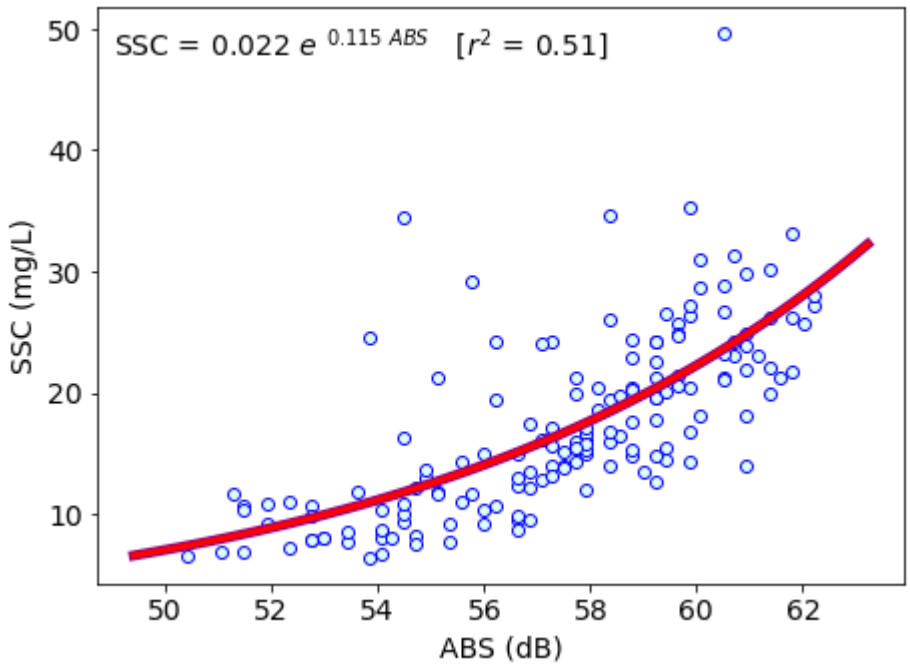

Source: The author (2021)

Transport Decomposition

The calculation of the mechanisms of advective transport of salt followed the approach described by Miranda et al. (2002), based on Bowden (1963), Fisher (1976), Hunkins (1981), Dyer (1974) and Kjerfve (1986). For a given laterally homogeneous estuarine channel, the decomposition of current *u* and salinity *S* are given by

$$\begin{aligned} u(x,z,t) &= u_a(x) + u_t(x,t) + u_s(x,z) + u'(x,z,t) \\ S(\mathrm{x,z,t}) &= S_a(x) + S_t(\mathrm{x,t}) + S_s(\mathrm{x,z}) + \mathrm{S'(x,z,t)} \end{aligned} \quad (4)$$

where u_a and u_a are the respective temporal and spatial averaged values, or $\langle\bar{u}\rangle$ and $\langle\bar{S}\rangle$. The over bar denotes vertical averaging, and the brackets denote time averaging. The terms u_t and $S_t$represent the deviation on time, physically the periodic tidal effects, given by $u_t = \bar{u} - u_a$and $S_t = \bar{S} - S_a$, and the terms u_s and S_s represents the deviation on space in the water column, physically the stationary tidal effects, given by $u_s = \langle u\rangle - u_a$ and $S_s = \langle S\rangle - S_a$. The last terms, u' and S', are residuals, which can be attributed to small-scale physical processes, are given by $u' = u - u_a - u_t - u_s$ and $S' = S - S_a - S_t - S_s$.

The water column thickness *h* also varies with the tide and can also be decomposed in time as $h(x,t) = h_a + \eta_t(x,t)$, where h_e is the local time averaged water depth $\langle h\rangle$, and $\eta_t$is the tidal variation of the water level. The averaged salt transport per one or more tidal cycles T_S is given by

$$T_S = \frac{1}{T}\int_0^T \int_0^h \rho\, uS dz dt \quad (5)$$

where *h* is the water column thickness, ρ is the water density, *u* is the longitudinal component of the current speed, and *S* is the salinity. The substitution of the different decomposition in the Eq. 4 produces 32 parcels of transport, from which seven have physical significance and are non-zero. Then, the total averaged salt transport per one or more tidal cycles can be written as

i *ii* *iii* *iv* *v* *vi* *vii*

$$T_S = \bar{\rho}(u_t h_a S_a + \langle h_t u_t\rangle S_a + h_a\langle u_t S_t\rangle + h_a\overline{u_s S_s} + h_a\langle\overline{u'S'}\rangle + \langle u_t S_t h_t\rangle + u_a\langle S_t h_t\rangle) \quad (6)$$

where the seven terms inside the parenthesis can be attributed to (i) fluvial discharge or storage term, (ii) Stokes' drift, (iii) tidal velocity-concentration correlation, (iv) gravitational circulation, (v) oscillatory shear, (vi) tidal sloshing, and (vii) tidal concentration-depth correlation (Miranda et al., 2002). The terms from Eq. 5 were divided by the mean depth of the sampling station (~7.5 m) to allow the comparison with Medeiros & Kjerfve (2005) results. The decomposition applied by these authors is based on Kjerfve (1986), for well mixed estuaries and did not solve the fourth term of gravitational mechanism. All the other terms represent same mechanisms. The Equation 6 was applied into 12:20 windows, which consider 75 temporal samples running over the whole time series. The results were reduced to mean and standard deviation of each term of the equation.

RESULTS

Time variation of water level, salinity, longitudinal velocity and SCC are presented in Figure 4. The statistics summary is presented in Table 1. The tidal signal displayed a symmetrical pattern, with equivalent periods of flood and ebb. The tidal range was ~2.3 m, which is the regional mean spring tide range. The currents displayed a phase-lag, with its peaks occurring at the end of the of the flood and ebb periods, respectively. The velocity was asymmetric, with maximum ebb velocity (-0.87 m/s) stronger than the maximum flood velocity currents (0.69 m/s).

Figure 2.4. Time series of (a) water level, (b) salinity, (c) longitudinal velocity and (d) suspended sediment concentration.

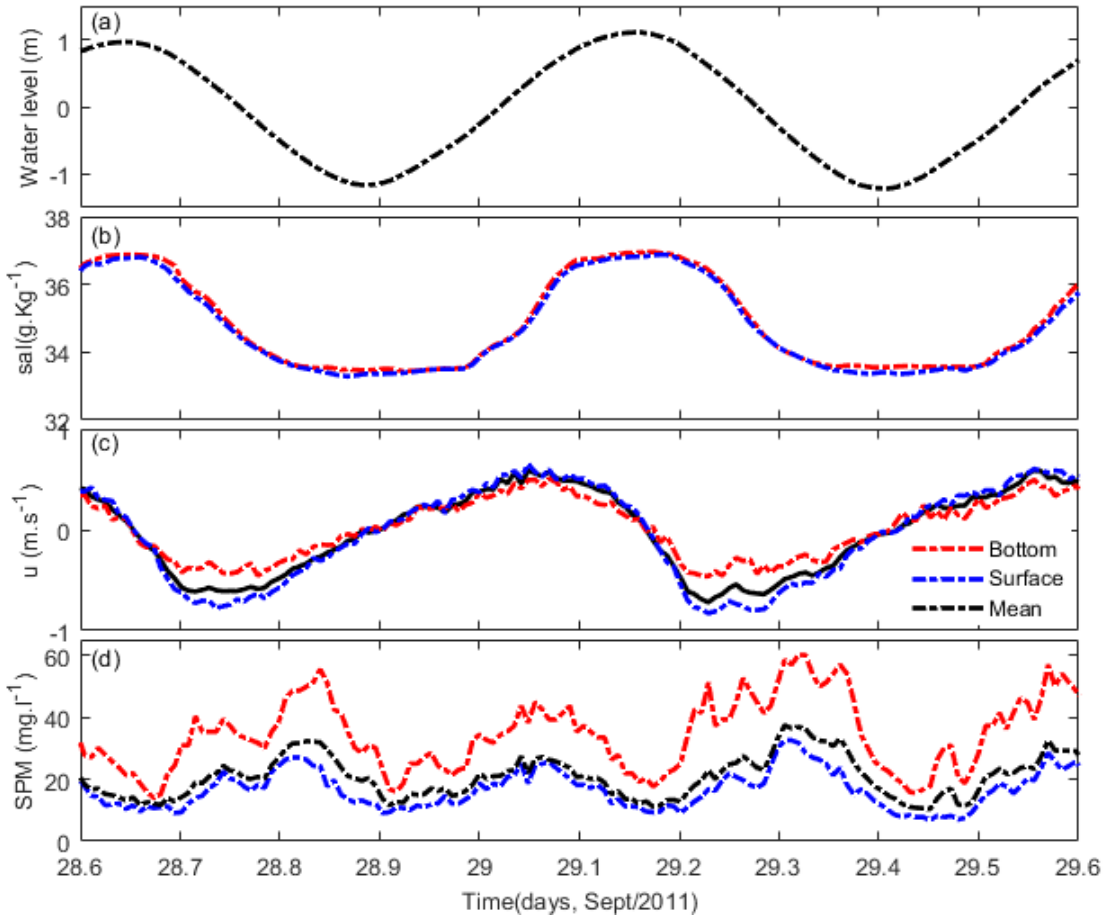

Source: The author (2021)

Temporal evolution of salinity followed the water level (Figure 4b), with maximum value (37.0 g/kg) at high tide and minimum value (33.0 g/kg) at low tide, indicating a light degree of dilution by freshwater inflow although it cannot be defined as hypersaline conditions as previously stated The salinity at the surface was on average 0.08 g/kg lesser than the salinity at the bottom, and the highest stratification occurred during at the low tide. The temperature (not presented in Figure 4) showed a maximum intra-tidal variation of 1 °C, with highest values of 27.8 °C at the high tides. The SSC ranged between 7 (at the surface) and 60 mg/L (at the bottom), with highest values during the current velocity peaks and near to the bottom.

Figure 2.5 presents the vertical and temporal distributions of the longitudinal current velocity and SSC with a 0.35 m of vertical resolution, what allows a better inspection on the data derived from the ADCP. In this figure is better visualized the longer flood and shorter ebb current periods. The currents were virtually unidirectional, reversing

from ebb to flood vertically monotonic. The SSC presented a quarti-diurnall pattern, with events of higher concentration coinciding with the current velocity peak. During the periods of slack waters, at high and low tide, the vertical SSC decreased in the whole water column.

Table 1: Summary of basic statistics of current velocity, salinity, temperature and SSC.

Parameter	Maximum	Minimum	Mean
U flood (m/s)	0.69		0.36
U ebb (m/s)		-0.87	-0.41
Salinity surface (g/kg)	36.9	33.3	34.8
Salinity bottom (g/kg)	36.9	33.4	34.9
Temperature surface (°C)	27.8	26.7	27.3
Temperature bottom (°C)	27.8	26.8	27.3
SSC (mg/L)	60.0	6.7	20.0

Source: The author (2021)

.

.

Figure 2.5. Temporal and vertical variation of (a) longitudinal velocity (m/s) and (b) SSC (mg/L). MAB means meters above the bed.

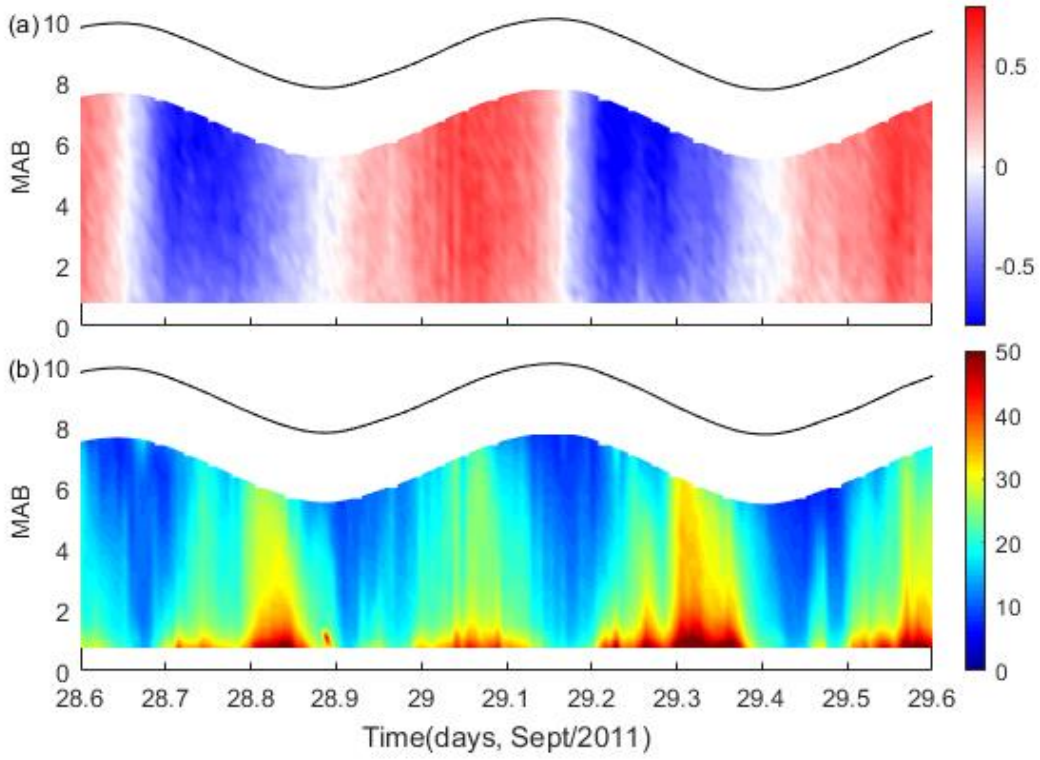

Source: The author (2021)

The relationship between the current velocity and the water level, the tidal stage diagram, is presented in Figure 6. The evolution of the tide condition presented an up-side down rain drop shape, near circular what indicates a standing wave regime when there is no mass transport by the wave movement. The current velocity asymmetry is indicated by the displacement for the negative (ebb) values. The relationship between current velocity and SSC presents an asymmetric butterfly shape, with indication of hysteresis during the ebb period (i.e. the water tends to maintain the same asymmetric shape).

Figure 2.6. (a) the tide stage diagram, relating the variation of the velocity and water level, and (b) the relationship between current velocity and SSC at surface and at bottom.

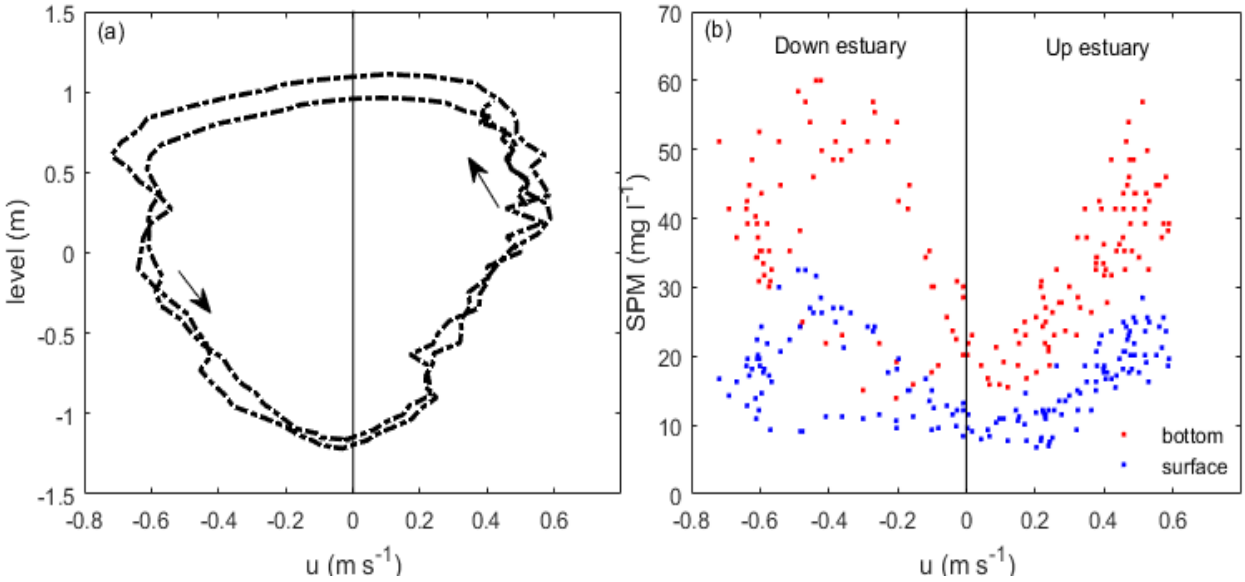

Source: The author (2021)

The results from the decomposition of the transport of suspended sediments are presented in Table 2 and Figure 7. The total transport was -2.12 kg/m.s, with the negative sign indicating seawards. The dominant mechanisms were the mean transport and the tidal correlation, with similar values and seawards. The other relevant mechanisms were the Stokes drift, gravitational circulation and tidal shear, all with about the same magnitude and landwards. All mechanisms displayed a temporal variability; however, this was clearer for the largest ones, presenting a semi-diurnal pattern.

Figure 2.7. Temporal variation of each right-side term of Equation 6, listed in the color indication legend.

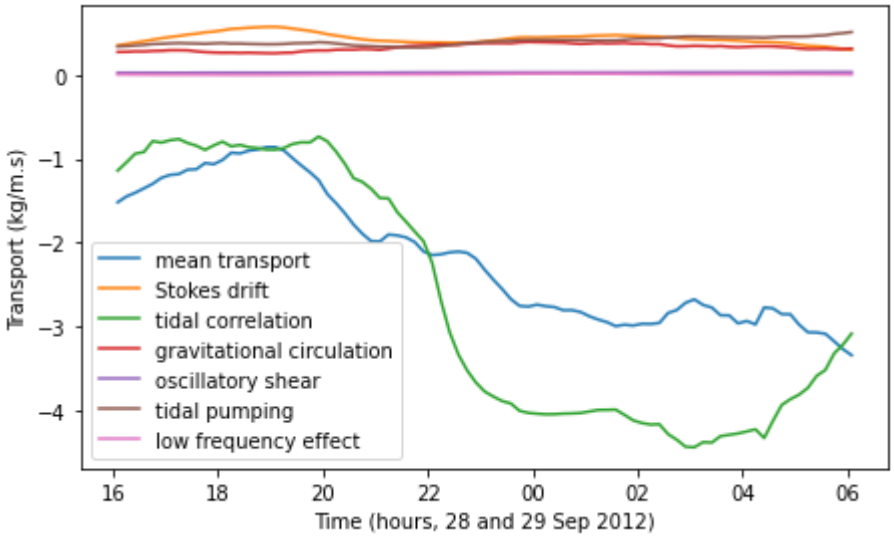

Source: The author (2021).

DISCUSSION

Along the Pernambuco shores occurs several coastal embayments. We may separate them in two groups: those with larger drainage basins, and others with reduced drainage basins. Thelarger ones are still relatively small, not exceeding 10,000 km^2 (e.g., Capibaribe and Una Rivers). Further, as they are subjected to semi-arid climate at the countryside, their water production is below the average for systems with equivalent size. During dry period, their flowrate is low, and they will work as efficient traps, retaining sediments and other river borne materials such as pollutants. The occurrence of estuarine turbidity maxima in these systems is a strong indicator of that (Schettini et al., 2016; Arruda-Santos et al., 2018).

During the wet period, extreme precipitation events occur (Ratisbona, 1976), and can produce massive injections of materials to the coastal zone. A single extreme event can produce more material transport than the expected one during years under average conditions (Schettini, 2002). Once in the shelf, these materials will be dispersed according with the shelf currents and waves. During the wet period the currents are predominately northwards (Schettini et al., 2017; Domingues et al., 2017), and this could allow these material be exchanged with other estuaries by the tidal action (Wolanski et al., 1992; Schettini et al., 2013). The IIES is located a short distance from the highly polluted Capibaribe estuary (Oliveira et al*.,* 2014; Régis et al., 2018), which is a pollutant source for the coastal area (Maciel et al., 2016). So, despite the IIES is relatively depopulated and preserved, it may be trapping materials delivered by the Capibaribe estuary.

Our survey provided a snapshot of the circulation and sediment dynamics, capturing the spring tidal regime, during the transition period between wet and rainy periods. The freshwater content can be easily assessed by the salinity. Regional continental shelf salinity is ~36.5 g/kg (Schettini et al., 2017), and the average salinity at the monitored station was ~35 g/kg, what disregarding other more complicated factor controlling the salinity distribution (Dyer, 1997), indicates that 96% of the water volume moving back and forth forced by the tides are marine one. Further, we can scale the relative importance of the freshwater inflow by the flow ratio: the ration between the freshwater volume contributions during ½ tidal periods to the tidal prism volume. The tidal prism can be scaled by the product between the system area and

the tidal range (Kjerfve, 1990). The West channel of the Itapessoca Island has area of ~20 km^2, and with the tidal range of 2.3 m, the tidal prism is ~46 × 10^6 m^3. There is no river discharge data available, but we may guess a value about 1.5 m^3/s based on Medeiros and Kjerfve (1996). The resulting flow ratio is ~7 × 10^{-4}. It reads, the water exchange with adjacent shelf contributes 1000 times more than the local river inflow.

Thus, we can hypothesize that all other properties measured at that point are driven mostly by tides, with negligible freshwater or river-borne materials content. Obviously, the sediments are river-borned, but then they are reworked materials from past freshets events. Their source could be either the local drainage or the exchange with the shelf.

The presence of suspended sediments in the water is a matter of energy/turbulence to keep the high-density particles suspended in a less dense environment, and material availability. Turbulence is produced by vertical shear caused by the bottom drag, being higher during the peaks of currents during flood and ebb. The highest SSC were recorded during these moments (Figure 5 and 6b), indicating that the main source of material is the ressuspension from the bed instead horizontal advection (e.g., Schettini et al., 2013). This is corroborated by the relationship between the depth-averaged SSC and the bottom SSC (Figure 8)(e.g. Nichols, 1984; Siegle et al 2009), which can be used as indicator of the suspended sediment source. Good agreement (high r^2) suggests the bottom as source, meanwhile poor agreement indicates other source then bottom.

Figure 2.8. Relationship between depth-averaged SSC and bottom SSC. MSE: mean squared error.

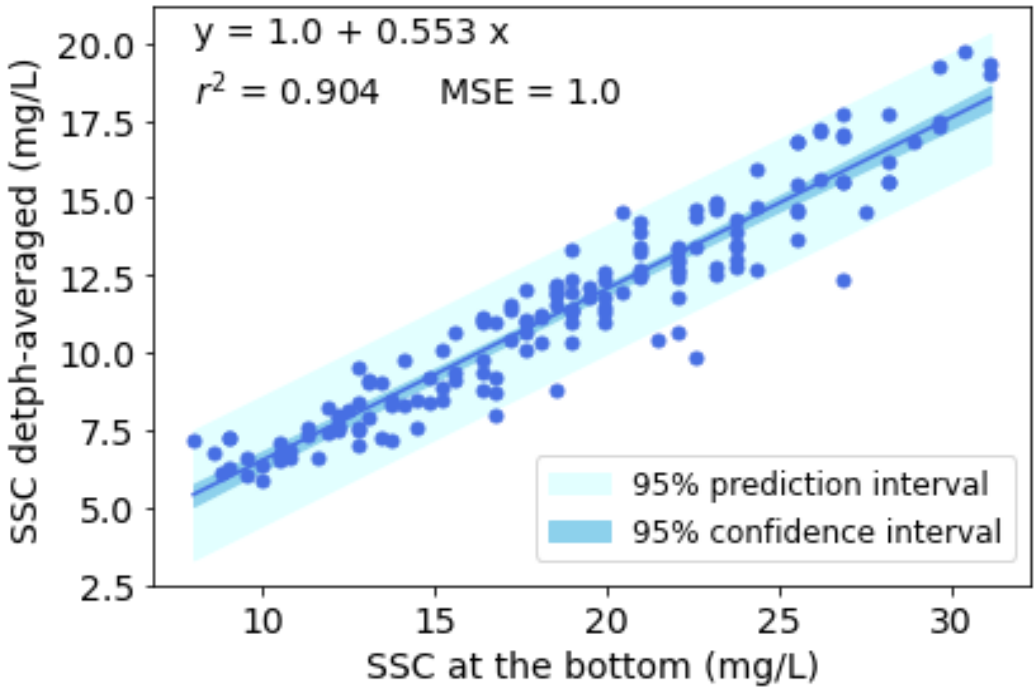

Source: The author (2021)

The Caravelas Estuary (Bahia, Brazil) is a relatively like the Itapessoca system. They share similar climate, similar tidal regime e present common fisiographic features, such as small drainage basin and multiple inlet system. There are more assessments on the Caravelas Estuary dynamics (Schettini and Miranda, 2010; Pereira et al., 2010; Schettini et al., 2013; Andutta et al., 2013; Sousa et al., 2014). However, an important distinction is the adjacent shelf. The shelf off Caravelas is wider by the presence of Abrolhos Bank, with large carbonate reefs affecting the coastal dynamics and allowing mud accumulation in the inner shelf. The shelf off IIES is narrow and dominated by sand and carbonate biogenic sand-gravelly poorly sorted sediments with low organic matter contents of marine natural origin (Barcellos et al., 2020). The fine sediment availability is lower, and this is reflected on the levels of SSC. In Caravelas, the SSC can be >300 mg/L during the spring tides (Schettini et al., 2013), while in Itapessoca the highest SSC was ~30 mg/L. This is particularly puzzling when one considers the extensive areas of mangrove in the system. This suggests that the systems may be one ‘sediment starving system’ which depends on the allochthonous sources (e.g., Willemsen et al., 2016), what is a concern in face of the sea level rise.

CONCLUSIONS

In this manuscript we assessed the circulation and the dynamics of suspended sediments in the western channel of the Itapessoca Island. It is part of the Itamaracá-Itapessoca Estuarine System. The assessment was based on a field survey that capture two complete tidal cycles, at spring tide. Our results showed that the hydrodynamics was primarily ruled by the tides, with negligible effects of freshwater inflow. Currents were ebb-dominant, as well as the residual suspended sediment transport. The source of suspended sediment was the erosion from the bottom, and the concentration was much lower than other similar estuaries. This suggest this system is ‘sediment starving system’.

Table 2: Mechanisms of the advective transport of suspended sediments calculateded by Equation 6.

Terms	Transport (kg/s.m)
i (mean transport)	-2.17 ± 0.78
ii (Stokes drift)	0.44 ± 0.06
iii (tidal correlation)	-2.69 ± 1.47
iv (gravitational circulation)	0.33 ± 0.04
v (tidal pumping)	0.03 ± 0.00
vi (tidal shear)	0.40 ± 0.04
vii (low frequency fluctuations)	0.01 ± 0.00
Residual	-3.57 ± 2.1
Total	-2.12 ± 0.76

Source: The author (2021)

3.2 ARTIGO 2 - RESIDUAL CIRCULATION IN A SEMI-ENCLOSED TROPICAL EMBAYMENT WITH COMPLEX GEOMETRY

Oliveira Filho, José Cavalcante de1; Schettini, Carlos Augusto França[4]; Sottolichio, Aldo[2]

Huybrechts, Nicholas[3]

Artigo submetido para o jornal “Regional Studies in Marine Sciences

Status atual: aceito com minor revisions. Revisão submetida.

ABSTRACT

Along the Brazilian northeast, occurs dozens of short estuaries, which present morphology as a result of tectonics and sea-level rise, showing complex geometry with multiple channels, islands, and intertidal areas. Some of these systems present small drainage basins with little freshwater inflow and sediment production. Here we present an assessment of the hydrodynamics and residual circulation of the Itamaracá-Itapessoca Estuarine System (IIES) based on field observations and numerical modeling. Field data was gathered during 15 days during the wet season (July 2013). Water level, currents, and salinity were recorded with moored instruments at two locations. This data allowed calibrating and validating a 3-D numerical model which was used to assess the whole system circulation patterns. As the system is composed of multiple branches and islands, we focused on the investigation of the residual circulation between the inlets (Catuama and Orange inlets) and the ocean. The main findings are (a) the main harmonic of the tide (M2) present hypersynchronous pattern with amplification landwards; (b) the hydrodynamic conditions slightly changed between wet and dry periods, however, there was an increase in the residual flow seawards (c) cross-sectional residual along estuary velocity presented laterally sheared distribution. The inflow was twice larger at the northern inlet than in the southern one which yields a net volume transport towards the estuarine head.

INTRODUCTION

Estuaries are highly biological productive ecosystems in the continent-ocean interface. They are transitional environments that are characterized by strong physical and ecological gradients and work as filters in the transport of scalars originated in the drainage basin in their flux towards the sea (Schubel e Carter, 1984). They are distributed throughout the world with different characteristics and also are natural habitats and breeding sites for many species of birds, reptiles, and mammals (Wolanski *et al.*, 1992). Although estuaries represent less than 1 % of the earth`s surface area, 22 of 32 of the world's largest cities are located in estuarine environments (Valle-Levinson, 2010).

The main characteristic of most estuaries is the longitudinal density gradient produced by differences in water salinity, from ~ 0 at the head to the coastal salinity usually >30 $g.kg^{-}$. This gradient tends to produce the gravitational circulation where the sub-tidal flow presents an upper, lighter layer moving seawards, and a lower, denser layer moving landwards (Fischer, 1976; Geyer e MacCready, 2014; Kreeke, Van de, 1993). This sub-tidal flow is called residual flow since the semi-diurnal tidal oscillation must be removed to depict it. It is about one order of magnitude weaker than instantaneous tidal flow, however, it is a major determinant for the transport and distribution of scalars (Prandle, 2009).

Despite the residual flow may be related firstly to the longitudinal density gradient in estuaries with sizeable river inflow, residual flows can be produced on short, low inflow estuaries (Largier, 2010), by the wind (Gutierrez de Velasco and Winant, 2004; Valle-Levinson et al., 2009), and even by the tidal interaction with the bathymetry (Burchard *et al.*, 2011). The residual flow produced by tides is strongly related to the system's geometry(Li e O'Donnell, 1997) where the cross-sectional shape and/or channel curvature can rule the lateral variability of the flow (Ross *et al.*, 2017; Valle-levinson, 2008; Valle-Levinson e Schettini, 2016). The residual flow in multiple inlets presents further complexity, since each inlet may present a different response to the physical forcing, and results that an inlet can act as a net importer while the other can be an exporter of water and scalars (Holtermann, Burchard e Jennerjahn, 2009; Schettini *et al.*, 2013; Schettini e Miranda, de, 2010; Waterhouse, Valle-Levinson e Winant, 2011)

The Itamaracá-Itapessoca Estuarine System (IIES) is one among dozens of relatively short coastal embayment located along the Brazilian northeast tropical shore. This area is formed by an indentation of the coastline surrounded by tertiary high plains, the Barreiras Geological Formation (Knoppers, Ekau e Figueiredo, 1999). There are remaining rocky hills that affected the shoreline evolution, which resulted in drowned valleys forming two major islands and connected to the sea by two inlets (Figure 1). The Itamaracá Island is nearly rectangular (13 x 5 km) separated from the continent by a channel with relatively uniform width (~300 m), with the Orange Inlet at the south and Catuama Inlet at the north. The Itapessoca Island (8 km long) extends from the Catuama Inlet northwards sided by two similar-sized channels (~ 300 m wide), which are connected by a shallower and narrower one sub-tidal channel (~50 m wide and < 1 m deep) bordering the northern part of the island within a mangrove, mud deposit surrounding it.

The IIES is relatively large when compared with neighboring systems, like the Goiana estuary at the north (Arruda-Santos, de *et al.*, 2018) and the Capibaribe estuary at the south (Schettini et al., 2016a). Its channel area is ~24 km^2, and the intertidal mangrove area is ~35 km^2 (Figure 1). On the other hand, its drainage basin is comparatively much smaller than its neighbors (~750 km^2; Goiana ~2,800 km^2; Capibaribe ~ 7,500 km^2). The basin is located near the shore, with its hinterland limit ~35 km from the sea and inserted in the tropical wet climate stripe along the coast (the Bush Zone, or *Zona da Mata*) where the precipitation rate can exceed 2,000 mm/year, contrasting with the semi-arid countryside where the precipitation is ~600 mm/year. The estimated freshwater flow to the estuary varies from null during the dry period to ~50 m^3/s during the wet period, debouching through five small streams.

A small drainage basin yields to low freshwater input and the same can be said about sediment production (Dyer, 1995). However, when one considers the relatively large mangroves areas and mud deposits of the Itamaracá and Itapessoca Estuaries, it seems to be paradoxical. Mangroves are efficient sediment traps and can retain most of the river borne suspended sediments (Wolanski, 1995; Schettini et al., 2020). In this context, mangroves would be river-sediment-starving if the sediment supply would be solely due to the local drainage basin. On the other hand, it may be possible that the estuary-shelf exchange processes could be an important source, if not the main one, of materials (Schettini *et al.*, 2013; Wolanski, Nhan e Spagnol, 1998) if residual flow is landwards.

The largest rivers debouching on the Not it has drainage basins ranging between 5,000 to 10,000 km^2. Their mean contribution of materials to the shelf is limited because of the countryside's semi-arid climate and is likely to be null during the dry period. However, intense rain events occur during the wet period, producing episodic pulses of materials. Once delivered on the shelf, these materials produce a turbid coastal boundary layer (Figure 2), and sediments will be distributed along the shelf and feed sediment-starving estuaries like the IIES.

In this sense, to assess the above-stated hypothesis, we addressed the estuarine circulation and estuary-shelf exchange processes coupling observations and numerical modeling. The main goals are to evaluate the system's residual circulation, tide propagation, and volume balance. At last, we want to address the system's budget for creating a conceptual model indicating the fate of waterborne material.

Figure 3.1 (a) Satellite image of the Itamaracá and Itapessoca Estuarine System from the Sentinel 2B sensor. (b) Map with the main river mouth and intertidal mangrove areas and the Orange (C1) and Catuama (C2) inlets. (c) Model grid and bathymetry. The entire model domain is presented in the top/right box.

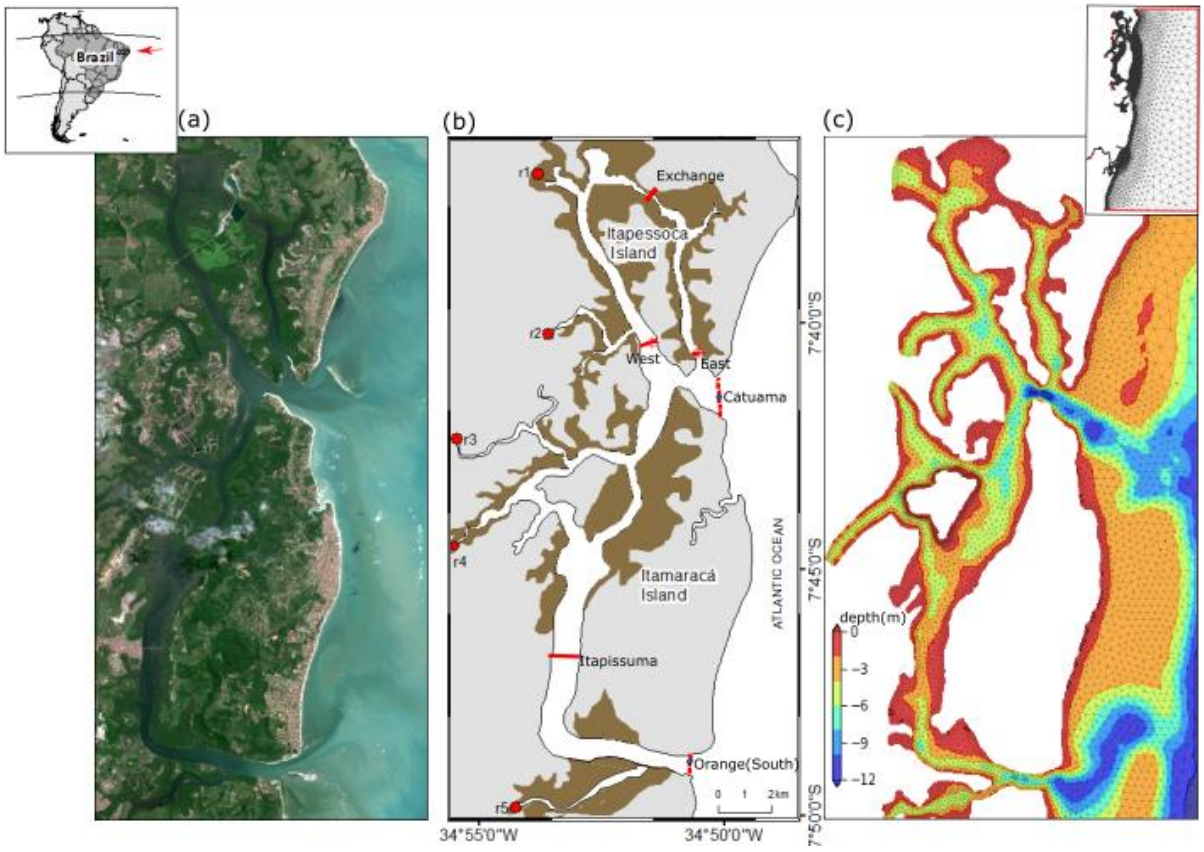

Source: The author (2021).

Figure 3.2. Stretch of Pernambuco shore from the city of Recife (south) to the Goiana estuary (north) at dry (left panel) and wet (right panel) periods, highlighting the presence of the turbidity coastal boundary layer during the wet period.

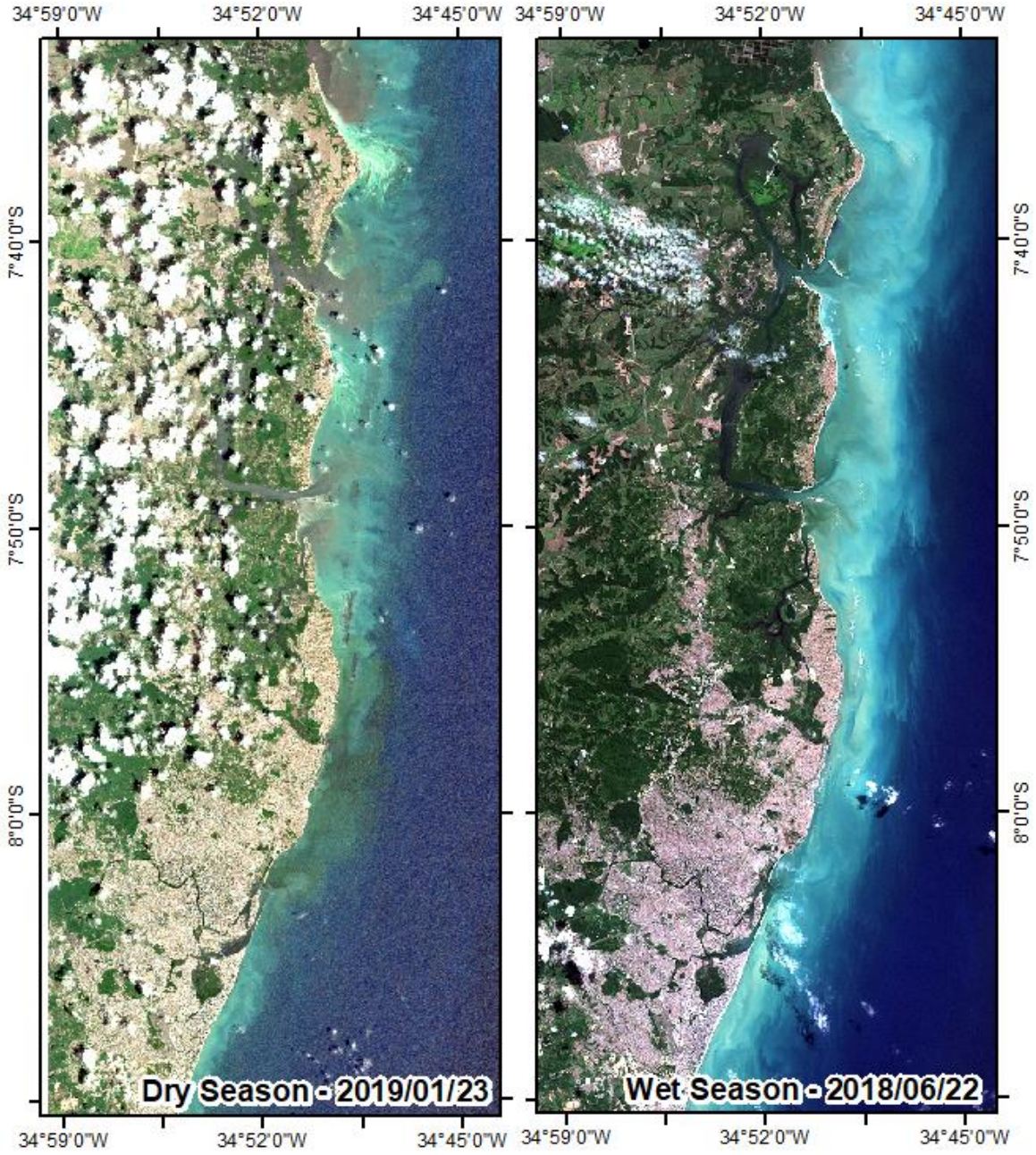

Source: The author (2021).

STUDY AREA

The IIES is located 40 km north of Recife, State Capital of Pernambuco, Brazil (7°36' - 8°12' south; 35°06' - 34°36' west; Figure 1). It can be described by three faulted U-shaped main channels: Santa Cruz channel, which extends from Orange inlet in the southern part of the system to Catuama inlet in the north, surrounding Itamaracá Island; Catuama channel (hereafter referenced as East Channel – EC), which extends from Catuama inlet to the northern part of the system; and Itapessoca channel (referenced as West Channel –WC) that presents similar morphology to Catuama channel, but extends in the western part of the system surrounding Itapessoca Island.

The existence of alongshore sandstone reefs is a main geologic feature that retains the local coastal circulation and exchange of the system. These shore-parallel lines of beach rocks/reefs bring protection to the coast but are interrupted many times by inlets that form excellent harbors as in the case of Capibaribe and IIES estuaries (Knoppers et al., 1999; Mabesoone and Coutinho, 1970; Mabesoone, 1964). The presence The IIES is similar to other shallow, convergent, mangrove-fringed estuaries (Asp *et al.*, 2018; Schettini *et al.*, 2013; Valle-Levinson e Schettini, 2016).The inlets are relatively deep (18 m deep in the Catuama inlet and 14 m in the Orange inlet), but the overall system is shallow (< 3 m) with large intertidal areas (~ 35 km^2).

The regional climate of the Brazilian Northeast region is semi-arid (Kopen's Aw, tropical savannah), however along the east shore occurs a stripe (~ 100 km wide) named Zona da Mata (Bush Zone), where the climate is tropical wet (Kopen's Am, tropical monsoon). The mean annual temperature is 25.5 °C, ranging from 23.9 and 26.6 °C in august and February. In the countryside, the annual precipitation rate is ~600 mm/year, with 5/6 dry months. At the shore, precipitation rate can exceed 2,000 mm/year, with rains concentrated in May-July months, although rain events occur all year long. There are sharp changes in the precipitation regime along the Zona da Mata caused by orography (Pereira, 2013). To characterize the IIES drainage basin climatology, we adopted values provided by Francisco et al. (2017) for the Caaporã Town, ~20 km north. The mean annual precipitation and evapotranspiration rates are 1,917 and 1,508 mm/year, with a strong seasonal

modulation. The rainy period is from May to July, and the dry period is from October to December (Figure 3A).

There is no river flow measurement in the IIES drainage basin. Figure 3B shows the monthly climatology of flow for the Tracunhaém River. This river borders the western side of the IIES drainage basin (gauged area = 1,230 km^2) and reflects the behavior of the IIES streams. The river flow follows strictly the balance between precipitation and evapotranspiration. The maximum monthly mean occurs in July at the end of the rainy period, and the minimum occurs in December at the end of the dry period. The maximum mean value is ~ 20 m^3/s and minimum < 2 m^3/s. However, the Tracunhaém drainage basin extends towards the country where the climate changes to semiarid and a higher flow may be expected towards the coast in proportion to the drainage area.

Figure 3.3. (A) Monthly precipitation and evapotranspiration rates for the Caaporã Town situated 20 km north from the IIES. (B) Monthly mean and median river flow of Tracunhaém River that flows along the western border of the IIES drainage basin.

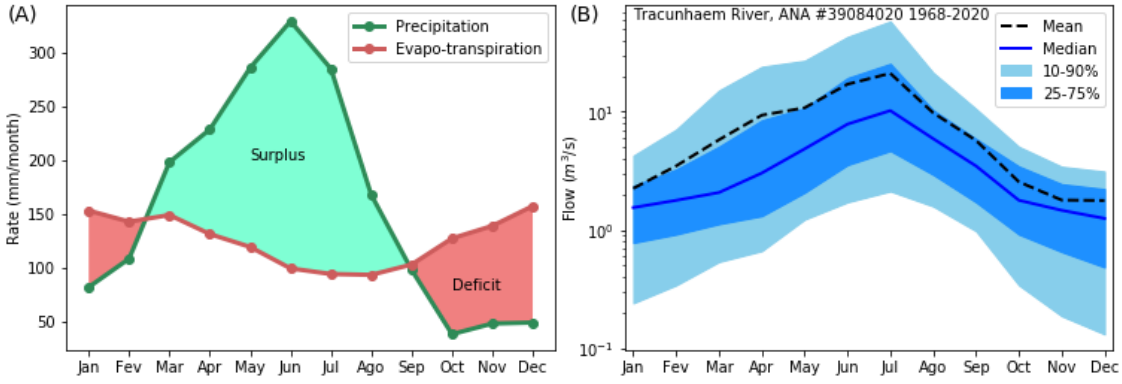

Source: The author (2021).

The first hydrographic assessment of the Itamaracá Estuary was made by Medeiros and Kjerfve (1993). They found hypersaline conditions in the dry season with a maximum of 38 psu in the inner part of the estuary. Further, longitudinal fluxes of salt and suspended sediment of the Santa Cruz Channel (Itamaracá) were reported by Medeiros and Kjerfve (2005). They concluded that net advective salt and sediment transport are not in a steady-state and can be explained by river discharge. More recently, the circulation and transport of salt and suspended sediment were observed by Oliveira-Filho and Schettini(2015). A landward residual transport of salt

and suspended sediment occurred in the Itapessoca channel although the ebb-dominance was observed in both channels.

MATERIAL AND METHODS

Field Data

A field survey was conducted in July 2013 to gather hydrodynamics, salinity/temperature, and suspended sediment concentration (though the latter is not used in the present study). Water level, current velocity, and direction were recorded with an Acoustic Doppler Current Profiler (ADCP) moored in two sites at east and west channels bordering the Itapessoca Island (Figure 1). The instruments, by Nortek model Aquadopp Profiler of 1,000 kHz, were moored at the thalweg at 7 and 11 m at the east and west channel, respectively. Data were recorded at 10 min-interval from 2-minute bursts with vertical resolution of 0.3 m and blank distance of 0.4 m. The deployments lasted from 16 to 29-July, capturing an incomplete neap and a spring tidal cycle.

The currents were decomposed to the main axis by principal component analysis. Seawards currents were assigned positive, and landwards currents negative if the channel orientation is north-south. For the inlets, Catuama and Orange, the negative sign represents inflow whilst positive values represent outflow.

The IIES bathymetry is partially charted, available in the Brazilian Navy chart N.o 910 “Proximidades de Itapessoca” (proximity of Itapessoca) from 1961. A bathymetric survey was carried out in July 2016 covering the whole system to complete the bottom topography, especially on the uncharted regions. We used a simple fish-finder by Garmin model GPSmap 420S, and a RBR Virtuoso water level recorder to make the tidal corrections. The data was leveled to the Port of Recife spring low to adjust with the available charted data. The mangroves’ topography had to be guessed. We considered the boundary between channels and mangrove with the level of neap tide high water, and the boundary between the mangrove and dry lands with the level of spring tide high water. The values of water level between these limits were interpolated linearly.

Freshwater Inflow

The knowledge of the freshwater inflow into an estuary is paramount to assess its hydrodynamics. However, the streams which debouche into the IIES are not gauged and there is no information available on freshwater flow. The streams debouching into the IIES are the Itapessoca, Carrapicho, Arataca, Botafogo and Igarassú rivers. According to the Pernambuco State Water Resources Company (CPRH, 2003), the total drainage area of these rivers is 746 km^2.

Medeiros and Kjerfve (1993) scaled the freshwater inflow based on the hydrological balance and an estimated runoff ratio, detailed in Kjerfve et al. (1996), suggesting values ranging from < 1 to ~ 56 m^3/s during the dry and wet periods, respectively, considering the drainage basin area of 824 km^2. Oliveira Filho (2015) assessing the water budget for the Itapessoca estuary suggested values ranging from 0 and 13 m^3/s during the dry and wet periods, respectively, considering the drainage basin area of 125 km^2. Adjusting linearly these values to the reference area (746 km^2) gives us 50 and 77 m^3/s for the wet period, from Medeiros and Kjerfve (1993) and Oliveira Filho (2015), respectively. Considering the simplest water budget, the balance of precipitation and evapotranspiration (Figure 3) integrated for the drainage area, utilizing the values from the plot in Figure 3A we get the maximum potential river discharge of 66 m^3/s.

Numerical Modelling

Hydrodynamic models became a robust tool to investigate the dynamics of coastal systems(Cheng, Valle-Levinson e Swart, De, 2011; Fernandes, Dyer e Moller, 2005; Scully, Geyer e Lerczak, 2009). Complementary to field observations, which are costly and limited in time and space, models allow us to widen our perspective in time and space otherwise impossible. The hydrodynamic numerical models rely on the *Navier-Stokes* equations to numerically solve the 3D free-surface flows through different numerical techniques. The main numerical discretization methods are the finite differences, finite elements and finite volumes. Despite the finite differences method allows to develop high order schemes at lower computational cost using orthogonal meshes, the finite element method allows a better representation of complex geometries by using triangular elements (Hervouet, 2007; Hirsch, 2007). In the present study, we adopted the open source TELEMAC

3D (www.opentelemac.org), which uses flexible mesh discretized on finite elements and is particularly suited for the complex geometry of the IIES.

The model bathymetric grid was built using a triangular mesh generator function which creates and defines triangular elements superimposed in 10 vertical layers. The domain encompasses ~70 km of shore (from 8.25° to 7.55°S) extending 35 km offshore from the coastline, reaching the isobaths of 50 m, which locally is close to shelf break (Schettini et al., 2017b). Table 1 summarizes the mesh characteristics.

Table 1. Metrics of the 3D mesh created for the Pernambuco Shelf. The bathymetry data were interpolated into a 2D grid which was extended in the vertical direction.

Mesh Characteristics	Total
Nodes	27470
Vertical layers	10
Elements	47617
Minimum Element Area (m^2)	10
Mean Element Area (m^2)	40837

Source: The author (2021).

Initial and Boundary Conditions

The initial conditions of the numerical simulations were prescribed under constant salinity (36g.kg^{-1}) and temperature (27 °C) which are the mean values on the adjacent shelf (Schettini, Carvalho, *et al.*, 2017). The open ocean boundaries were forced by sea-surface height and currents generated from tidal harmonics of the Topex-Poseidon altimetry database (TPXO9) (Egbert and Erofeeva, 2002), which includes eight primary harmonic tidal constituents (M2, S2, N2, K2, K1, O1, P1, Q1), two long-period (Mf, Mm) and 3 non-linear (M4, MS4, MN4). The mesh domain presents two types of open, liquid boundaries: i) the oceanic boundary which is a tidal boundary condition described above and ii) the river boundary, which presents a clamped boundary condition with prescribed and constant values of freshwater and tracer (salinity and temperature) input.

Freshwater inflow was prescribed at the points where the main streams reach the domain. We simulated two scenarios to represent modal seasonal conditions of dry and wet periods. The dry period was set up with null freshwater discharge. This

sounds true especially at the end of the dry period when most of the aquifers may empty. This is corroborated with hyper-salinity (38 $g.kg^{-1}$) observed by Medeiros and Kjerfve (1993) during the dry period.

For the wet period, we used a reference river discharge of 75 m^3/s. This value is higher than our estimates above, but we have it to compensate limited period of simulations (2 months) and to emphasize the wet period conditions. The flow for each stream Itapessoca/Carrapicho/Arataca/Botafogo/Igarassu was scaled by the proportion of the drainage area as 0.08:0.08:0.32:0.32:0.20, respectively, and using constant flow.

Each simulation lasted 60 days and we used the last 15 days for calibration and validation when the simulations were synoptic to the observations. The model was defined to compute on timesteps of 10 s. The calibration was carried out by comparing the modeled and observed currents from the east channel mooring ADCP. Table 2 summarizes the keywords of TELEMAC's input file that resulted in stable runs and best agreement between observations and model. For the Bottom friction coefficient, the used approach was from Nikuradse scheme (Nikuradse, 1950). To solve the vertical and horizontal turbulence we chose a mixing length model based on Nezu and Nakagawa approach (Nezu, Nakagawa e Jirka, 1994).

Table 2. Keywords values used for calibrating the setup configuration case file of TELEMAC 3D numerical simulations.

Keyword	Value	Meaning
Bottom friction coefficient	0,02 and 0,05	Nikuradse Law
Scheme for advection	5	Locally semi-implicit predictor-corrector scheme (MURD scheme)
Horizontal turbulence model	4	Smagorinsky
Vertical turbulence model	Mixing length	Nezu and Nakagawa
Wind Forcing	No used	No
Air Pressure	No used	No

Source: The author (2021).

Water level and along estuary velocity validation were achieved by comparing the East Channel mooring ADCP derived data (O_i) and the same variable from the modeling results $(P)_i$ (Figure 4 a and b). Table 3 shows the statistics indexes and errors. Root Mean Squared Error $(RMSE = \sqrt{\frac{\sum_{i=1}^{N}|O_i - P_i|^2}{N}})$ varied from 0.20 and 0.21.

The NMRSE which stands for Normalized–RMSE (i.e. RMSE divided by the range of the observed data) was 17,2 and 8,5%. The correlation coefficient (r^2) was 0.89 for both velocity/water level comparisons. Further, a skill score ($d = 1 - \frac{\sum_{i=1}^{n}[(P_i - \bar{O}) - (O_i - \bar{O})]^2}{\sum_{i=1}^{n}[(P_i - \bar{O}) - (O_i - \bar{O})]^2}$) (Willmott, Robeson e Matsuura, 2012) of 0.93 and 0.97 was computed. The errors are low enough and the skill is near to 1, which means a satisfactory agreement according toWillmott et al. (2012).

Figure 3.4. Validation for the east channel mooring. (a)observed and simulated water level; (b) observed and simulated depth averaged longitudinal velocity; (c) measured profiles of longitudinal velocity and d) simulated profiles of longitudinal velocity.

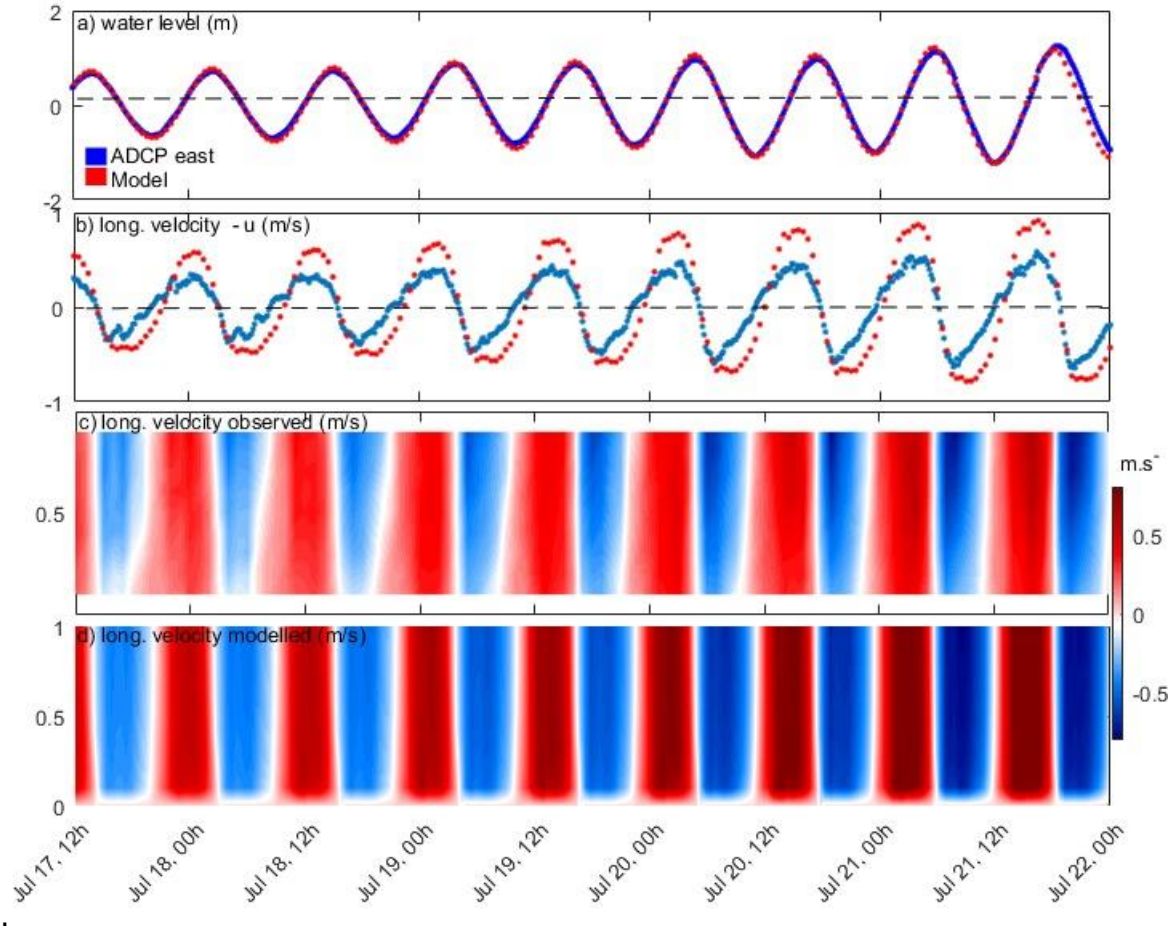

Source: The author (2021).

Table 3.Model verification statistics, Root Mean Squared Error (RMSE) and Normalized RMSE comparing the observed data against the modelled one.

EC (Catuama)	Long.Velocity	Water Level
RMSE	0.20	0.21
N-RMSE	17.2%	8.5%
r^2	0.89	0.89
Index of Agreement	0.93	0.97

Source: The author (2021).

RESULTS

The possibilities of assessment from model results are wide. However, the reach and robustness of these results rely on the model skill to reproduce observations. We are aware that our observations are very limited to a few days and at some points. However, the model was able to reproduce reasonably well the water levels and currents. The currents responded very well for phase but less than desired for amplitude. Our approach doesn't allow a precise evaluation of the salinity field, but qualitatively the model generated a partially mixed pattern during the wet period, which indeed was observed however with different gradients and amplitude due to errors associated with the freshwater input estimation or differences in the intertidal geometry.

This said we cannot lay eyes on details but extract main patterns on the system hydrodynamics. In this section, we will explore (i) the tidal regime in the system, (ii) the synodical variability of the vertical structure of currents in the thalweg of the inlets, (iii) the cross-sectional variability of the residual currents at the inlets for 15 days, and (iv) the residual flow exchanges between the inlets and around the islands. Despite this session is called 'Results', there are insertions of specific methods used in each sub-section, for sake of organization and clearness.

Tidal Circulation

Tidal dynamics in the IIES were assessed based on the variation of the amplitude of the main lunar semi-diurnal tidal constituent M_2 and its main over tide M_4, and the amplitude of tidal currents. The ratio M_4/M_2 is an indicator of the non-linearities caused by the frictional effect during the tidal propagation up-estuary

(Speer et al., 1991). We selected 49 locations along the channels (Figure 5a) to extract water level and currents. The water level was analyzed by harmonic tidal analysis using the Python package T_tide, a transcription of the original code in Matlab by Pawlowicz et al. (2002). T_tide for Python is available at https://github.com/moflaher/ttide_py/. With the tidal amplitude, we calculated the tidal excursion D by

$$D = \frac{U_0 T}{\pi}$$

where *T* is the dominant tidal period in seconds and U_0current amplitude (e.g. Parsa and Shahidi, 2010). This equation is computed by integrating over a half-tidal cycle. The tidal excursion provides an estimate of the water parcel displacement from a given point.

To present the results of this analysis we considered the origin of the system as being the Catuama inlet, with the distances negative towards the Orange inlet, and positive towards the east and west Itapessoca channels. The tidal current is stronger near the inlets and its amplitude decreases up-estuary. From Orange inlet, it decreases gradually towards the Catuama inlet, and there is a steep increase at -2 km, in the intersection between the Santa Cruz and west channel. From this point, the current amplitude decreases gradually to the head of the west channel. Similar behavior occurs at the east channel.

The current pattern is not related to the spatial variability of the M_2. There is a mild amplification of the M_2 from the inlets upward, reaching the maximum values at the mid reach of the Santa Cruz channel (~ -8 km) and the head of the west channel. The M_4/M_2 ration displayed an inverse pattern of the M_2, indicating that the amplification of the M_2 is not followed by the frictional non-linearities, transferring energy to over tides.

The tidal excursion is a linear transformation of the current amplitude however furnishes the spatial scale of water parcel displacement. At the mouths, the values are >20 km, which is about twice the system length (inlet to head or mid-reach of Santa Cruz Channel). The values decrease, and between -4 and -8 km from Catuama de tidal excursion is less than 1 km. This indicates that this region is a ‘null zone’ with sluggish tidal currents and higher residence time.

Figure 3.5. At the top (a) is a sketch of the IIES with the location of the sampling points. The lower panels present the spatial variation of the (b) current amplitude, (c) M_2 amplitude, (d) M_4/M_2 ratio, and (d) the tidal excursion. The distances are referenced to the Catuama inlet.

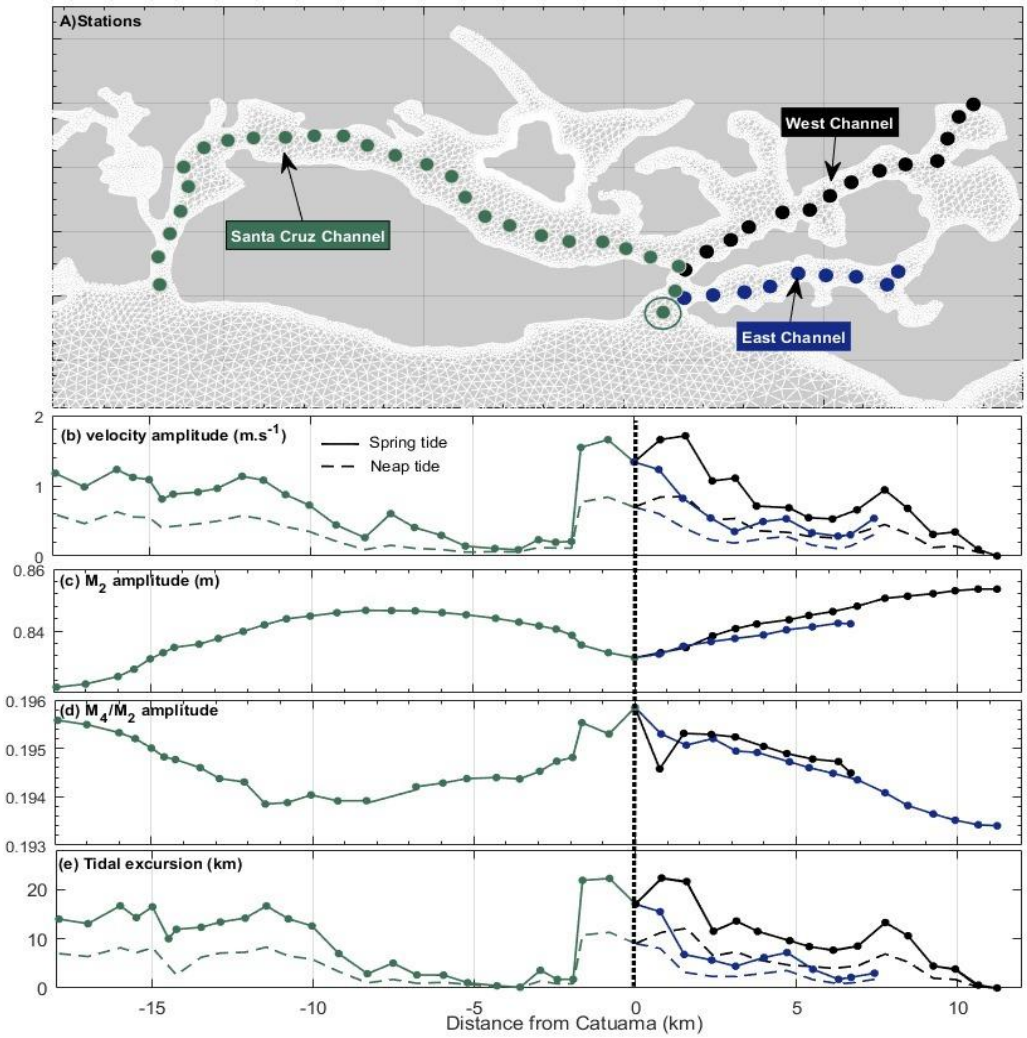

Source: The author (2021).

Vertical Structure of Residual Currents

The vertical structure of residual currents has been assessed at three locations that represent the system connections to the sea: at the Orange inlet (#South), and the two sections formed by the bifurcation of the Catuama inlet. The one that connects to Santa Cruz and West channels, #West, and the one that opens northwards, #North. The time series were filtered using a Butterworth filter with a cut-off period of 40 hours.

Vertical residual structure of velocity in South station for both wet and dry periods along with modeled salinity and water level is shown in Figure 6. Under wet conditions, the estuary displayed a vertically uniform landward residual flow, reaching

0.025 m.s^{-1}. On the contrary, under wet conditions, the vertical distribution of the residual circulation turns into an inverse estuarine circulation, with outflow in the lower part of the profile against a residual inflow on the upper portion.

Figure 3.6. Model results at orange inlet (#South), with (a) tidal signal, residual currents at (b) dry and (c) wet period and (d) salinity at the wet period.

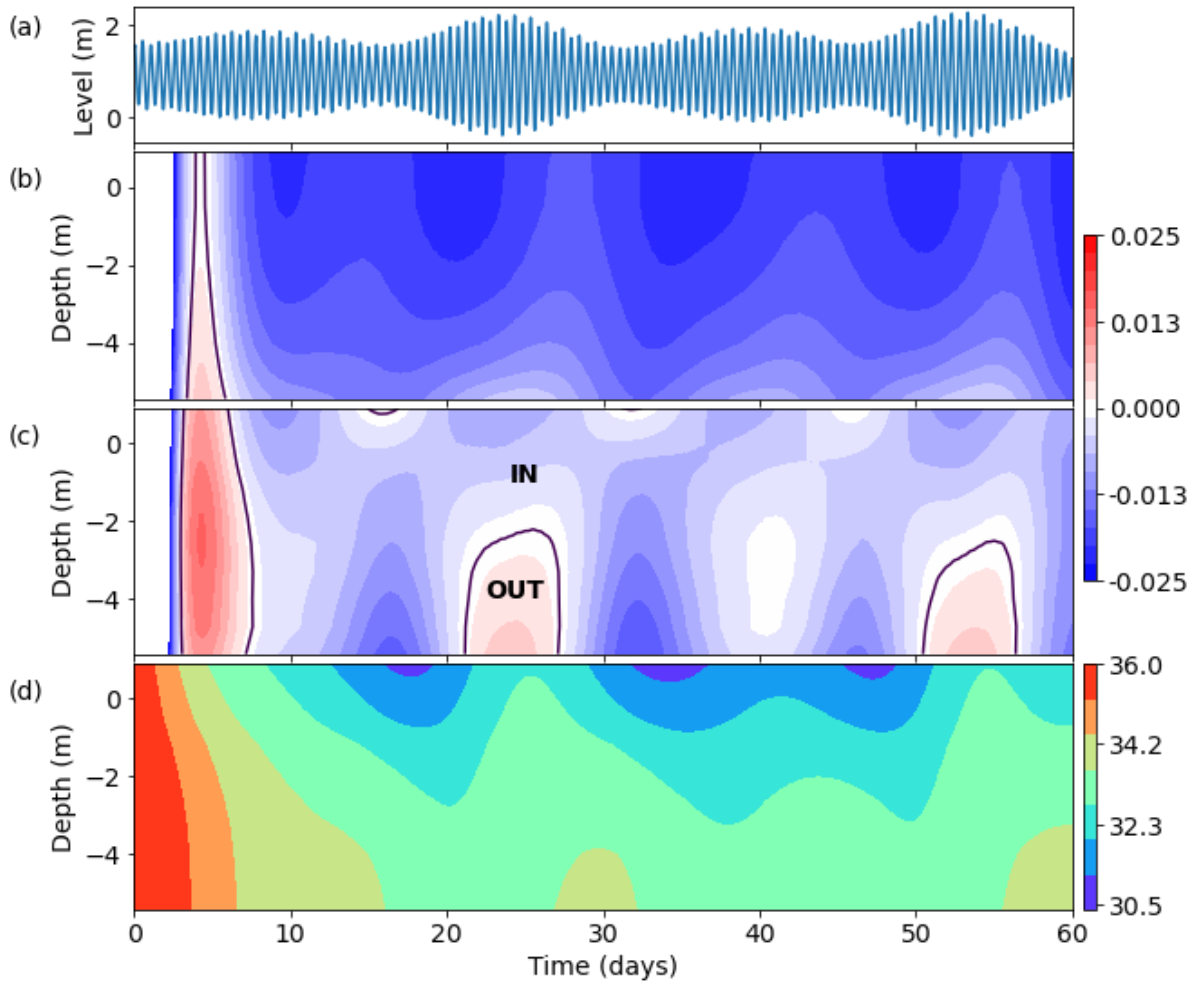

Source: The author (2021)

Similarly, the vertical residual structure for the West Channel of Catuama Inlet displayed a vertically bidirectional pattern (Figure 7), following the inverse of the classical estuarine circulation with maximum values varying from 0.1 to - 0.1 m.s^{-1}. This configuration is magnified under spring tidal conditions but reduces in the wet season if compared to the dry season.

Figure 3.7. Model results at Catuama inlet (West channel), with (a) tidal signal, residual currents at (b) dry and (c) wet period, and (d) salinity at the wet period. .

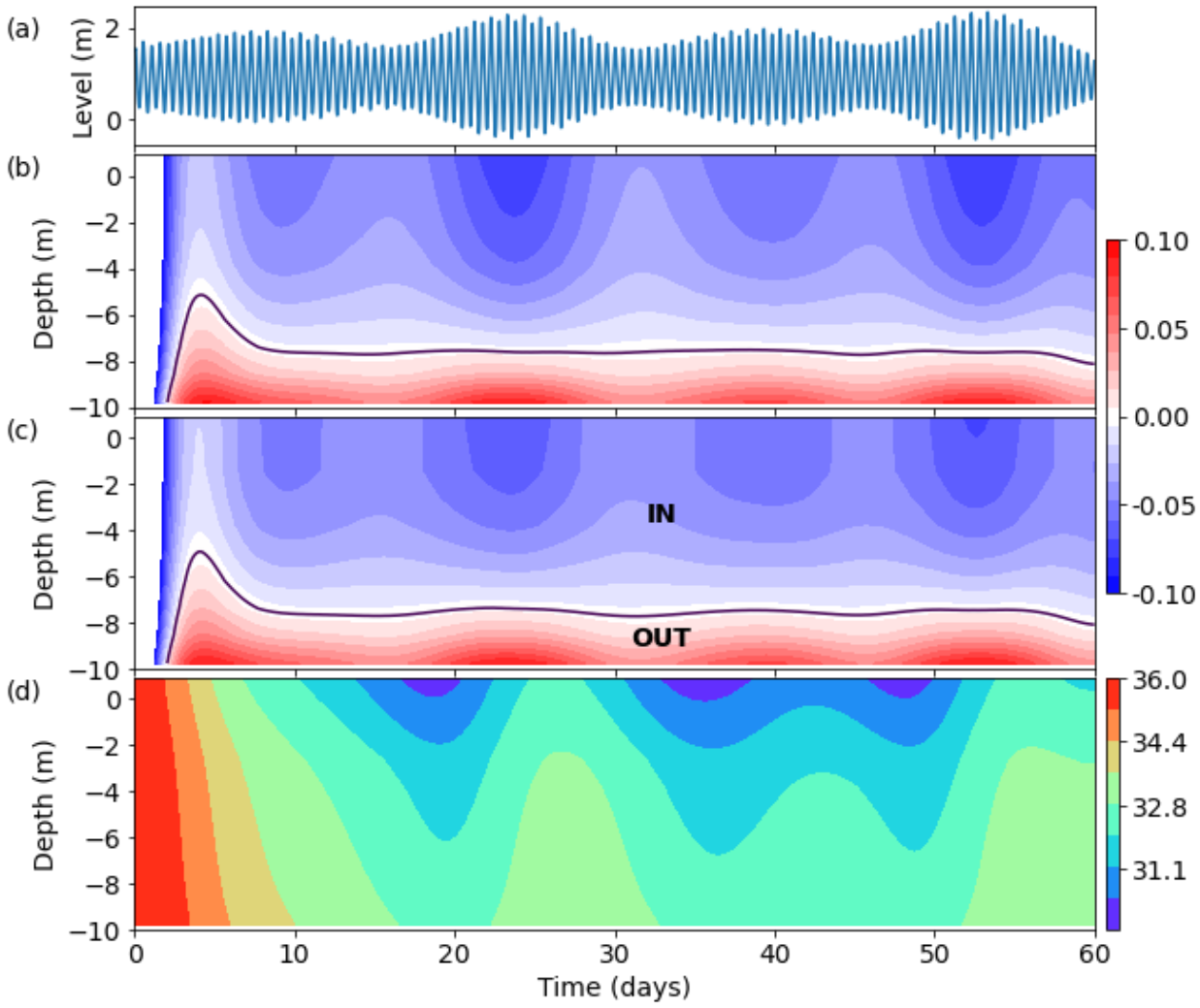

Source: The author (2021).

In contrast to the other two stations, the #North inlet displayed a classical estuarine circulation pattern with landward inflow occurring on the lower part (0.05 $m.s^{-1}$) whilst a net outflow occurred on the upper section (-0.05 $m.s^{-1}$)

Figure 3.8. Model results at Catuama inlet (East Channel), with (a) tidal signal, residual currents at (b) dry and (c) wet period and (d) salinity at the wet period.

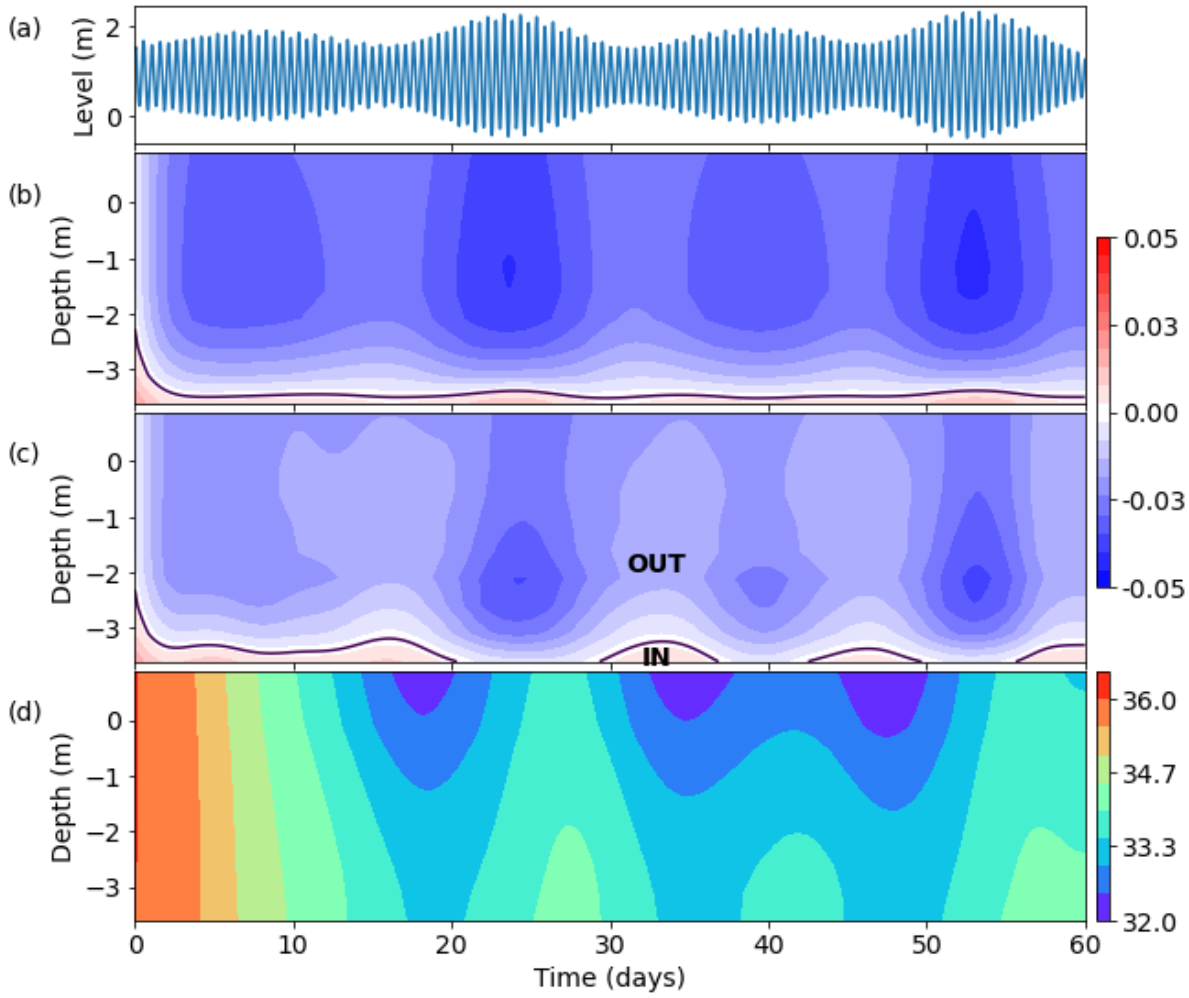

Source: The author (2021).

Cross-sectional Residual Flow and Flow Rates

To spatially assess the residual flow and volume balance we selected six cross-sections across the domain that encloses segments of the systems. The instantaneous water discharge was extracted using the provided Python 3 library (Audouin *et al.*, 2019), and the tidal signal was removed using Butterworth filter with a cut-off period of 40 hours.

Figure 3.9. Time series of the sub-tidal flow of Orange and Catuama inlets. During the neap tide periods the water budget in the inlets is tidal-balanced however during the spring tides occurs a net flow from Orange to Catuama. This net flow is magnified during the spring tide with a higher tidal range.

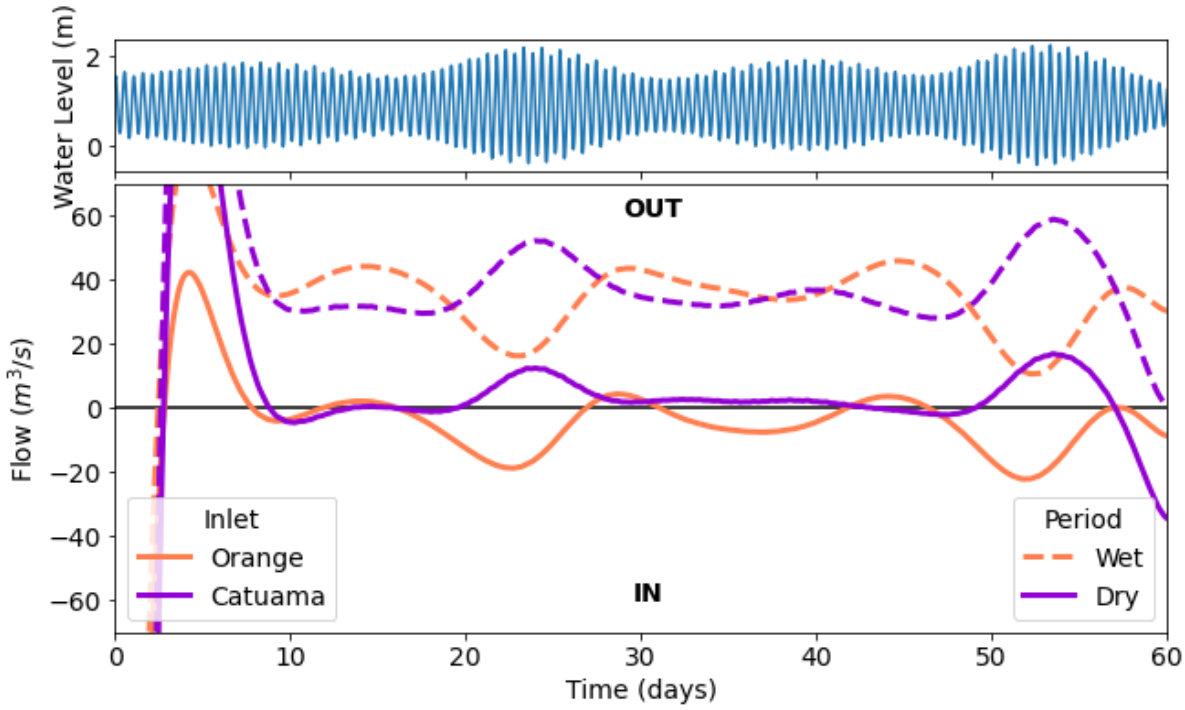

Source: The author (2021).

The cross-sectional residual flow variability on a fortnightly basis, under wet and dry conditions, is presented in Figure 10. We selected the three main entrances of the channels to depict the residual flow aspects. The Orange (south) cross-section displayed a main net inflow in the center and outflow on the flanks with maximum values reaching 0.3 $m.s^{-}$ in the shoals and 0.1 $m.s^{-}$ in the channels in dry conditions. The same pattern of a laterally sheared flow is observed for west and east cross-sections during the dry season.

Figure 3.10. Cross-sectional residual flow distributions in three selected locations at the entrances of the main channels (Orange, West, and East). The lower panels represent 15 days' averaged salinity. The sections are referenced looking landward and positive values depict inflow for west and east cross sections. The signal is inverted on orange cross section due to its orientation shore-parallel. Negative values depict inflow therefore in Orange and outflow in West and East channels.

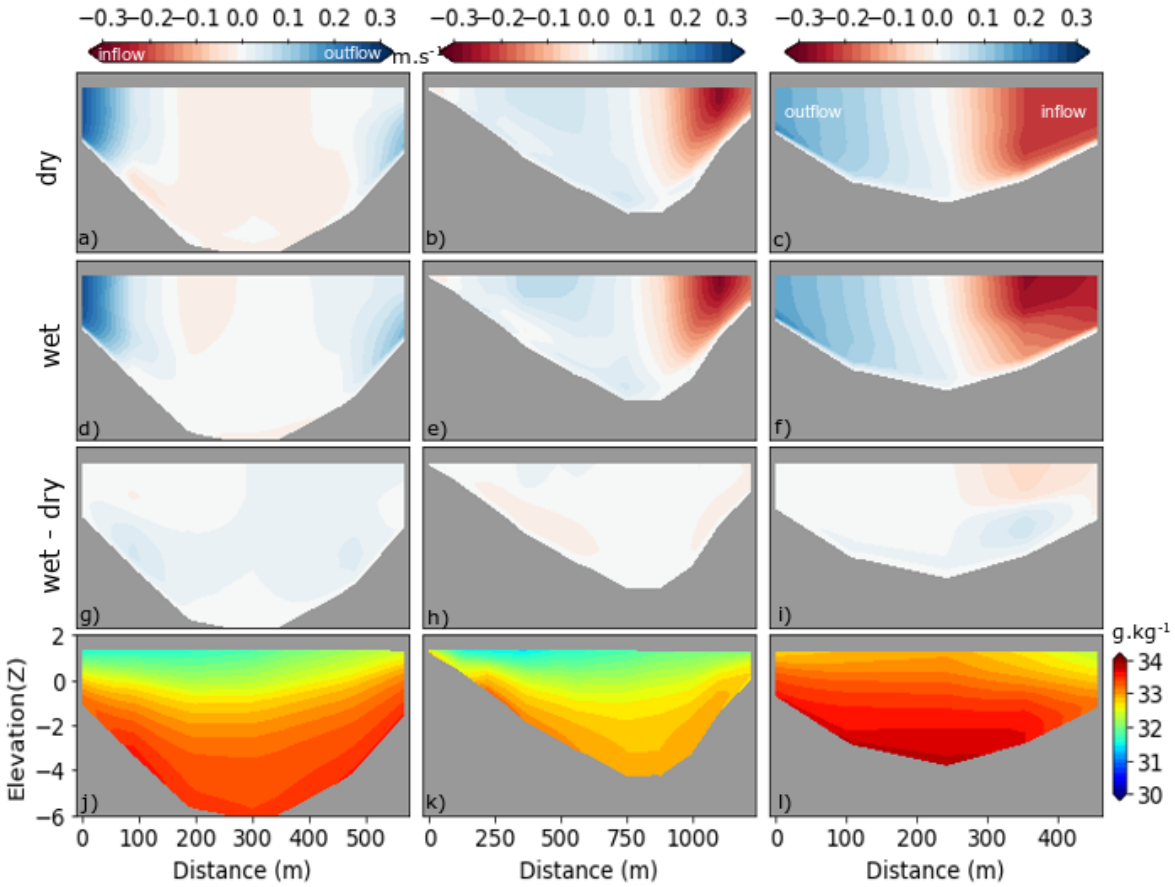

Source: The author (2021).

In wet conditions, the residual outflow becomes stronger in the flanks but reduces in the main channel for the three cross-sections. There is no vertical change in the structure of circulation from dry to wet conditions. The 15 days averaged salinity field followed the flow with minimum salinities ocurring in the upper part (30 $g.kg^{-1}$) along with residual outflow and maximum values of 35 $g.kg^{-1}$ occurring in the lower part following the residual inflow.

Regarding the volumetric flow rate, the detailed values for each cross-section are showed in table 4. It is possible to notice in dry conditions, a subtidal flow rate of

10.3 $m^3.s$ seawards in Catuama Inlet. In opposite direction, orange inlet cross-section presented -.6 $m^3.s^-$

Table 4. Fortnightly averaged flow rate for the chosen cross-sections. Positive values depict seaward flow while negative depicts landward volume transport in the main inlets of the system, Orange (South) and Catuama (West and East). For Sta Cruz cross- section, West and East Channel cross-sections, positive values depict northward flow while negative values display southwards, seaward flow.

	Dry conditions($m^3.s^{-1}$)					
	Orange	Sta Cruz	West Channel	East Channel	Intersection*	Catuama
Fortnightly	-6,6	4,9	39,1	-40,6	-39,2	10,3
Spring	-23,5	18,4	-30,8	-76,7	-53,5	174,7
Neap	3,7	3,2	32,3	-32,3	-31,9	3,2
	Wet conditions ($m^3.s^{-1}$)					
	Orange	Sta Cruz	West Channel	East Channel	Intersection*	Catuama
Fortnightly	30,4	-17,7	24,5	-41	-40,3	55,3
Spring	45,2	-29,9	-70,5	-63,3	246	34,1
Neap	7,3	0,1	128,2	-31,7	-51,9	-137

Source: The author (2021).

DISCUSSION

The main goals of this study are to assess tidal propagation and to investigate the seasonal influence on the variability of the residual circulation and volume exchange. The hydrodynamics of the IIES proved to be well represented by the 3D numerical model. We discuss in this section the main drivers of residual flow structure in the system and the water balances in the system.

The IIES is a tropical, faulted estuary that receives low freshwater input under mesotidal conditions. The tide enters at both Orange (South) and Catuama (North) inlets and attenuates upwards estuary due to frictional effects and shallow depths (Waterhouse, Valle-Levinson e Winant, 2011). The three main channels of the system (Santa Cruz, West, and East channels) are ~5 m depth with the deepest part of the system just in front of the Catuama inlet (-18 m deep). This null zone coincides with the shallowest depths of the system where the lowest values of current amplitude and tidal excursion match the two largest mud deposits of the system. The

presence of a nodal point approximately -7 km from Catuama Inlet was predicted by (Medeiros and Kjerfve, 2005). The model results suggest a similar feature for Santa Cruz Channel but points out another null tidal point in the northern part of Itapessoca Island (West Channel). The tidal dynamics in the IIES are determined by a balance between friction and pressure gradient (Geyer e MacCready, 2014; Waterhouse, Valle-Levinson e Winant, 2011). The tidal amplitudes and velocities attenuate to zero when a characteristic length in the along-estuary direction, separating the two inlets, is large such that the tidal energy will be dissipated, so that there will be no flushing around the middle region of the waterway (Smith e Pierce, 1983). For IIES, the tide propagates in three different waterways and maximum attenuates upwards however the presence of a second inlet with greater depth inhibits the propagation between the south and north part of the system. Such conditions can change during the wet season not only by tidal nonlinearities but also due to baroclinic effects on the residual circulation since IIES can turn into inverse estuarine circulation conditions (Largier, 2010; Medeiros e Kjerfve, 2005)

The tidal or densimetric Froude number $\boldsymbol{Fr_o}$(Valle-Levinson e Schettini, 2016) scales the ratio between the tidal advective accelerations (scaled by the amplitude of tidal currents $\boldsymbol{U_0^2}$) and baroclinic pressure gradient which is scaled based on reduced gravity and mean depth ($\boldsymbol{g'H}$)**,** where$\boldsymbol{g' = g.\frac{\Delta\rho}{\rho_0}}and\boldsymbol{\Delta\rho = \frac{\partial\rho}{\partial z}}$**.,**g is gravity (9.8 $m.s^{-1}$) and ρ_0 is a reference density (1025 $kg.m^{-3}$ for instance). Figure 11, lower panel, displays the neap-spring variability of $\boldsymbol{Fr_o}$ derived from observations on the east channel mooring.

Figure 3.11. log10 of Tidal Froude number variation for East Channel mooring (lower panel). The upper panel shows the temporal variability of tidal amplitude (U) along with the reduced gravity distribution.

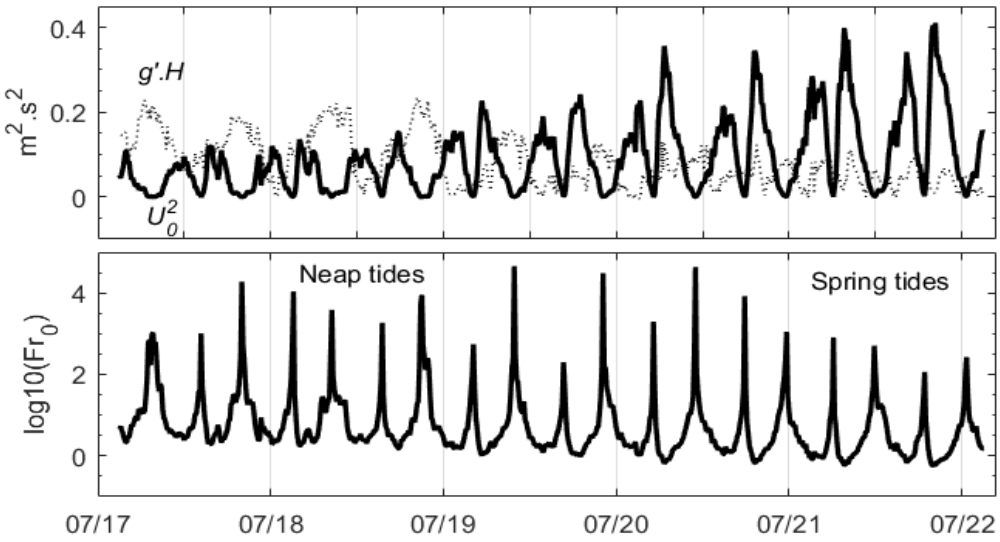

Source: The author (2021).

Considering a mean channel depth of ~5 m and vertical salinity gradient ($\Delta\boldsymbol{\rho}$), the values of $\boldsymbol{Fr_o}$ remain lower than 1 in most of the synodical cycle however it exceeds the threshold at the end of every ebbtide $\boldsymbol{Fr_o} > 1$ due to the weakening in tidal amplitude. Similar results were found by Ross et al.(2017) and Valle-Levinson and Schettini (2016) in other systems, indicating that tidal nonlinearities rule the residual circulation over density gradients. For IIES, however this condition can change under strong wet season episodic events of rainfall as reported by Schettini et al. (2017a) or under strong dry conditions when the evaporation rates can exceed precipitation as found by (Juarez, Valle-Levinson e Li, 2020; Valle-Levinson e Schettini, 2016).

Regarding volume balance in the system, the exchange between the two inlets and the ocean follows an inverse pattern under dry conditions. In general, the water enters through the south inlet and flows northwards until reaches Catuama, North Inlet, where it will exit the system. From Catuama inlet northwards, there is a clockwise volume transport around Itapessoca Island coming from the West channel (Figure 12). This pattern is intensified during spring tide conditions, becoming weaker until invert direction under neap tide conditions, although this sub-tidal flowrate is less

than 3 $m^3.s^-$. On the other hand, during wet conditions, occurs the expected seaward volume transport in both inlets under influence of larger river discharge.

Figure 3.12. Drawn scheme of the volume transport patterns around IIES in wet conditions. The red arrows represent volume transport coming from the southern inlet, while blue arrows stand for volume transport around Itapessoca Island, coming from the west channel.

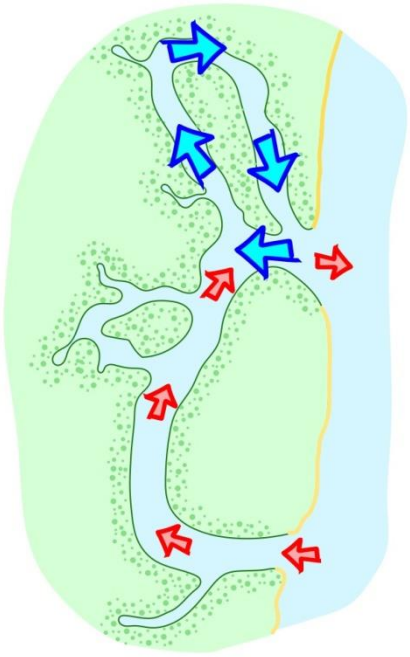

Source: The author (2021).

The coastal water near IIES mangroves are very shallow and friction effects dominate the tidal dynamics in these waters. This prevents the formation of ebb-tidal jets at the mouth (Victor *et al.*, 2004; Wolanski *et al.*, 1992). Instead, the ebb tide flow is fan-like (Wolanski e Ridd, 1990). This implies that, in the absence of longshore currents, the return coefficient (i.e., the fraction of the water that leaves the estuary at ebb tide that returns at the following flood tide) is large. If the coastline is mangrove-fringed, all creeks along a length of a coastline are linked. It may well be that the water leaving one creek at ebb tide subsequently re-enters another creek at flood tide. Water becomes coastally trapped and mixes only slowly with offshore water (Elliott *et al.*, 2019; Wolanski *et al.*, 1992; Wolanski, Nhan e Spagnol, 1998). This conceptual model seems to be represented by IIES once it may be acting as a deposit from the neighborhood shelf waters.

CONCLUSIONS

Residual circulation, tidal propagation, and volume balances of the system were assessed in the IIES estuary. Results from 3D numerical model agreed with observations and were used to depict the physical response of the system to wet and dry conditions. The tide propagates into the three main channels and attenuates landwards due to the presence of mangrove, mud deposits with an opposite amplification of M_2. We conclude that the presence of two inlets in the system change inhibits tidal propagation and create null zones. The tidal Froude number was computed to explain the main driver of residual flow and showed that tidal forcing is dominant in the system most of the time but can switch to density gradient forcing in dry conditions. Despite the volume exportation pattern in the wet season, the water tends to enter in orange inlet and exit in the Catuama inlet, but curiously part of the volume is transported clockwise around the Itapessoca Island.

ACKNOWLEDGMENTS

The authors would like to thank the Brazilian Project Funding Agency (FINEP), and Brazilian National Council of Research (CNPq) National Institute of Science and Technology AmbTropic for financial support under Rehmansa project. Also, we thank to Ernesto Domingues, Bárbara Paiva, Felipe Facó, Paulo Sigauque and Samuel Valentim for the help on the field surveys. We appreciate also the help of all EPOC (Université de Bordeaux) people and CAPES (Coordination for higher Education Staff Development) PDSE funding.

3.3 ARTIGO 3 – TROCAS ESTUÁRIO-PLATAFORMA EM UM SISTEMA DE RIA COM GEOMETRIA COMPLEXA

Oliveira Filho, J.C.; Schettini, C.A.F.; Sottolichio, A.

RESUMO

O presente trabalho investiga as trocas de material particulado em suspensão entre um sistema de estuários com geometria complexa e a plataforma. Foram utilizados resultados derivados de um modelo numérico 3D hidrodinâmico de alta resolução como input de um modelo lagrangeano. Neste sentido, foram encontradas a origem a o destino de traçadores passivos suspensos em superfície e fundo com origem em nove pontos no domínio, 5 dentro do sistema e 4 fora representando as fontes alóctones. Os resultados mostraram que existe uma combinação de forçantes e condições que favorecem o acúmulo de partículas dentro do sistema. Uma estimativa de densidade por Kernel e a distribuição temporal do acumulado de partículas dentro dos polígonos de controle mostraram que o sistema está sendo preenchido por sedimentos oriundos da plataforma.

ABSTRACT

The present study aims to assess estuarine-shelf exchange processes between an estuarine system and its adjacent shelf. Derived 3D numerical model data were used as input for a lagrangian particle trajectory modelling. Thus, origin and fate of SPM (suspended particulate matter) in bottom and surface layers in 9 different origins:5 located inside the estuarine system and another 4 originating in the shelf and inside an adjacent estuary to represent allochthonous sediment sources. Results showed that a combination of drivings and conditions makes the estuary prone to be filled by sediment from outside. The KDE density estimation and the temporal distribution of cumulative particle number inside of the control polygons showed the estuary has been being filled by sediments from the shelf.

INTRODUÇÂO

Os ambientes estuarinos são definidos como corpos de águas semifechados onde á água do mar é mensuravelmente diluída pela água fluvial proveniente da drenagem continental, possui pelo menos uma conexão com o oceano e tem seu limite definido pela máxima propagação da maré (Perillo, 1995). Os estuários são a principal rota do sedimento em suspensão do continente para o oceano. Rio abaixo, o sedimento suspenso (aqui referido como MPS) é distribuído em constantes ciclos de deposição, ressuspensão e transporte na sua forma suspensa (Dyer, 1995; Prandle, 2009). Parte do material mais grosseiro fica retido nas planícies costeiras, sendo liberado apenas quando ocorre preamar de sizígia. A variação da morfologia estuarina depende diretamente do volume de sedimento que aporta para preencher os canais, além da fração do sedimento que é trazido do oceano adjacente. Onde a descarga é baixa, os estuários não estão sendo preenchidos (Wolanski, Nhan e Spagnol, 1998).

Plataformas continentais passivas que são forçadas por correntes de contorno oeste estão entre as regiões oceânicas menos produtivas dentre as margens continentais, a não ser que ocorra grande aporte de material particulado em suspensão (MPS) pelos rios, ou zonas de ressurgência. (Chen *et al.*, 2004; Hsu, Chen e Ogston, 2013; Walsh, 1995). A plataforma continental Nordeste (NE) do Brasil é um bom exemplo deste tipo de margem passiva. A plataforma é estreita e relativamente rasa, além de estar no caminho da oligotrófica Corrente Sul Equatorial (CSE), e receber baixo aporte fluvial e sedimentar das dezenas dos estuários locais (Knoppers, Ekau e Figueiredo, 1999; Schettini, Carvalho, *et al.*, 2017).

Os estuários apresentam uma grande variabilidade na sua geomorfologia e nas suas forçantes físicas (Perillo, 1995). O modelo conceitual mais citado na literatura idealiza os estuários por uma circulação estuarina clássica, onde a água fluvial, menos densa, escoa na camada superficial em direção ao oceano, enquanto a água marinha, mais densa, entra no ambiente estuarino pela camada inferior, em direção ao continente, por uma conexão com o mar (Geyer e MacCready, 2014; MacCready e Geyer, 2010). No entanto, o que se observa é uma grande variabilidade de estuários quanto a sua morfologia, circulação e transporte de material entre o estuário e a plataforma. Por exemplo, para sistemas com duas ou mais conexões com o mar, a solução do modelo conceitual não é direta e se torna

complexa, pois o ambiente apresenta mais de uma saída para o material (Schettini *et al.*, 2021; Waterhouse, Valle-Levinson e Winant, 2011)..

Os estuários da costa NE do Brasil são caracterizados por serem dominados por marés, enquanto o volume de água fluvial que chega é baixo e varia sazonalmente com o regime chuvoso (Juarez, Valle-Levinson e Li, 2020; Largier, 2010). Na costa de Pernambuco, especificamente, é possível notar a presença de dezenas de estuários pequenos, preenchidos por lama e manguezal. Em especial, o Sistema Estuarino de Itamaracá e Itapessoca (SEII) é um protótipo ideal de estuário pequeno, dominado por maré e que está sendo preenchido por sedimento, além de possuir duas conexões com o oceano (Medeiros e Kjerfve, 1993; Oliveira-Filho e Schettini, 2015; Schettini *et al.*, 2021).

O SEII está localizado na costa NE do Brasil e apresenta geometria complexa com a presença de vários canais e pequenos rios. As suas duas conexões, Orange, mais ao sul, e Catuama que limita o sistema ao norte, são interligadas pelo Canal de Santa Cruz, circundando a Ilha de Itamaracá. Mais ao norte, o sistema apresenta a ilha de Itapessoca e dois canais principais, que recebem o aporte dos rios Itapessoca, Catuama e Carrapicho. O SEII apresenta características de um vale de rio inundado durante o aumento do nível do mar no Holoceno o qual não foi preenchido devido à baixa produção sedimentar do local. Juntos, em média, todos os rios do sistema fornecem uma média de 66 $m^3.s^{-1}$. A baixa produção fluvio-sedimentar do local, no entanto, não condiz com a presença de grandes depósitos de sedimentos finos dentro do sistema, pois, uma vez que não existe aporte fluvial ou este é baixo, a tendência seria um sistema com necessidade de aporte sedimentar fluvial.

Assim, uma explicação para a origem desses depósitos de sedimento dentro do SEII seria uma fonte alóctone oriunda da plataforma continental ou estuários adjacentes. Uma fonte provável deste material seria a erosão da formação barreiras que está presente na porção continental do Nordeste Brasileiro, assim como proposto por (Knoppers, Ekau e Figueiredo, 1999). Deste modo, o presente artigo tem como objetivo principal identificar as trocas entre o estuário e a plataforma utilizando modelagem numérica especificamente, tem-se como objetivos a caracterização geral da circulação local por uma perspectiva lagrangeana, identificação da origem e destino dos traçadores passivos (aqui considerados como MPS) e tendências de acúmulo dentro de zonas específicas dentro do estuário.

ÁREA DE ESTUDO

O SEII está localizado 40 km ao norte da cidade de Recife, capital de Pernambuco, Brasil (Figura 1). O sistema está inserido no contexto da formação Barreiras e apresenta geomorfologia complexa com uma pequena planície de maré circundada por ravinas. A área dos canais é, aproximadamente, 30 km^2 com área intermareal coberta por manguezal de 47 km^2. A profundidade média dos canais é 3 m e o ponto mais profundo, na barra de Catuama, apresenta 18 m de profundidade.

O clima local da região Nordeste do Brasil é semiárido (Kopen's Aw, Savannah tropical), no entanto, na zona costeira ocorre um cinturão (Zona da Mata) onde o clima é classificado como tropical-úmido (Koppens Am, tropical monsoon). A plataforma continental adjacente é estreita (40 km) e apresenta predominância de material sedimentar bioclástico com pouca matéria orgânica.

Não existe monitoramento da descarga fluvial dos rios no SEII, no entanto, os dados de (Francisco *et al.*, 2017) para a cidade de Caaporã (distante 20 km ao norte do SEII) foram usados como referência para base climatológica do rio Tracunhaém. Este rio faz fronteira com a borda oeste da bacia de drenagem do SEII e reflete o mesmo comportamento dos rios locais do ambiente. Deste modo, foi estimado um valor médio de 20 $m^3.s^{-1}$ para o máximo da quadra chuvosa e um mínimo de 2 $m^3.s^{-1}$ durante o período de estiagem (Schettini *et al.*, 2021).

Figura 4.1. Área de estudo em um contexto da America do Sul. São mostradas as posições dos fundeios para aquisição dos dados, bem como os polígonos de controle para análise o acúmulo de partículas.

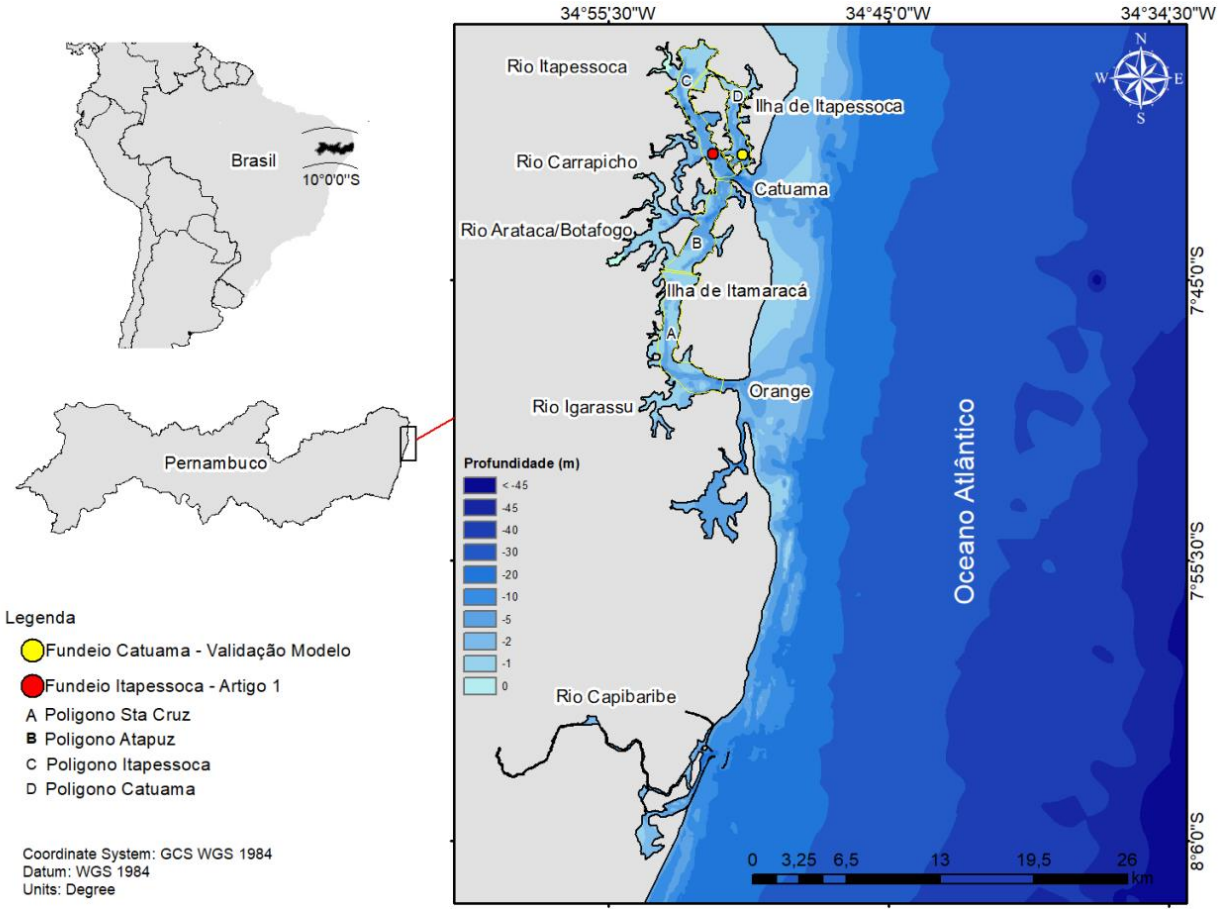

Fonte: o autor (2021).

MATERIAL E MÉTODOS

Dados Observacionais e validação do modelo numérico hydrodinâmico 3D

Os dados coletados para a validação do modelo numérico foram obtidos em uma campanha oceanográfica que se estendeu de 15 a 31 de julho de 2013, durante a estação chuvosa. Dois Perfiladores Acústicos de Corrente por efeito Doppler (PACDs) foram fundeados nos dois principais talvegues dos canais de Itapessoca e Catuama (Oeste e Leste, respectivamente, em relação à ilha de Itapessoca). Os dados do PACD do canal de Itapessoca sofreram influência das fortes correntes e o equipamento tombou, comprometendo a coleta de dados. No entanto, o PACD do canal leste, Catuama, registrou cinco dias completos das componentes da

velocidade u, v e w (zonal, meridional e vertical). Estes dados foram usados para validação do modelo numérico Telemac 3D (www.opentelemac.org). Para o detalhamento da calibração e validação, consultar (de Oliveira Filho et al., *in press*)

Modelo Numérico Hidrodinâmico

As trajetórias das partículas foram integradas utilizando os resultados das simulações numéricas do modelo Telemac 3D supracitado. O modelo resolve as equações de *Navier-Stoke/Saint-Venant* nas suas formas hidrostáticas e não hidrostáticas, utilizando o método dos elementos finitos. Para mais detalhes a respeito da suíte Telemac, favor consultar (Hervouet, 2007). O grid triangular para construção da malha amostral do modelo, foi criado no software *BlueKenue* (https://nrc.canada.ca/en/research-development/products-services/software-applications/blue-kenuetm-software-tool-hydraulic-modellers). Foram gerados 27250 nós dos elementos triangulares e estes são verticalmente extrapolados em 10 camadas verticais. O modelo foi forçado nas bordas oceânicas abertas pela solução global de maré derivada do TPXO 09 (https://www.tpxo.net/global) o qual fornece os componentes u e v da velocidade, bem como o nível da maré.

Nas bordas continentais dos rios, o modelo foi forçado por uma descarga fluvial constante que totalizou 66 $m^3.s^{-1}$ durante o período chuvoso para o SEEI e 100 $m^3.s^{-1}$ para a borda continental do rio Capibaribe, obtidos em (Domingues *et al.*, 2017; Schettini, Carvalho, *et al.*, 2017). Além disso, outro cenário foi criado quando o modelo foi forçado por um vento constante de 10 $m.s^{-}$ em direção Norte. Foram simulados quatro cenários que são exemplificados na tabela 1, bem como os valores usados como condição inicial do modelo. Para salinidade e temperatura, os valores iniciais usados foram de 27 °C e 36 $g.kg^{-1}$ constante em todo domínio. O coeficiente de fricção de fundo foi considerado 0.02 $m^2.s$ para a abordagem de *Manning*.

Tabela 1. Cenários simulados e os respectivos valores de condição inicial usados para as simulações hidrodinâmicas.

Cenário	Maré	Vazão Fluvial	Vento
A	sim	não	não
B	sim	Sim	não
C	sim	não	sim
D	sim	sim	sim

Fonte: o autor (2021)

Modelo Lagrangeano

Para a obtenção das simulações da trajetória das partículas, foi adotado o modelo lagrangeano OpenDrift (Dagestad *et al.*, 2018), um *framework* baseado em Python, *open-source*, para modelagem lagrangeana. Este modelo opera em modo *offline,* ou seja, necessita de um input externo de outro modelo hidrodinâmico para poder resolver a trajetória das partículas. O OpenDrift possui vários módulos para simular trajetória de óleo, sedimento, "*search and rescue*", deriva de navio e plâncton. Neste estudo, contudo, foi considerado o módulo mais geral OceanDrift que descarta propriedades específicas das parcelas ou partículas. As trajetórias foram computadas em intervalos de 5 minutos e se estenderam durante um ciclo sinodical, incluindo quadratura e sizígia (15 dias). O OpenDrift fornece várias diferentes configurações que podem ser ajustadas antes de iniciar a simulação. A posição das partículas é atualizada através um esquema de integração de Runge-Kutta de quarta ordem, no entanto o modelo oferece alternativas como Euller e Runge-Kutta de segunda ordem.

As partículas passivas que representam o MPS foram lançadas em superfície e fundo, em nove pontos distintos, inicialmente, e em um raio de 200 metros de dispersão em torno de cada ponto inicial para reduzir tendências na obtenção das trajetórias. Não foram considerados movimentos verticais de partículas. Apesar de reconhecer que existe um movimento vertical de sedimentos em suspensão, os sedimentos em suspensão caracterizados para o rio Capibaribe foram de ordem 25 µm (Schettini *et al.*, 2016) o que justificaria rejeitar uma possível velocidade terminal de partículas. Essas foram lançadas em 9 pontos diferentes dentro sistema, três na plataforma continental (Plat 0, Plat 1 e Plat 2), ao sul do rio Capibaribe, um ponto dentro do estuário do rio Capibaribe (aqui denominada Pina) e mais 5 pontos espalhados de sul para norte no SEII (Itapissuma, Sta Cruz, Atapuz, Itapessoca e Catuama – Figura 2). A estratégia de lançamento ocorreu de forma que uma partícula fosse lançada em cada ponto a cada 30 minutos ou um passo de tempo do modelo, totalizando 6480 partículas no domínio inteiro e 721 partículas lançadas em cada um dos 9 pontos.

Figura 4.2. Estratégia de amostragem para lançamento dos traçadores passivos no sistema. Nove pontos foram selecionados e cores diferentes foram atribuídas a cada um para fins de

monitoramento da origem e destino. Um total de 6480 partículas foi lançado em 15 dias de simulação.

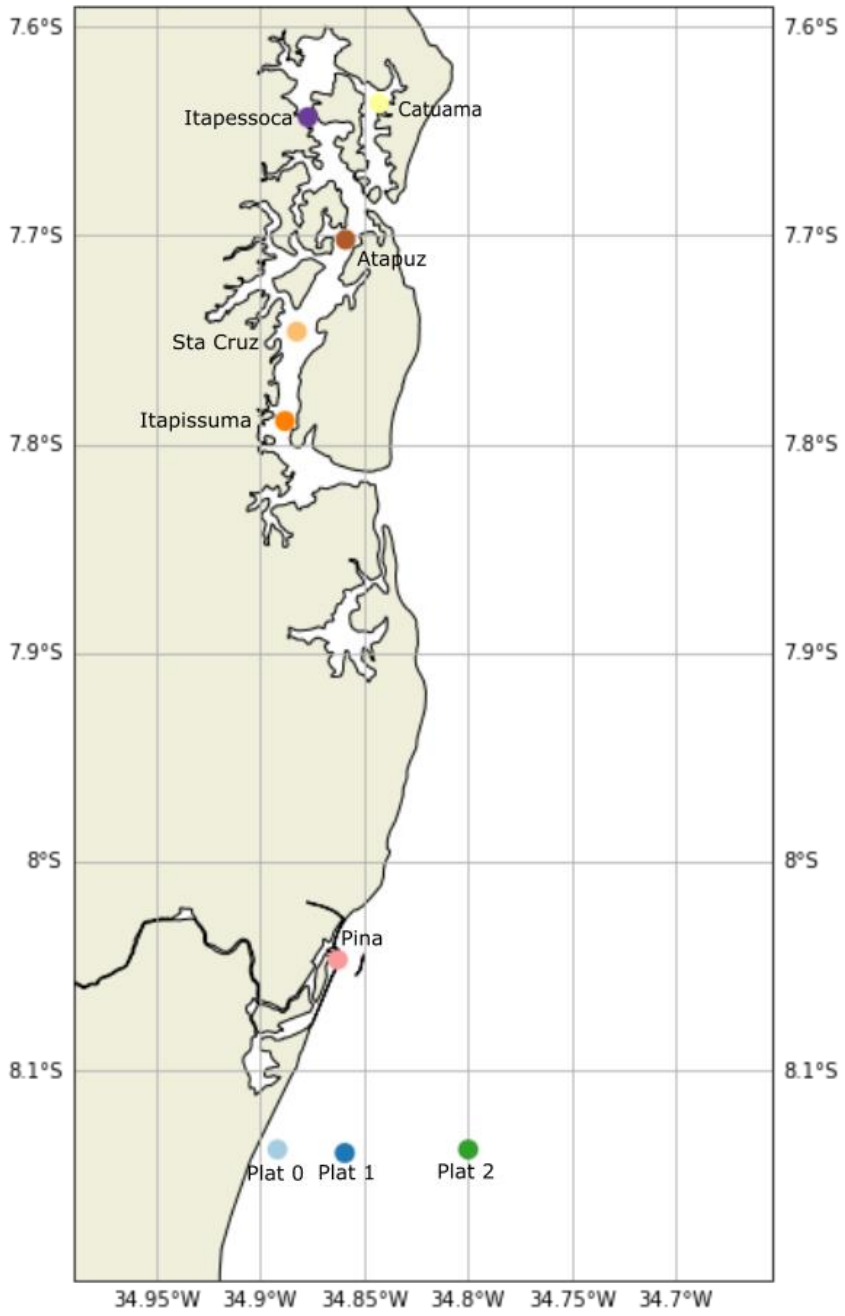

Fonte: o autor (2021).

Por fim, foram selecionados quatro polígonos de controle (exibidos na figura 3) dentro do SEII que representam as regiões com depósitos sedimentares dentro do sistema. A cada timestep, a presença dessas partículas foi testada dentro dos polígonos e acumuladas ao longo do tempo. Em paralelo, foi aplicada uma Estimativa de Densidade por Kernel (KDE) (e.g. Cantrell et al., 2018) para se

encontrar a distribuição das partículas, em relação a sua densidade, dentro do sistema.

Figura 4.3. Polígonos de interesse para análise das tendências de acúmulo dentro do SEII. De Sul para Norte: polígono Sta. Cruz, polígono Atapuz, polígono Itapessoca e polígono Catuama.

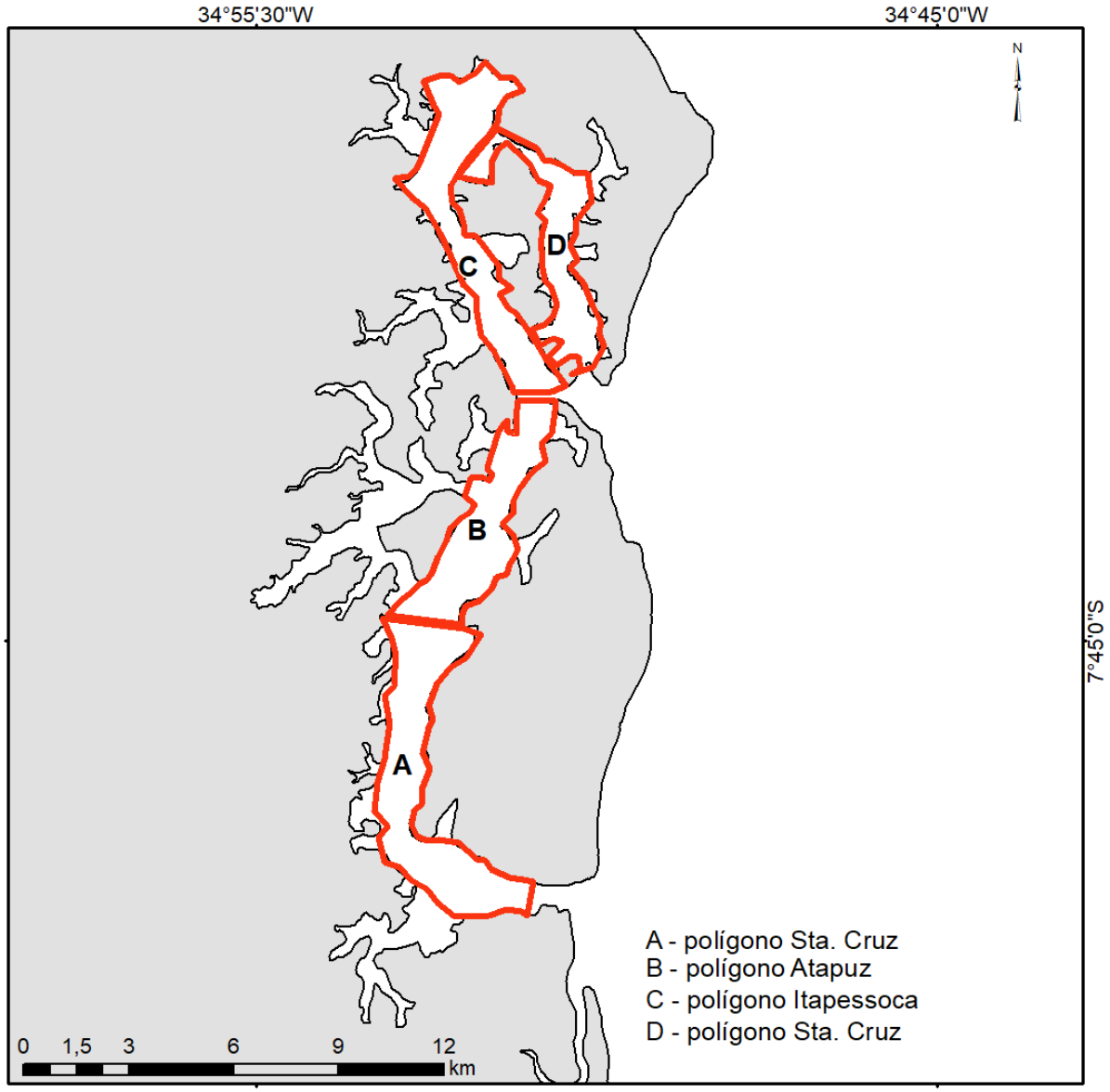

Fonte: o autor (2021).

RESULTADOS

Os resultados obtidos das simulações das trajetórias das partículas foram organizados em quatro partes, baseando-se nas forçantes da simulação os resultados são organizados de acordo com o cenário da simulação: i) maré, ii) maré + vento, iii) maré + fluvial e iv) maré + vento + fluvial. A Figura 4 mostra a posição das partículas após 15 dias de simulação em condições forçadas apenas com maré para superfície e fundo.

Figura 4.4 Posição das partículas após 15 dias de simulação e suas respectivas trajetórias desde o início da simulação. O painel a) representa as partículas em camada superficial e o painel b) representa as partículas próximas ao fundo. Condição utilizando somente maré.

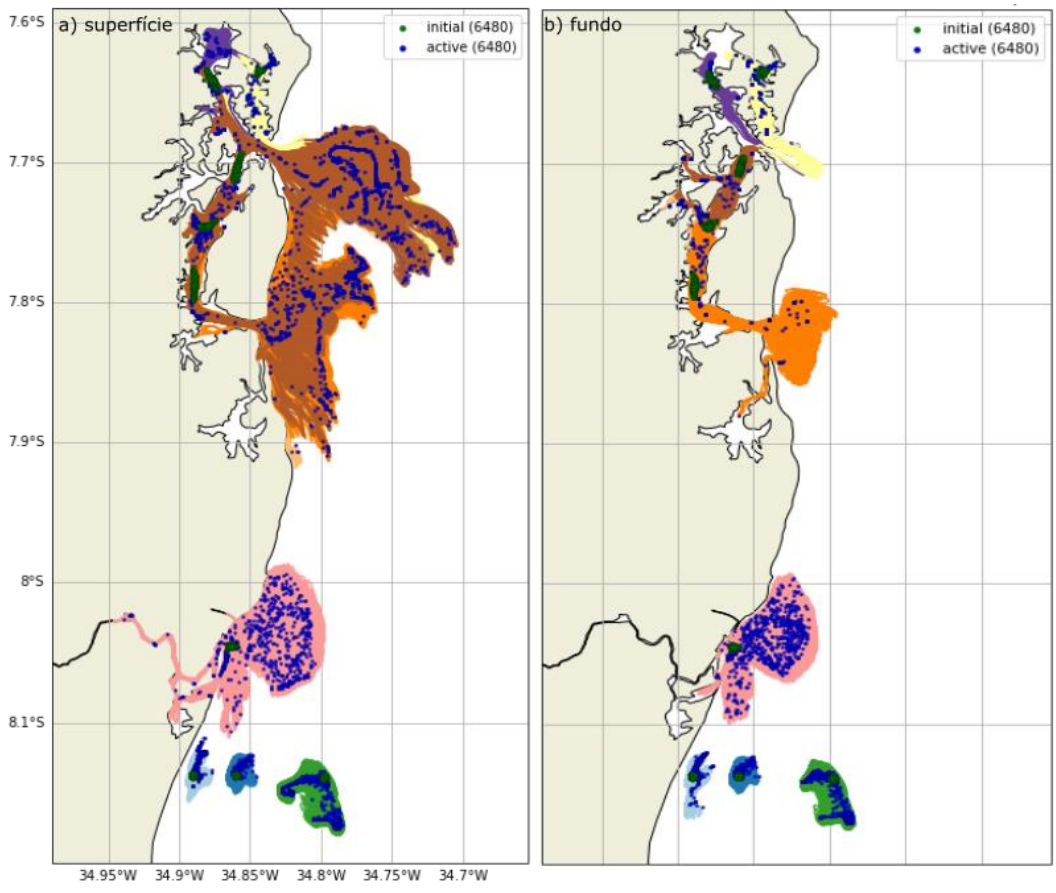

Fonte: o autor (2021)

As partículas lançadas em condições apenas de maré, em superfície, seguiram a dinâmica mareal com pouco deslocamento na plataforma e uma tendência de exportação nas partículas com origem no ponto Pina. É possível notar uma tendência de entrada dos traçadores em superfície para montante do estuário.

Mais ao norte é possível notar que as partículas com origem em Atapuz tendem a percorrer todo o SEII, sendo exportado para fora do estuário por Orange e Catuama.

Da mesma maneira, o experimento realizado considerando maré e descarga fluvial como forçantes, apresentou distribuição de partículas diferente à condição supracitada. A posição final das partículas após 15 dias de simulação é mostrada na figura 5.

Figura 4.5. Posição das partículas após 15 dias de simulação e suas respectivas trajetórias desde o início da simulação. O painel a) representa as partículas em camada superficial e o painel b) representa as partículas próximas ao fundo. Condição utilizando somente maré e descarga fluvial.

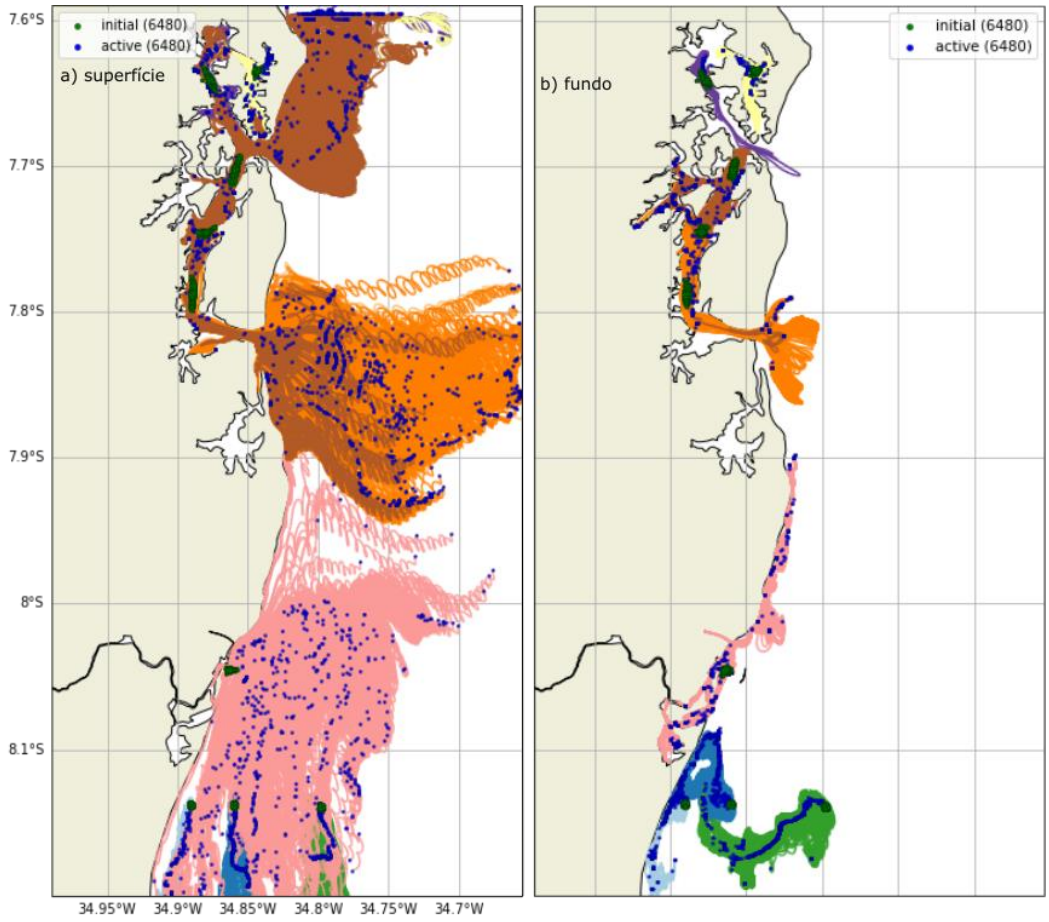

Fonte: o autor (2021).

Em condições com maré e descarga atuando no sistema, as partículas de superfície com origem na plataforma tendem a derivar para o norte. Para as partículas com origem no Pina, a nuvem de dispersão é mais expressiva devido a influência da descarga fluvial. Esta deriva das partículas com origem no Pina

acontece para sul e para norte próximo a linha de costa. No SEEI, as partículas com origem em Atapuz, tendem a se deslocar por todo o sistema e sair pela barra de Catuama em direção ao Norte. De maneira contrária, as partículas que têm origem em Itapissuma e Sta Cruz tendem a deixar o sistema pela barra Orange, mais ao sul, criando uma nuvem de dispersão a frente do estuário. Nas mesmas condições, as partículas próximas ao fundo tendem a permanecer dentro do estuário com exceção das que tem origem no Pina, ou estuário do rio Capibaribe, que tende a se deslocar aproximadamente. Para as ouras origens, a tendência que ocorre é o transporte para montante dos estuários.

As duas situações descritas acima são totalmente modificadas quando é adicionado um vento em direção ao modelo (Figura 6). Primeiramente, em condições forçadas apenas por maré e vento, na superfície, as partículas com origem na plataforma e no Pina se deslocam para o Norte até atingir o SEII. Parte das parcelas com origem no Capibaribe entra no SEII e outra parte deriva em direção ao Norte.

Figura 4.6. Posição das partículas após 15 dias de simulação e suas respectivas trajetórias desde o início da simulação. O painel a) representa as partículas em camada superficial e o painel b) representa as partículas próximas ao fundo. Condição utilizando somente maré e vento Norte de 10 $m.s^{-}$.

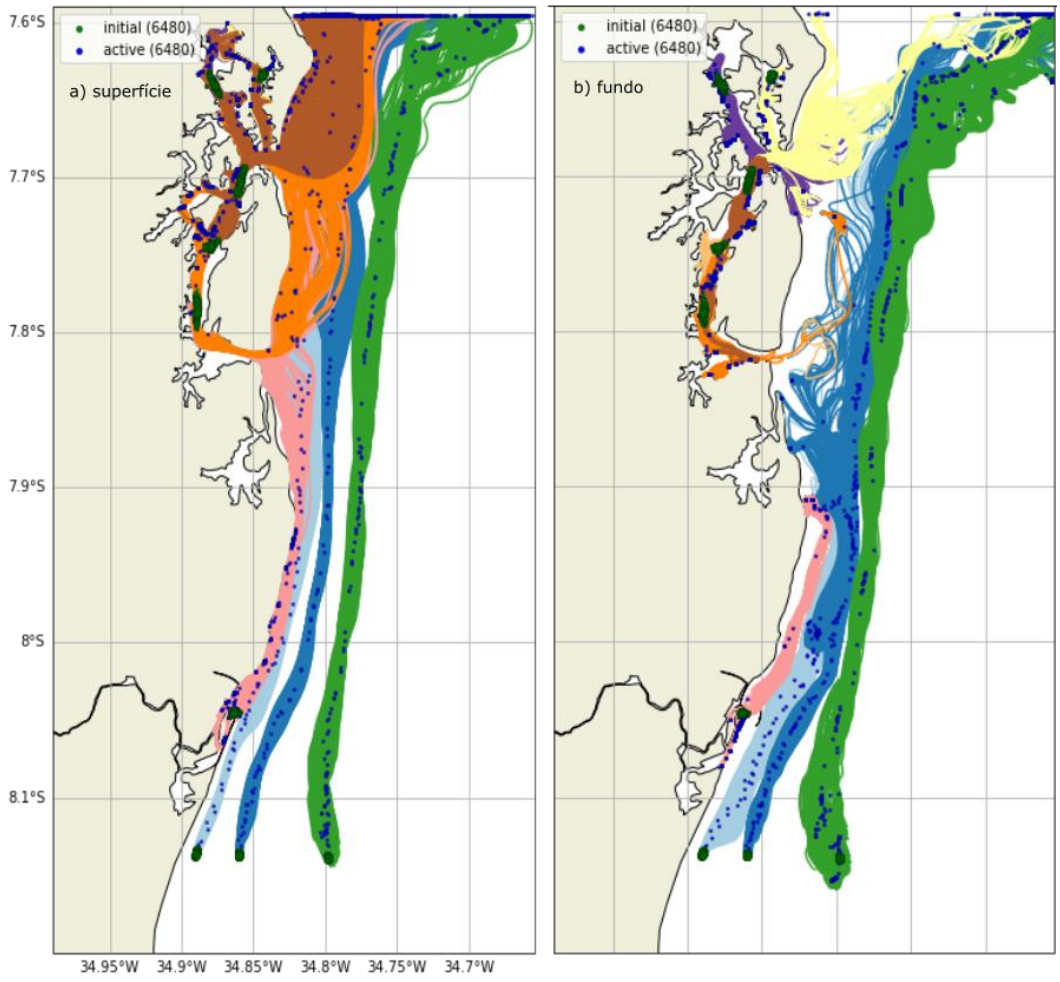

Fonte: o autor (2021).

Próximo ao fundo, as partículas que tem origem na plataforma continental seguem a mesma trajetória das partículas superficiais, no entanto, as partículas com origem no Pina ficam retidas aproximadamente 15 km da origem. As partículas com origem em Itapissuma, Atapuz, Sta Cruz e Itapessoca tendem a ficar próximas as suas origens. No entanto, é possível notar que as partículas que tem origem em Atapuz circundam todo o sistema. Por sua vez, as partículas com origem em Itapessoca tendem a serem exportadas para norte. Nessas condições, é possível notar pela primeira vez a entrada de partículas provenientes do rio Capibaribe e da Plataforma para dentro do SEII.

Da mesma forma, se forem consideradas as forçantes maré, vento e descarga fluvial em conjunto, existe uma tendência de importação de material da plataforma pelo SEII. A figura7 mostra a posição final das partículas dentro do sistema.

Figura 4.7. Posição das partículas após 15 dias de simulação e suas respectivas trajetórias desde o início da simulação. O painel a) representa as partículas em camada superficial e o painel b) representa as partículas próximas ao fundo. Condição utilizando maré, descarga fluvial e vento de 10 $m.s^{-1}$

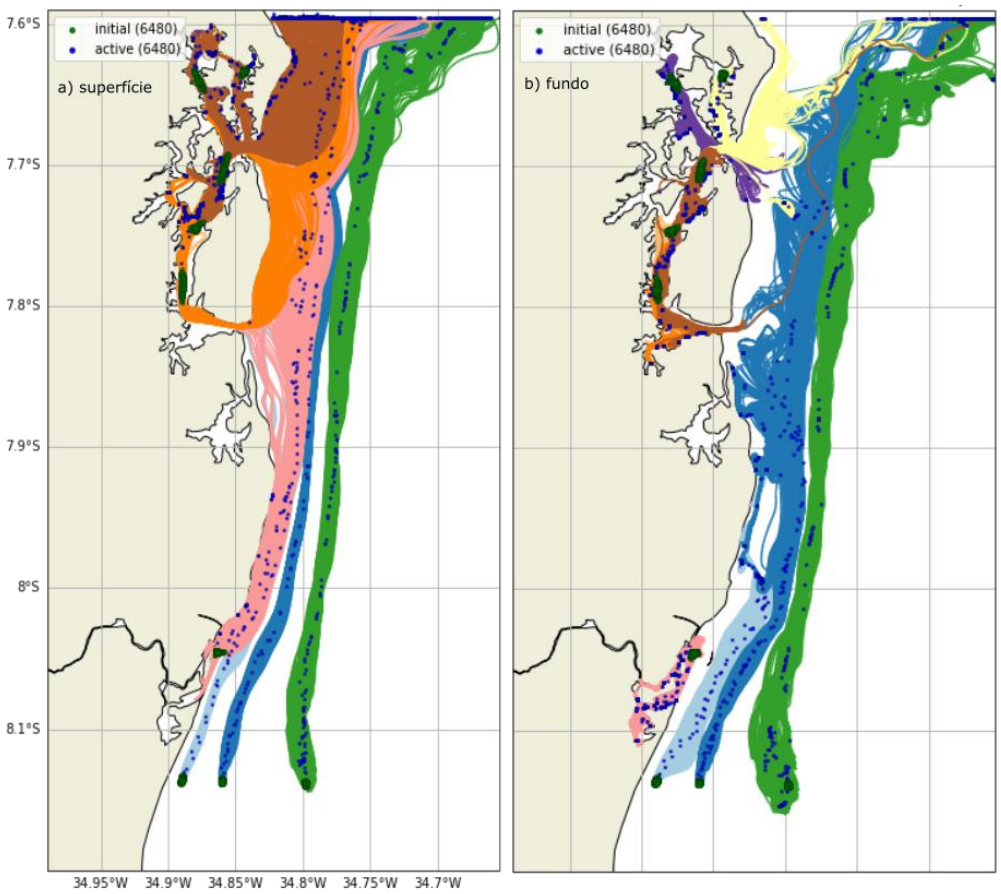

Fonte: o autor (2021).

.

Para ter uma ideia da frequência de entrada e saída das partículas dentro do SEII, os valores das posições das partículas foram filtrados por um passa-baixa por uma abordagem Butterworth com período de corte de 30h. Em seguida, foram acumulados ao longo do tempo a cada passagem por dentro dos polígonos de controle do SEII (Figura 3). O acúmulo temporal de partículas dentro dos polígonos de controle para condições apenas de maré, é mostrado na Figura 8.

Figura 4.8. Evolução temporal da quantidade de partículas dentro dos polígonos de controle em condições forçadas apenas por maré após a aplicação de um filtro passa-baixa com período de corte de 30h. O eixo y representa a quantidade de partículas que está dentro dos polígonos a cada passo de tempo durante uma simulação de 15 dias e é compartilhado para todos os quadros. O eixo x representa os dias do mês de julho, 2013. As linhas contínuas representam as partículas em superfície e as tracejadas representam a quantidade de partículas no fundo.

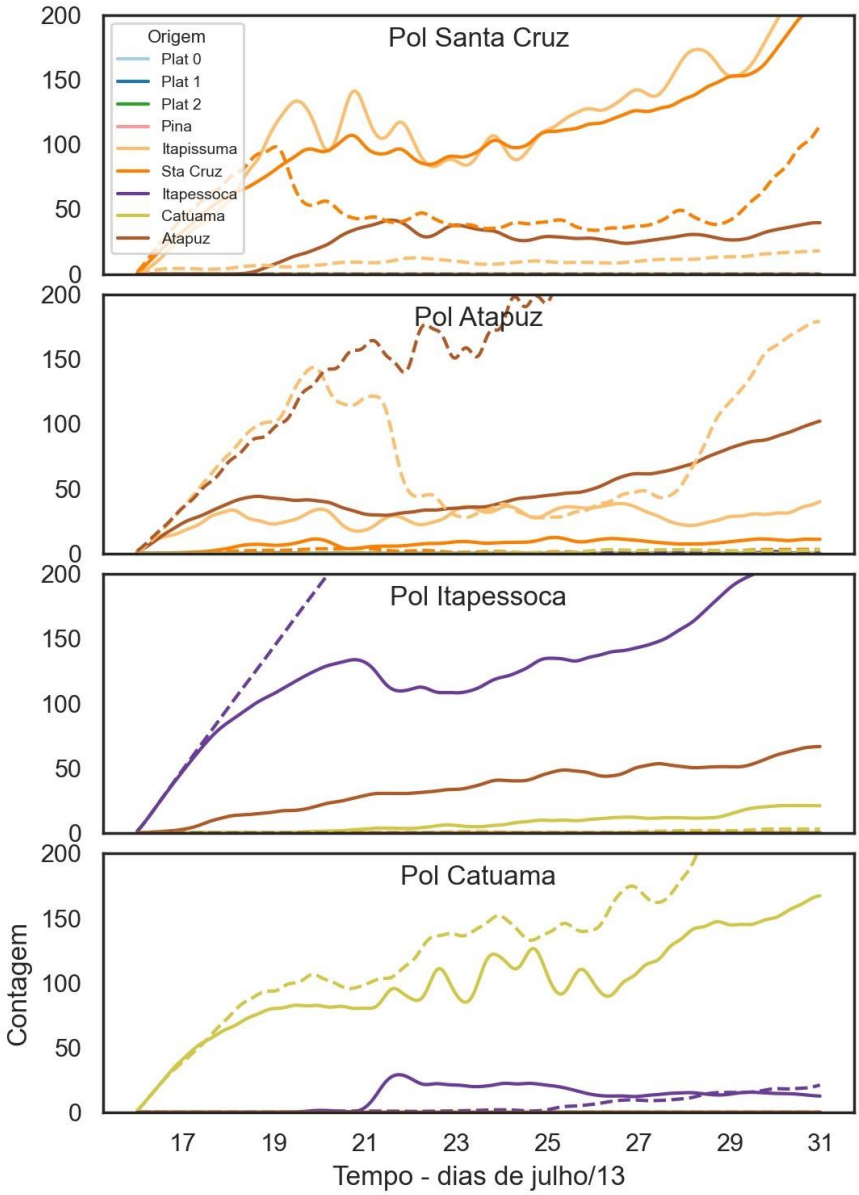

Fonte: o autor (2021).

De maneira geral, cada polígono tende a acumular a quantidade de partículas da origem que está inserida no mesmo. No polígono Sta. Cruz (painel superior), é possível notar a presença de três classes distintas da origem das partículas. As que são originadas em Itapissuma, Atapuz e Sta. Cruz (Figura 2), ou seja, não existe

fonte alóctone para o canal de Sta. Cruz nessas condições em superfície e fundo. Essa situação é semelhante ao polígono de Atapuz (painel “Pol Atapuz”- Figura 7) e apenas três classes de origem das partículas são percebidas dentro do polígono. De maneira diferente, para o polígono de Itapessoca (painel “Pol Itapessoca”) é possível notar a presença de partículas provenientes do canal de Sta. Cruz (origem Atapuz) na superfície, além do acúmulo de partículas originárias de dentro do polígono (origem Itapessoca). Por fim, no polígono de Catuama, à leste da Ilha de Itapessoca, é possível notar a presença de partículas originadas no canal Itapessoca à Oeste da ilha, evidenciando uma circulação em torno da ilha em superfície.

Em condições forçadas pela maré e pela descarga fluvial, é possível notar uma distribuição temporal diferente de partículas em comparação à supracitada. Os dados relativos ao acúmulo temporal dentro do SEII, em condições de maré e descarga fluvial são mostrados na Figura 9. Os polígonos Sta Cruz, Atapuz e Catuama apresentam partículas que são originadas no próprio local, sem influência externa. No entanto, no polígono de Itapessoca (painel “Pol Itapessoca”) é possível nota a presença de partículas originadas em Atapuz, mais ao sul, evidenciando a interconectividade entre as ilhas.

Figura 4.9. Evolução temporal da quantidade de partículas dentro e fora dos polígonos de controle em condições forçadas por maré e descarga fluvial. O eixo y representa a quantidade de partículas que está dentro dos polígonos a cada passo de tempo durante uma simulação de 15 dias e é compartilhado para todos os quadros. O eixo x representa os dias do mês de julho, 2013. As linhas contínuas representam as partículas em superfície e as tracejadas representam a quantidade de partículas no fundo.

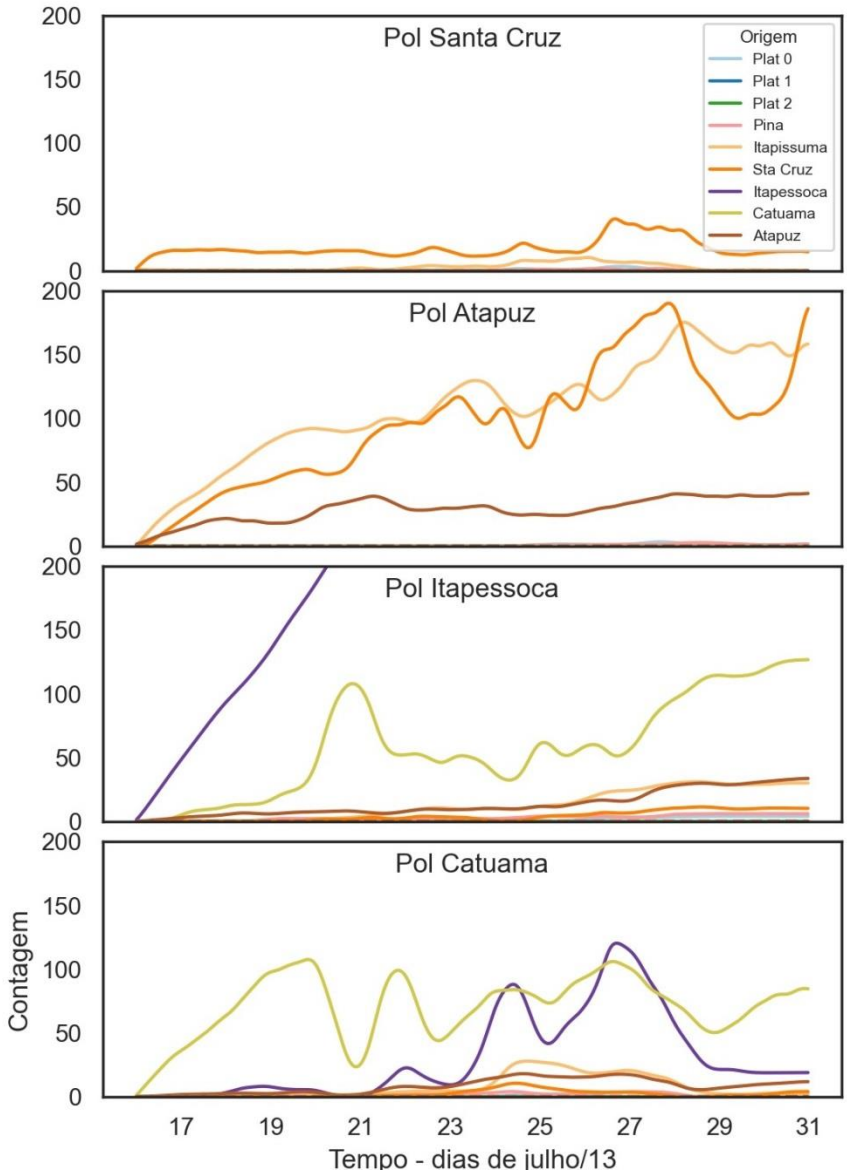

Fonte: o autor (2021).

Ao adicionar vento às condições unicamente com maré, as partículas lançadas na plataforma e mais ao sul do SEII (Plat 0, Plat 1, Plat 2 e Pina) tendem a se deslocar, primariamente, seguindo a influência do vento para Norte. No entanto, devido à circulação residual do SEII, algumas partículas tendem a entrar no sistema, evidenciando a influência externa no ambiente. A Figura 10 mostra a distribuição

temporal do acumulado de partículas em condições com maré e vento norte de 10 $m.s^{-1}$.

Figura 4.10. Evolução temporal da quantidade de partículas dentro dos polígonos de controle em condições forçadas por maré e vento norte de 10 $m.s^{-1}$. O eixo y representa a quantidade de partículas que está dentro dos polígonos a cada passo de tempo durante uma simulação de 15 dias e é compartilhado para todos os quadros. O eixo x representa os dias do mês de julho, 2013. As linhas contínuas representam as partículas em superfície e as tracejadas representam a quantidade de partículas no fundo. O eixo y foi colocado em escala logarítmica para evidenciar a influência externa.

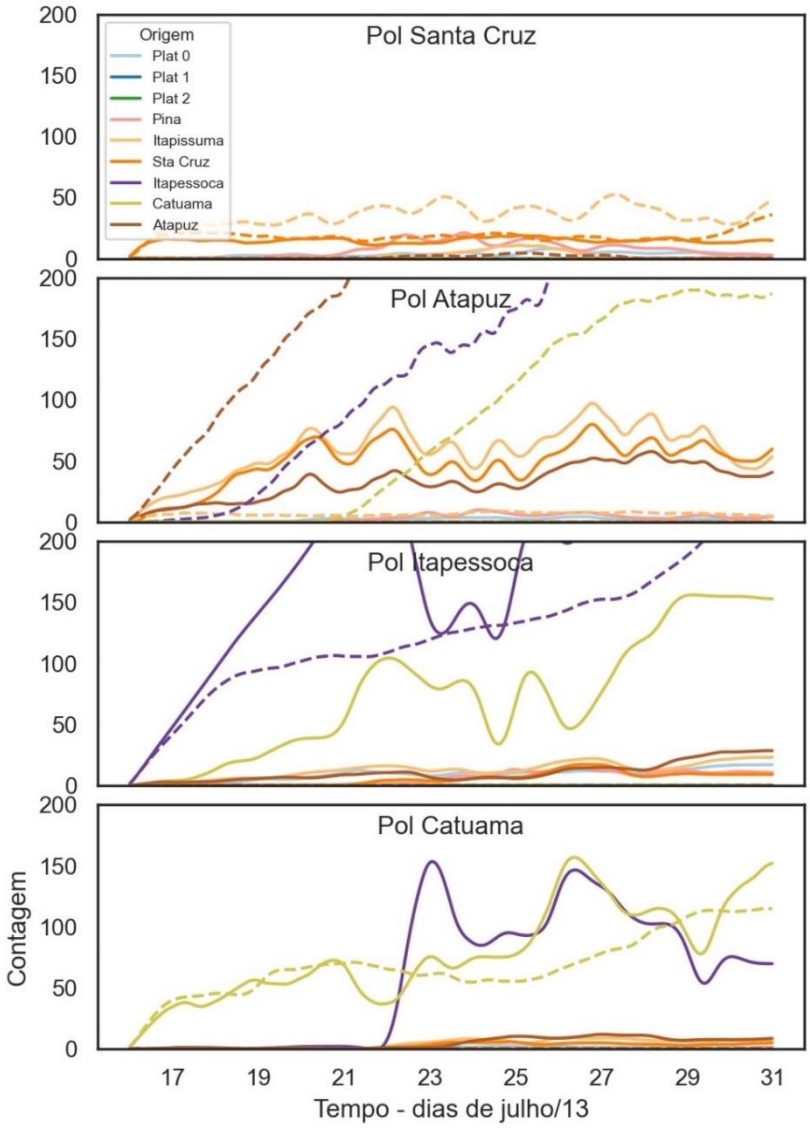

Fonte: o autor (2021).

É possível notar a presença de partículas alóctones em todos os polígonos e locais do estuário, evidenciando a origem externa do material inserido no sistema. Da mesma forma, se a influência da descarga fluvial for adicionada a maré, juntamente ao vento norte de 10 $m.s^{-1}$, também é possível notar influência alóctone no sistema. A distribuição do acumulado para a condição supracitada é mostrada na Figura 11.

Figura 4.11. Evolução temporal da quantidade de partículas dentro e fora dos polígonos de controle em condições forçadas por maré, descarga fluvial e vento norte de 10 $m.s^{-1}$. O eixo y representa a quantidade de partículas que está dentro dos polígonos a cada passo de tempo durante uma simulação de 15 dias e é compartilhado para todos os quadros. O eixo x representa os dias do mês de julho, 2013. As linhas contínuas representam as partículas em superfície e as tracejadas representam a quantidade de partículas no fundo. O eixo y foi definido como logarítmico para melhor exibir a presença de partículas externas aos polígonos.

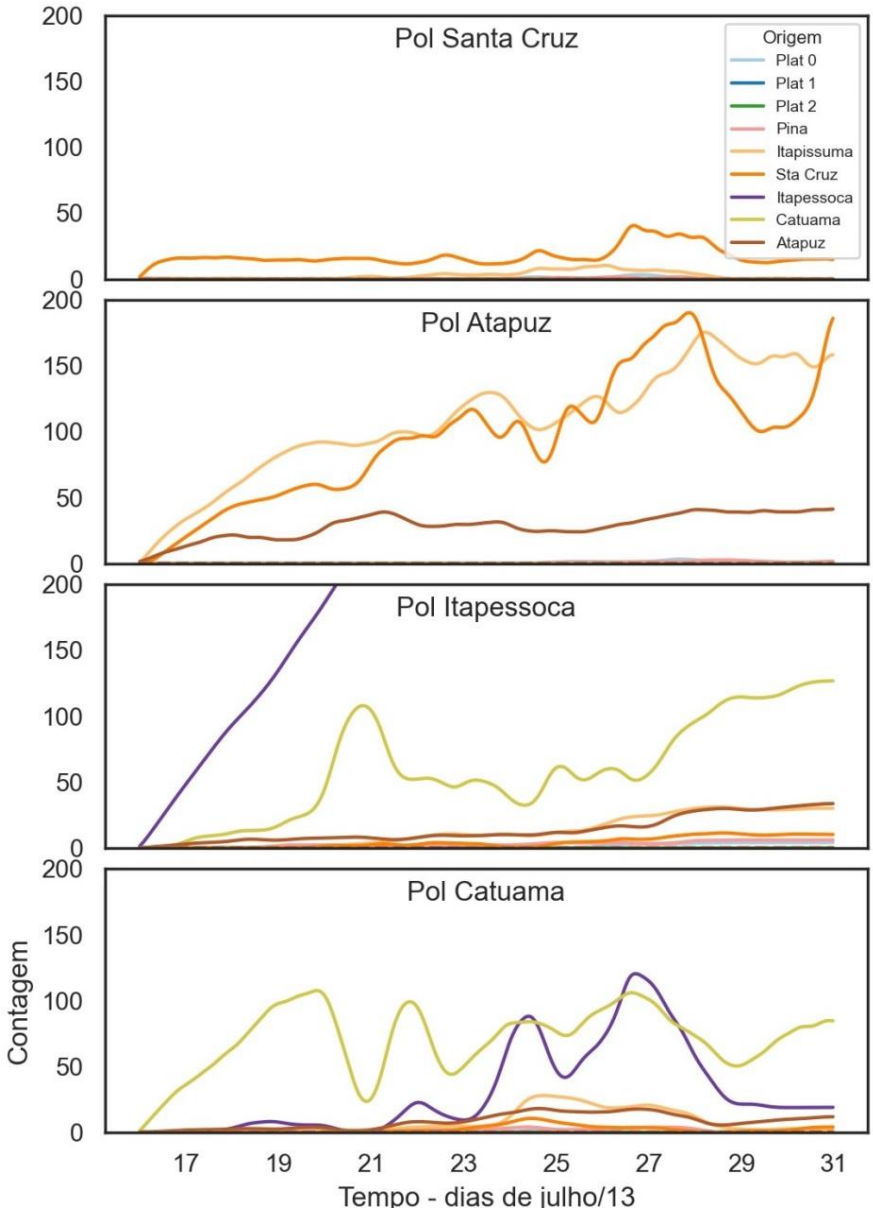

Fonte: o autor (2021).

Em condições com vento, descarga fluvial e maré atuando, é evidenciada e influência externa no ambiente em todos os polígonos de controle. Seguindo a quantidade de partículas com origem na plataforma e na origem “Pina”, é possível observar que os traçadores percorrem um caminho entrando pela entrada sul do sistema, cabo Orange, percorrendo um caminho em direção ao norte. Além disso, é possível notar uma quantidade de partículas pela entrada Norte do sistema, Catuama, que ficam se acumulando no polígono Catuama, leste da Ilha de Itapessoca.

DISCUSSÃO

A presença de grandes depósitos de sedimento no estuário do SEII é paradoxal em relação ao aporte pelos rios. As simulações das trajetórias das partículas mostraram que existem fontes alóctones do MPS para dentro do sistema. Apesar das limitações e parametrizações do modelo numérico hidrodinâmico e das simulações lagrangeanas, foi possível diagnosticar a dinâmica dos derivadores (ou partículas) aplicados para o SEII, em superfície e próximo ao fundo, em uma base sinodical (ciclo de quadratura e sizígia). De acordo com a teoria clássica da dinâmica do MPS nos estuários, a principal fonte de material para dentro destes ambientes são os rios (Dyer, 1995; Prandle, 2009). Mais recentemente, a plataforma continental vem sendo investigada como fonte potencial de volume e MPS para dentro dos estuários, atuando no controle do tempo de residência (Brasseale, Diego e Maccready, 2021; Pawlowicz *et al.*, 2010). Para o SEII, apenas a ação da maré não é suficiente para transportar material da plataforma para dentro do sistema, no entanto, é possível notar que existe uma relação entre o estuário de Itapessoca e o de Santa Cruz. Devido à presença de duas conexões permanentes com o oceano, a propagação da maré no sistema cria zonas nodais onde não ocorre amplitude de correntes e do nível da água, criando zonas nulas. Tal efeito foi reportado inicialmente por (Medeiros e Kjerfve, 1993, 2005) e recentemente confirmado (de Oliveira Filho et al.*no prelo*; Schettini et al., 2021). Isso implica que existem zonas prováveis de acúmulo de material no sistema.

Ao analisar os padrões das trajetórias das partículas, é possível notar que o principal agente de transporte de MPS na zona costeira é o vento, no entanto, a importação para dentro dos estuários ocorre devido à circulação residual estuarina. A descarga fluvial, por sua vez, é responsável por distribuir o MPS na zona costeira superficialmente e manter o processo constante de exportação por um estuário que recebe maior aporte fluvial, e importação por outro que não possui descarga fluvial expressiva. A estimativa de densidade mostrada na Figura 12 mostra a tendência de acúmulo dentro do sistema.

Figura 4. 12. Densidade das partículas no SEII, após 15 dias de simulação, em condições de maré.

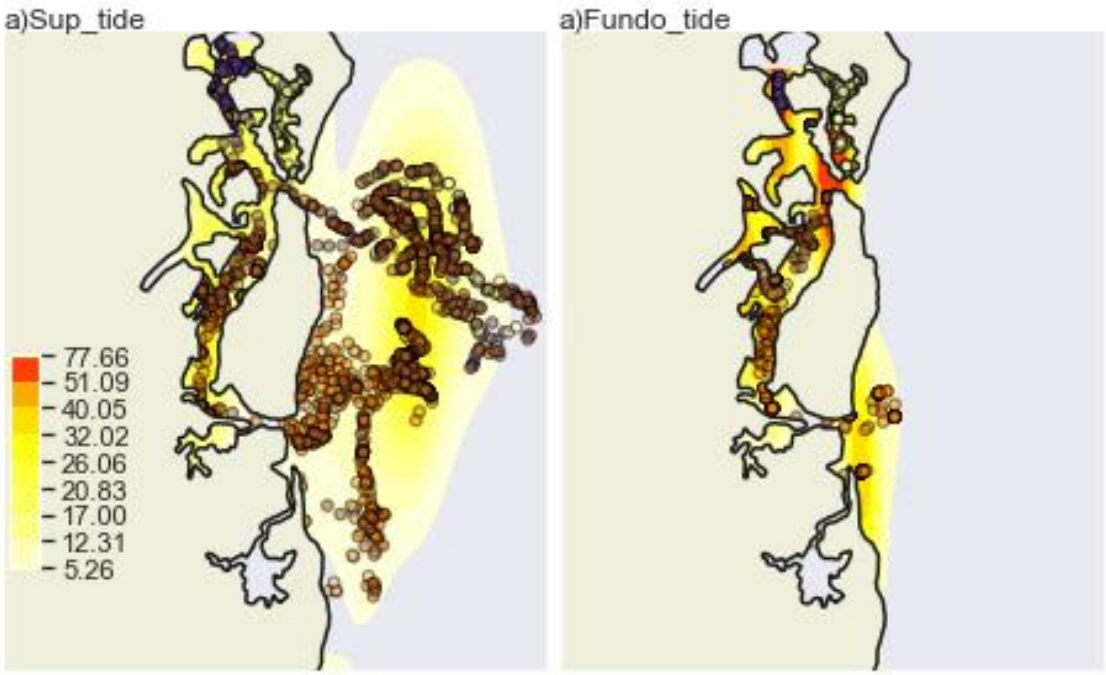

Fonte: o autor (2021).

Tal situação mostrada na Figura 12 evidencia a formação de uma nuvem superficial à frente do estuário, enquanto o material de fundo tende a ficar acumulado dentro do sistema. Ao analisarmos a condição anterior associada à descarga fluvial, a distribuição sofre alterações. A Figura 13 mostra o cenário de acúmulo em condições chuvosas. As partículas que são exportadas por Orange se juntam às partículas provenientes do rio Capibaribe, mais ao Sul, criando um caminho natural do MPS entre um estuário e outro.

Figura 4.13. Densidade das partículas no SEII, após 15 dias de simulação, em condições de maré. O eixo C, colorbar, representa a quantidade de partículas por pixel no domínio.

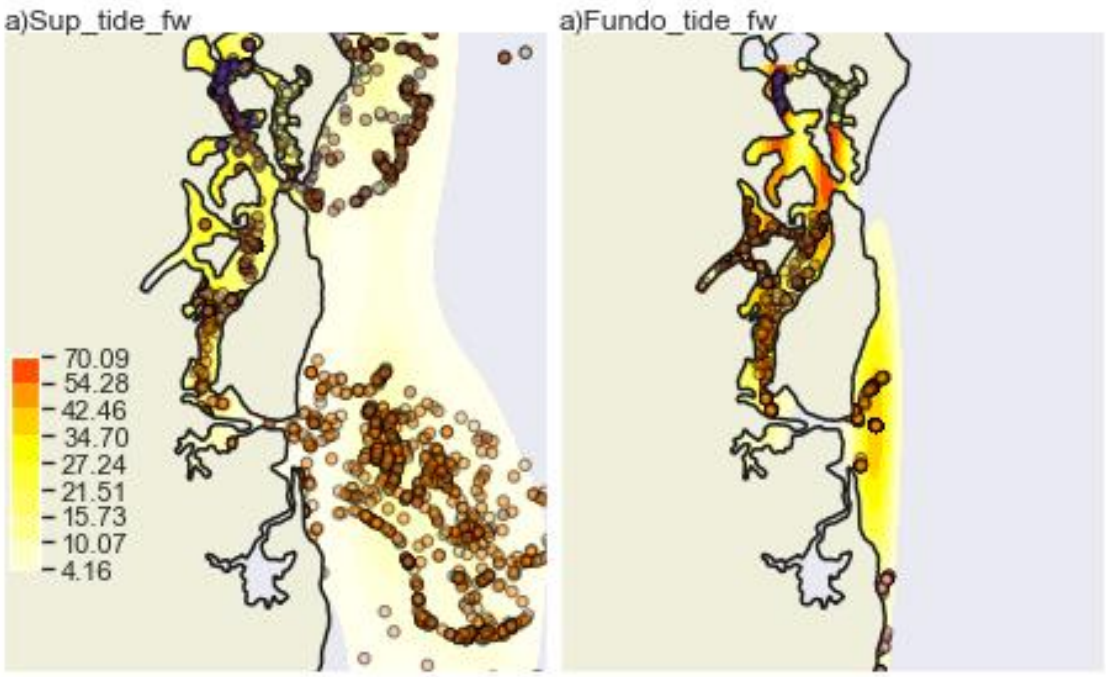

Fonte: o autor (2021).

A intensificação do processo de interação estuário-estuário e plataforma-estuário ocorre quando o vento é adicionado ao cenário. A Figura 14 representa a densidade das partículas em condições forçadas por maré e vento. A densidade de partículas tende a aumentar dentro do sistema devido a presença do MPS alóctone vindo da plataforma e do rio Capibaribe como mostrado anteriormente, deslocando o material para norte e aprisionando nos canais interiores de Santa Cruz e Itapessoca.

Tendo em vista a sazonalidade da região, onde o período chuvoso se concentra entre maio e julho (Schettini *et al.*, 2016; Schettini, Domingues, *et al.*, 2017), é possível que a intensificação do processo de aprisionamento de MPS dentro do SEII ocorra nesta época. No verão, entre dezembro e fevereiro, ocorre um vento médio de leste de 7,5 $m.s^{-1}$. Em tal situação, contudo, o MPS ficará retido dentro dos sistemas e o transporte ao longo da costa será suprimido. Por outro lado, nos meses entre julho e setembro, a intensidade média do vento é intensificada para 10 $m.s^{-1}$, onde se espera que ocorra a situação aqui mostrada de interação entre os estuários.

Figura 4.14. Densidade das partículas no SEII, após 15 dias de simulação, em condições de maré associada ao vento e a descarga fluvial. O eixo C, barra de cores, representa a quantidade de partículas por pixel no domínio e a tendência de acúmulo.

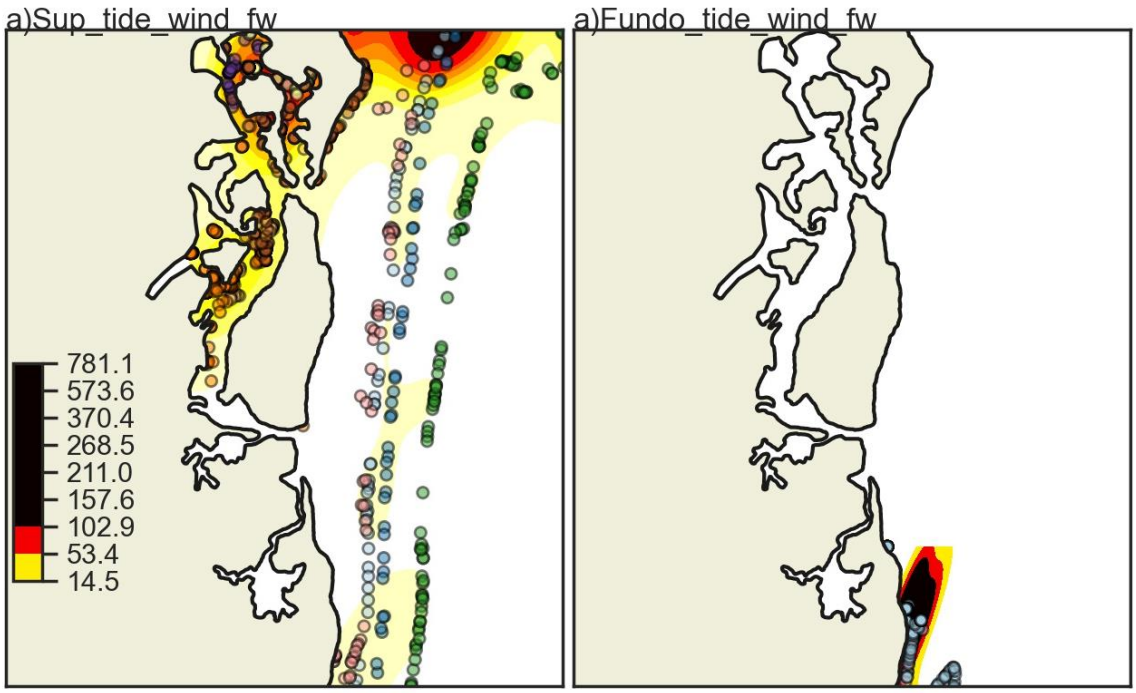

Fonte: o autor (2021).

É possível que ocorra processos similares de importação aqui discutidos para outros estuários semelhantes. No estuário do rio Mossoró, ao norte do SEII, ocorre circulação inversa estuarina e condições de hipersalinidade o que pode ainda mais favorecer o processo de importação de MPS (Largier, 2010; Valle-Levinson *et al.*, 2009; Valle-Levinson e Schettini, 2016). Tal situação também provavelmente ocorre no estuário do rio Caravelas, que possui duas conexões com o mar e está sujeito a mesa sazonalidade (Schettini e Miranda, de, 2010).

Adicionalmente, se forem observadas apenas as situações onde o vento Norte é usado como forçante, a influência alóctone é evidenciada e a hipótese de uma fonte externa é provada. As figuras 15 e 16 mostram apenas as partículas com origem na plataforma e na origem Pina, dentro do estuário do Capibaribe. Nestes casos, sem atentar muito para os valores da contagem acumulada que são relativamente baixos, devemos voltar atenção para os padrões de distribuição temporal, A Figura 15 mostra o acúmulo de partículas alóctones dentro do sistema em condições de maré e vento Norte.

Figura 4.15. Acumulativo temporal filtrado das partículas apenas com fonte alóctone ao SEII em condições de maré e vento Norte de 10m/s.

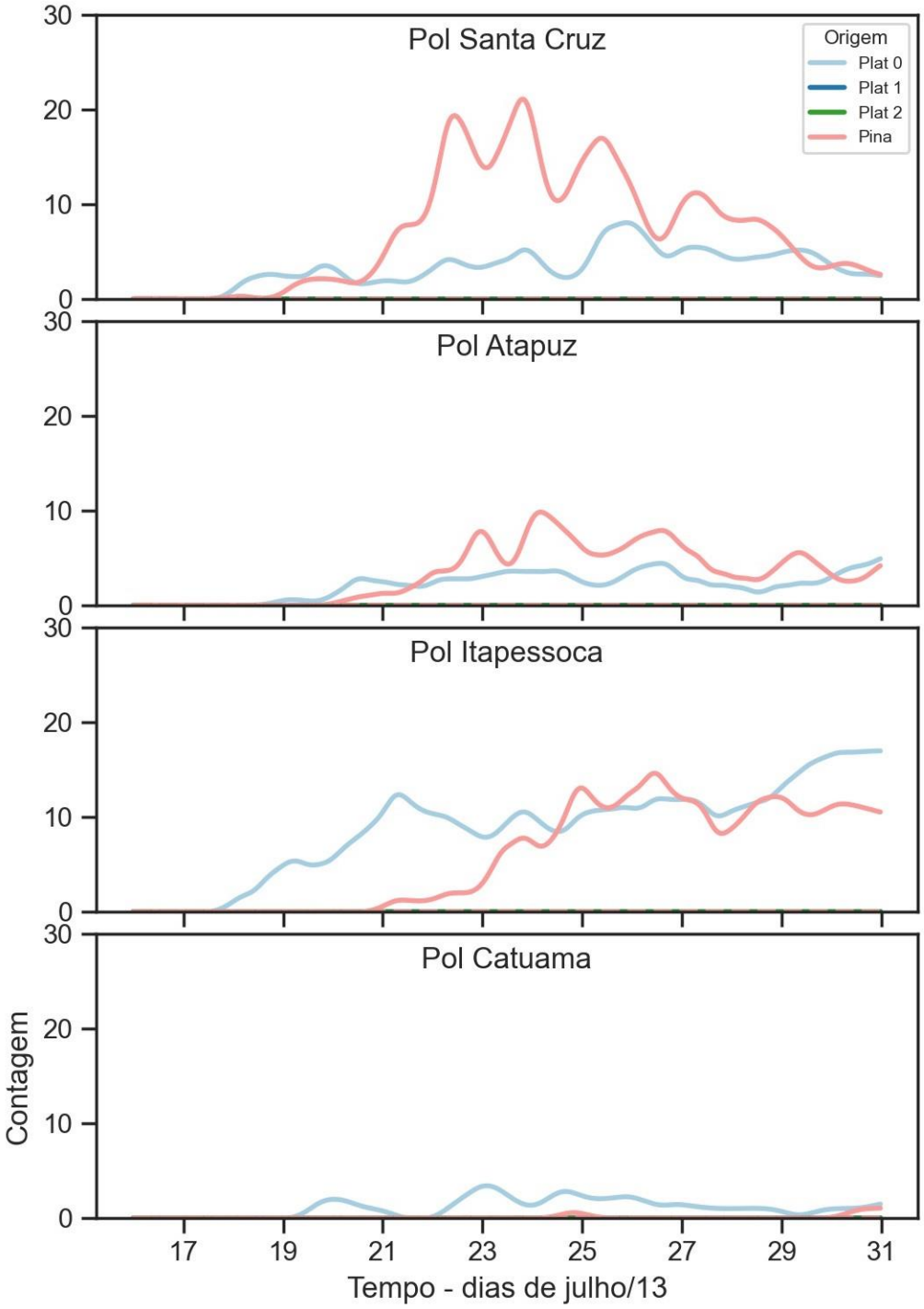

Fonte: o autor (2021).

Nesse mesmo contexto, a Figura 16 evidencia o acúmulo alóctone de partículas dentro do sistema.

Figura 4.16. Acumulativo temporal filtrado das partículas apenas com fonte alóctone ao SEII em condições de maré e vento Norte de 10m/s.

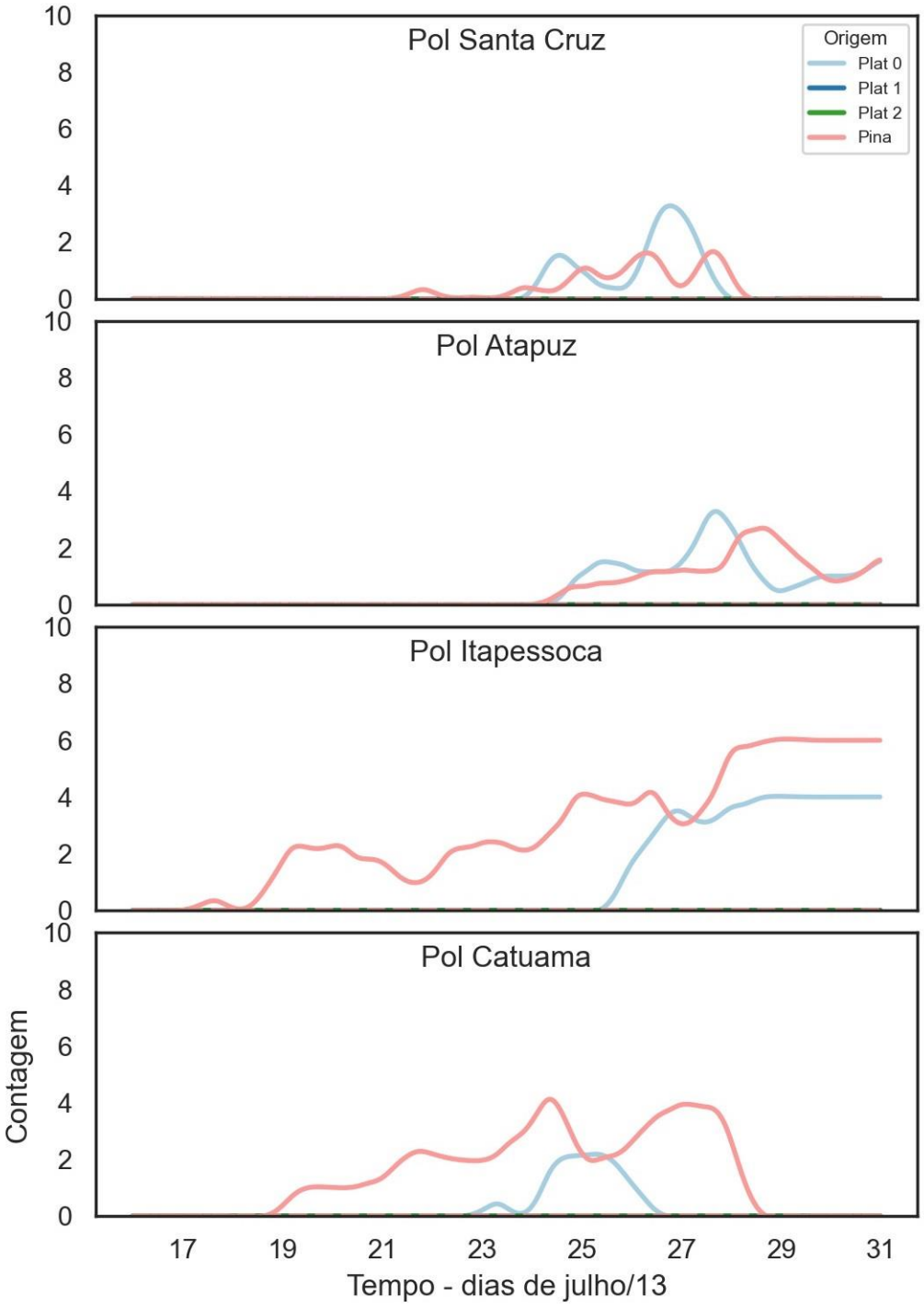

Fonte: o autor (2021).

Nas duas condições evidenciadas acima, os padrões nos polígonos de Itapessoca e Atapuz mostram que existe uma tendência de acúmulo de partículas dentro do sistema o que coincide com as maiores densidades estimadas anteriormente. Se essa situação for analisada no contexto de que a erosão da formação barreiras é a fonte como proposto por (Knoppers, Ekau e Figueiredo, 1999), a tendência é que

estes canais de Itapessoca e a parte central do SEII estejam em processo de preenchimento. Tal informação é crucial para tomada de decisão por exemplo para construção de um porto na localidade.

CONCLUSÕES

O estuário SEII é um estuário tropical dominado por maré que apresenta duas conexões principais com o oceano. Os objetivos principais e específicos desse estudo eram identificar as fontes e destino dos traçadores passivos (aqui tratados como MPS) sob quatro cenários diferentes. Disto, os principais aspectos identificados são:

i) Existe um transporte residual de partículas dentro do SEII, de sul para norte em superfície, em condições forçadas apenas pela maré, no entanto não é possível identificar interação entre estuários e importação da plataforma. As partículas tendem a acumular dentro do estuário no fundo e uma nuvem de partículas se forma em frente às duas entradas do sistema;

ii) Em condições forçadas por maré e descarga fluvial, o MPS que sai pela conexão Norte (Catuama), deriva para Norte, paralelamente à costa. Por outro lado, as partículas que são exportadas pela conexão sul derivam para sul, formando uma conexão com as partículas provenientes do estuário do rio Capibaribe;

iii) Em condições de maré associada a descarga fluvial e um vento norte, as partículas com origem na plataforma e no estuário do rio Capibaribe entram no sistema pelas duas conexões e tendem a se acumular a montante estuarina.

Por fim, tendo em vista a qualidade ambiental do rio Capibaribe e a relação comprovada entre um estuário/plataforma/estuário, esta investigação é um importante indicador para tomadas de decisões ambientais localmente e chama atenção para redução da qualidade ambiental de estuário menos impactado por um estuário altamente impactado.

4 CONSIDERAÇÕES FINAIS

Os resultados obtidos nos três artigos aqui apresentados, juntamente a literatura incluída nas discussões, permitem definir os principais processos dominantes na hidrodinâmica do estuário e as trocas que ocorrem entre estuário-plataforma em um contexto da dinâmica sedimentar e processos de preenchimento estuarino.

Do primeiro artigo, foi possível observar que o sedimento em suspensão sofre dominância de correntes de vazante e responde a um ciclo de erosão e ressuspensão de acordo com o ciclo mareal. O sistema foi caracterizado como “faminto” por sedimento continental e a principal fonte de MPS é o fundo estuarino.

Do segundo artigo, foi possível encontrar que ocorre um padrão de circulação no sistema que transfere propriedades de uma parte do sistema para outra. Além disso, a propagação da onda da maré no sistema sofre influência das duas conexões que existem e forma zonas propícias ao acúmulo de material.

Neste sentido, o artigo 3 comprova as hipóteses propostas mostrando que existem fontes alóctones de MPS para dentro do sistema com tendências de acumulação a montante dos canais estuarinos.

Apesar do mais, algumas questões e perspectivas ainda ficam em aberto. Por exemplo, qual escala temporal de reajuste do sistema a esse acúmulo de MPS? Qual a composição do MPS e qual o tamanho médio das partículas, além de sua natureza reológica?

REFERÊNCIAS

ANDUTTA, F., MIRANDA, L.B., SCHETTINI, C.A.F., SIEGLE, E., SILVA, M.P., PEREIRA, M.D.,MAZZINI, P., (2013). Temporal variations of temperature, salinity and circulation in the Peruípe river estuary (Nova Viçosa, BA). **Continental Shelf Researc**h.

ARRUDA-SANTOS, R. H. DE *et al.* Sources and distribution of aromatic hydrocarbons in a tropical marine protected area estuary under influence of sugarcane cultivation. **Science of The Total Environment**, v. 624, p. 935–944, 2018.

ASP, N. E. *et al.* Sediment dynamics of a tropical tide-dominated estuary: Turbidity maximum, mangroves and the role of the Amazon River sediment load. **Estuarine, Coastal and Shelf Science**, v. 214, n. August, p. 10–24, 2018.

AUDOUIN, Y. *et al.* A new Python3 module for TELEMAC-MASCARET dedicated to post-treatment: Postel. **Telemac & Mascaret User Club**, 2019.

BARCELLOS, R. L., MELO, M. C. S. S.; SIAL, A. N., & MANSO, V. A. V. (2020). Sedimentary Organic Matter Characterization on a Tropical Continental Shelf in Northeastern Brazil. I**nternational Journal of Geosciences**, 11(6), 393-419

BOWDEN, K.F. (1963). The mixing processes in a tidal estuary. **Journal of Air and Water Pollution** 7:343–356.

BRASSEALE, E.; DIEGO, S.; MACCREADY, P. The shelf sources of estuarine inflow. n. May, 2021. **Estuarine Coastal and Shelf Science.** 2021

BROWN, J. M. *et al.* Fate and pathways of dredged estuarine sediment spoil in response to variable sediment size and baroclinic coastal circulation. v**. 149, p**. 209–221, 2015. **Journal of Geop. Researc**. 2015.

BURCHARD, H.; SCHUTTELAARS, H.M.; RALSTON, D.K. Sediment trapping in estuaries. ***Annu. Rev. Mar. Sci.* 2018**, *10*, 371–395.

BURCHARD, H. *et al.* Drivers of residual estuarine circulation in tidally energetic estuaries: Straight and irrotational channels with parabolic cross section. **Journal of Physical Oceanography**, v. 41, n. 3, p. 548–570, 2011.

CAMERON, W.N; PRITCHARD. (1963). Estuaries, In: M.N. Hill [Ed.], **The sea. V**ol. 2. New York, John Wiley & Sons. p. 306-324.

CANTRELL, D. L. *et al.* The use of kernel density estimation with a bio-physical model provides a method to quantify connectivity among salmon farms: Spatial planning and management with epidemiological relevance. **Frontiers in Veterinary Science**, v. 5, n. OCT, p. 1–14, 2018.

CHEN, C. T. A. *et al.* Roles of continental shelves and marginal seas in the biogeochemical cycles of the North Pacific Ocean. **Journal of Oceanography**, v. 60, n. 1, p. 17–44, 2004.

CHENG, P.; VALLE-LEVINSON, A.; SWART, H. E. DE. A numerical study of residual circulation induced by asymmetric tidal mixing in tidally dominated estuaries. **Journal of Geophysical Research: Oceans**, v. 116, n. 1, p. 1–13, 2011.

COMPANHIA PERNAMBUCANA DO MEIO AMBIENTE (CPRH). (1998) Diagnóstico Sócio Ambiental e Mapeamento das Potencialidades e Restrições de Uso: Área Piloto da RBMA – Complexo de Igarassu, Itapissuma e Itamaracá. Recife, 1998. v. 01. in. **TOMO 1**

COMPANHIA PERNAMBUCANA DO MEIO AMBIENTE CPRH (2003). Agência Estadual do Meio Ambiente de pernambuco. In: d**iagnóstico socioambiental do litoral norte de pernambuco.** p. 43-56.

DAGESTAD, K. F. *et al.* OpenDrift v1.0: A generic framework for trajectory modelling. **Geoscientific Model Development**, v. 11, n. 4, p. 1405–1420, 2018.

DALRYMPLE, R. W.; CANADA, O. K. L.; ZAITLIN, B. A. Estuarine Facies Models: Conceptual Basis and Stratigraphic Implications: **PERSPECTIVE. v. 62, n. 6, p. 1130–1146, 1992.**

DALRYMPLE, R. W.; CHOI, K. Morphologic and facies trends through the fluvial-marine transition in tide-dominated depositional systems: A schematic framework for environmental and sequence-stratigraphic interpretation. **Earth-Science Reviews**, v. 81, n. 3–4, p. 135–174, 2007.

D'AQUINO, C.A; NETO, J.S.A, MANIQUE, G.A.B, SCHETTINI, C.A.F. (2011). Caracterização oceanográfica e do transporte de sedimentos em suspensão no estuario do rio mampituba, sc. I**n Revista Brasileira de Geofísica.** 29(2):217:230.

DEINES, K.L. (1999). Backscatter estimation using broadband acoustic Doppler current profilers. In: **Proceedings of the IEEE Sixth Working conference on Current Measurements**, San Diego, CA, 13-16 September 1999, p. 249–253.

DOMINGUES, E. D. C. *et al.* Hydrography and currents on the Pernambuco **Continental Shelf. Research 2017**.

DYER, K.R. (1995). Estuaries: a physical introduction. 2. **ed. Chichester, Wiley. 195 p.**

DYER, K.R. (1974). The salt balance in stratified estuaries. **Estuarine and Coastal Marine Science**, 2:273-281.

DYER, K.R., NEW, A.L., (1986). Intermittency in estuarine mixing. In: Wolfe, D.A. (Ed.), Estuarine Variability. **Academic Press, Orlando, Florida, USA**, pp. 321e339.,

DYER, K.R. (1997). Fine Sediment Particle Transport in Estuaries. In: **Hydrodynamic of Estuaries, Springer, Verlin,** 295-310,

DYER, K. R. Sediment transport processes in estuaries. **Developments in Sedimentology**, v. 53, n. C, p. 423–449, 1995.

EGBERT, G. D.; EROFEEVA, S. Y. Efficient inverse modeling of barotropic ocean tides. **Journal of Atmospheric and Oceanic Technology**, v. 19, n. 2, p. 183–204, 2002.

EISMA, D. Ge0 . Marine Particle Size of Suspended Matter in Estuaries. **In Situ**, p. 147–153, 1991.

ELLIOTT, M. *et al.* A synthesis: what is the future for coasts, estuaries, deltas and other transitional habitats in 2050 and beyond? *In*: **Coasts and Estuaries**. [s.l.] Elsevier, 2019. p. 1–28.

FAIRBRIDGE, RW (1980). The estuary: its definition and geodynamic cycle. In: Olausson E & Cato I (Eds.). Chemistry and biogeochemistry of estuaries. New York, J**ohn Wiley and Sons**, p. 1–35.

FERNANDES, E. H. L.; DYER, K. R.; MOLLER, O. O. Spatial Gradients in the Flow of Southern Patos Lagoon. **Journal of Coastal Research**, v. 21, n. 4 (214), p. 759–769, 2005.

FIDEM - Fundação De Desenvolvimento Da Região Metropolitana Do Recife. (1987). Proteção de Áreas Estuarinas de Pernambuco. Recife (Série Desenvolvimento Urbano e Meio Ambiente). **Notas Técnicas.**

FISCHER, H.B.(1976). Mixing and dispersion in estuaries. **Annual Review of Fluid Mechanics**, 8: 107–133.

FISCHER, H. B. Mixing and dispersion in estuaries. **Annual review of fluid mechanics**, v. 8, n. 1, p. 107–133, 1976.

FRANCISCO, P. R. M. *et al.* Revista Brasileira de Climatologia. **Revista Brasileira de Climatologia**, v. 20, p. 135–147, 2017.

GARTNER, J.W. (2004). Estimating suspended solid concentrations from backscatter intensity measured by Doppler current profiler in San Francisco Bay, **California. Mar. Geol.,** 211: 169–187.

GEYER, W. R.; MACCREADY, P. The estuarine circulation. **Annual Review of Fluid Mechanics**, v. 46, n. August 2013, p. 175–197, 2014.

GEYER WR, KINEKE GC (1995) Observations of currents and water properties in the Amazon frontal zone. **J Geophys Res** 100:2321–2339. doi: 10.1029/94JC02657 CrossRefGoogle Scholar

GEYER WR, BEARDSLEY RC, LENTZ EJ, CANDELA J, LIMEBURNER R, JOHNS WE, CASTRO BM, SOARES ID (1996) Physical oceanography of the Amazon shelf. **Cont Shelf Res** 16:575–616. doi: 10.1016/0278-4343(95)00051-8

GEYER, W.R, MACREADY, P. (2014). The estuarine Circulation. In**: Annual Review of Fluid Mechanics.** Florida, USA. 46:175-197.

HANSEN, D. V.; RATTRAY, M. (1965). Gravitational circulation in straits and estuaries. ***Journal of Marine Research*** 23:104–122.

HANSEN, D.V. & RATTRAY, M. (1966). New dimension in estuary classification. **Limnology and Oceanography,** 11(3):319-325.

HERVOUET, J.-M. Hydrodynamics of free surface flows: modelling with the finite element method. [s.l.] **Wiley Online Library**, 2007. v. 360

HOLTERMANN, P.; BURCHARD, H.; JENNERJAHN, T. Hydrodynamics of the Segara Anakan lagoon. **Regional Environmental Change**, v. 9, n. 4, p. 245–258, 2009.

HSU, T. J.; CHEN, S. N.; OGSTON, A. S. The landward and seaward mechanisms of fine-sediment transport across intertidal flats in the shallow-water region-A numerical investigation. **Continental Shelf Research**, v. 60, p. S85–S9**8, 2013.**

HUNKINS, K. (1981). Salt dispersion in the Hudson estuary. Journal of Physical Oceanography, 11:729-738.

JAY, D.J.; MUSIAK, J. D. Particle trapping in estuarine tidal flows. J**. Geophys. Res.,** v. 99, n. C10, p. 20445-20461, 1994.

JUAREZ, B.; VALLE-LEVINSON, A.; LI, C. Estuarine salt-plug induced by freshwater pulses from the inner shelf. **Estuarine, Coastal and Shelf Science**, v. 232, n. June 2019, p. 106491, 2020.

KJERFVE B, PROEHL JA, SCHWING FB, SEIM HE & MAROZAS M (1982). Temporal and spatial considerations in measuring estuarine water fluxes. In: KENNEDY VS (Ed.). Estuarine Comparisons. **New York, Academic Press,** p. 37–51.

KJERFVE, B. (1986). Circulation and salt flux in a well mixed estuary. In: Kreeke, van de. (Ed). **Physics of Shallow Estuaries and Bays. New York, Spring-Verlag,** p.22-29.

KJERFVE, B. (1990). Manual for investigation of hydrological processes in Mangrove Ecosystems. **New Delhi, UNESCO/UNDP. 79 p.**

KNOPPERS, B.; EKAU, W.; FIGUEIREDO, A. G. The coast and shelf of east and northeast Brazil and material transport. **Geo-Marine Letters**, v. 19, n. 3, p. 171–178, 1999.

KREEKE, J. VAN DE. **Physical processes in estuaries**. [s.l: s.n.]. v. 110

LARGIER, J. Low-inflow estuaries: hypersaline, inverse, and thermal scenarios. *In*: VALLE-LEVINSON, A. (Ed.). . **Contemporary Issues in Estuarine Physics**. [s.l.] Cambridge University Press, 2010. p. 247–272.

LI, C.; O'DONNELL, J. Tidally driven residual circulation in shallow estuaries with lateral depth variation. **Journal of Geophysical Research C: Oceans**, v. 102, n. C13, p. 27915–27929, 1997.

LESSA, G.C., DOMINGUEZ, J.M.L., BITTENCOURT, A.C.S.P., BRICHTA, A. (2001) The tides and tidal circulation of Todos os Santos Bay, Northeast Brazil. **Anais da**

Academia Brasileira de Ciências, 73(2), http://dx.doi.org/10.1590/S0001-37652001000200009

LOHRMANN, A. (2001). Monitoring sediment concentration with acoustic backscattering instruments. Nortek AS, Rud, Norway, **Nortek Technical Note N.** 03, 5 pp.

MABESONE, J. M.; COUTINHO, P. N. Littoral and shallow marine geology of northern and northeastern Brazil. Universidade Fedederal de Pernambuco. **Trab. Ocean**, v. 12, p. 214, 1970.

MABESOONE, J. M. Origin and Age of the Sandstone Reefs of Pernambuco (Northeastern Brazil). v. 34, n. 4, 1964. **Tropical Oceanography**. 1964

MACCREADY, P.; GEYER, W. R. Advances in estuarine physics. **Annual Review of Marine Science**, v. 2, n. 1, p. 35–58, 2010.

MACIEL, D.C.; SOUZA, J.R.B.; TANIGUCHI, S.; BICEGO, M.C.; SCHETTINI, C.A.F.; ZANARDI-LAMARDO, E. 2016. Hydrocarbons in sediments along a tropical estuary-shelf transition area: sources and spatial distribution. **Mar. Pollution Bul.,** 113(1-2):566-571. http://dx.doi.org/10.1016/j.marpolbul.2016.08.048

MEDEIROS, C.; KJERFVE, B. Hydrology of a tropical estuarine system: Itamaracá, Brazil. **Estuarine, Coastal and Shelf Science**, v. 36, n. 5, p. 495–515, 1993.

___. Longitudinal salt and sediment fluxes in a tropical estuary: Itamaracá, Brazil. **Journal of Coastal Research**, v. 21, n. 4, p. 751–758, 2005.

MIRANDA, L. B. *et al.* **Fundamentals of estuarine physical oceanography**. [s.l.] **Springer**, 2017. v. 8

MIRANDA, L. B. DE; KJERFVE, B.; CASTRO, B. M. Princípios de oceanografia física de estuários. **São Paulo: EDUSP**, 2002.

MCDOUGALL, T. J., BARKER, P.M. (2011): Getting started with TEOS-10 and theGibbs Seawater (GSW) oceanographic toolbox. **SCOR/IAPSO WG127 Rep., 34** pp. [Available online at http://www.teos-10.org/pubs/Getting_Started.pdf.]

MEDEIROS, C, KJERFVE, B. (1993). Hydrology of a tropical estuarine system: Itamaraca, Brazil. **Estuarine, Coastal and Shelf Science** 36, 495-515.

MEDEIROS,C. (1991). Physical characteristics and circulation-dispersion processes in the Itamaraca estuarine system, Brazil. Ph.D. **dissertation**, **Marine Science Program, University of South Carolina, Columbia, SC.**

MEDEIROS, C. And KJERFVE, B., (2005). Longitudinal salt and sediment fluxes in a tropical estuary: Itamaraca, Brazil. **Journal of Coastal Research, 2**1(4), 751-758. West Palm Beach (Florida), ISSN 0749-0208.

MIRANDA, L.B.; CASTRO, B.M. & KJERFVE, B.(2002). Princípios de Oceanografia Física de Estuários. **São Paulo, Editora da Universidade de São Paulo –** EDUSP. 424p.

NEZU, I.; NAKAGAWA, H.; JIRKA, G. H. Turbulence in open-channel flows. **Journal of Hydraulic Engineering**, v. 120, n. 10, p. 1235–1237, 1994.

NICHOLS, M.M. (1984). Effects of fine sediment resuspension in estuaries.In: MEHTA AJ (Ed.). Estuarine cohesive sediment dynamics. **Springer-Verlag, Berlin, p. 5–42.**

NIKURADSE, J. **Laws of flow in rough pipes**. [s.l.] N**ational Advisory Committee for Aeronautics Washington,** 1950. v. 2

OFFICER, CB (1977). Longitudinal Circulation and Mixing Relations in Estuaries. Estuaries, Geophysics, and the environment. Washington DC, N**ational Academy of Sciences**, pp. 13-21.

OFFICER,C.B.(1976). Physical Oceanography of Estuaries and associated coastal waters). **New York, Wile**y. 465p.

OLIVEIRA, T. S.; Barcellos, R. L.; Schettini, C. A. F.; Camargo, P. B. (2014) Processo sedimentar atual e distribuição da matéria orgânica em um complexo estuarino tropical, Recife, PE, Brasil. **J. Integr. Coast. Zone Manag, v**. 14, n. 3, p. 399-411.

OLIVEIRA-FILHO, J. C. DE;; SCHETTINI, C. A. F. Circulação e transporte de sal e sedimento em suspensão no sistema estuarino de Itapessoca, PE, Brasil. [s.l.] **DIssertação de mestrado**. Federal University of Pernambuco, 2015.

OLIVEIRA FILHO, J. C. DE *et al.* Residual circulation in a semi-enclosed tropical embayment with complex geometry. **Regional Studies in Marine Science**, [s.d.].

PARSA, J.; SHAHIDI, A. E. Prediction of tidal excursion length in estuaries due to the environmental changes. **International Journal of Environmental Science & Technology**, v. 7, n. 4, p. 675–686, 2010.

PAWLOWICZ, R. *et al.* The circulation and residence time of the strait of Georgia using a simple mixing - box approach The Circulation and Residence Time of the Strait of Georgia using a Simple Mixing-box A**pproach. v. 5900, 2010**.

PEREIRA, M. D.; SIEGLE, E.; MIRANDA, L. B.; SCHETTINI, C. A. F. (2010) Hidrodinâmica e transporte de material particulado em suspensão sazonal em um estuário dominado por maré: Estuário de Caravelas (BA). **Rev. Bras. Geof**., v. 28, n. 3, p.427-444.

PERILLO, G. Definitions and Geomorphologic Classifications of Estuaries BT - Geomorphology and Sedimentology of Estuaries. **Geomorphology and Sedimentology of Estuaries**, p. 17–47, 1995.

PRANDLE, D. (2009) Estuaries**:** dynamics, mixing, sedimentation and morphology. **Cambridge: Cambridge University Press.** 236 p.

PRITCHARD, D.W (1955). Estuarine Circulation Patterns. **Proc. Am. Soc. Civ. Eng.**, 81:717:1-11.

PRITCHARD, D.W. (1989) Estuarine Classification — A Help or a Hindrance. In: Neilson B.J., Kuo A., Brubaker J. (eds) Estuarine Circulation. **Contemporary Issues in Science and Society. Humana Pres**

RATISBONA. L.R. (1976). The climate of Brazil. p 219-93. In: Climates of South and Central America (Schwerdtfger W.,ed). **Elsevier Scientific Publishing Company,** Amsterdam, 532 pp.

RÉGIS, C.G., SOUCA-SANTOS, L.P., YOGUI, G.T., MORAES, A.S., SCHETTINI, C.A.F. 2018. Use of Tisbe biminiensis nauplii in ecotoxicological tst and geochemical analyses to assess the sediment quality of a tropical urban estuary in northeastern Brazi. **Marine Pollution Bulletim,** 137:45-55.

ROSS, L. *et al.* Lateral variability of subtidal flow at the mid-reaches of a macrotidal estuary. **Journal of Geophysical Research: Oceans**, v. 122, n. 9, p. 7651–7673, 2017.

SCHETTINI, C. A. F. *et al.* Residual fluxes of suspended sediment in a tidally dominated tropical estuary. **Continental Shelf Research**, v. 70, p. 27–35, 2013.

___. The circulation of the lower Capibaribe Estuary (Brazil) and its implications for the transport of scalars. **Brazilian Journal of Oceanography**, v. 64, n. 3, p. 263–276, set. 2016.

SCHETTINI, C. A. F.; CARVALHO, E. DE; *et al.* Seasonal variability of water masses and currents at the eastern Brazilian continental shelf (7 . 5 – 9 ◦ S). **Regional Studies in Marine Science**, v. 16, p. 131–144, 2017.

SCHETTINI, C. A. F.; DOMINGUES, E. DE C.; *et al.* Seasonal variability of water masses and currents at the eastern Brazilian continental shelf (7.5–9◦ S). **Regional Studies in Marine Science**, v. 16, n. November, p. 131–144, 2017.

SCHETTINI, C. A. F. *et al.* Circulation and fine-sediment dynamics in the Amazon Macrotidal Mangrove Coast. **Earth Surface Processes and Landforms,** v. 45, n. 3, p. 574–589, 2020.

SCHETTINI, C. A. F. *et al.* Transport processes in the Santa Cruz Channel, Brazil. **Regional Studies in Marine Science**, v. 45, p. 101812, 2021.

SCHETTINI, C. A. F.; MIRANDA, L. B. DE. Circulation and suspended particulate matter transport in a tidally dominated estuary: Caravelas Estuary, Bahia, Brazil. **Brazilian Journal of Oceanography**, v. 58, n. 1, p. 1–11, 2010.

SCHETTINI C.A.F. (2002). Near bed sediment transport in the Itajaí-Açu River estuary, southern Brazil. In: Winterwerp JC and Kranenburg C (Eds). Fine sediment dynamics in the marine environment. **New York, Elsevier, p** 499-512.

SCHETTINI, C.A.F. (1994). Determinantes Hidrológicas na Manutenção da Hipersalinidade da lagoa de Araruama, RJ. **Dissertação de Mestrado, Niterói. Universidade Federal Fluminense**. p 75.

SCHETTINI, C.A.F, CARVALHO, J.L.B. (1999). Caracterização Hidrodinâmica do estuário do rio cubatão, Joinville. **Nota técnicas FACIMAR**, 3:87-97.

SCHETTINI, C.A.F., RICKLEFS, K., TRUCCOLO, E.C., GOLBIG, V., (2006). Synoptic hydrograph of a highly stratified estuary. **Ocean Dynamics** 56 (3-4), 308–319.

SCHETTINI,C.A.F; MIRANDA, L.B. (2010). Circulation and Suspended Sediment Particulate Matter Transport in a Tidally Dominated Estuary: Caravelas Estuary, Bahia, Brazil. **Brazilian Journal of Oceanography,** 58(1):1-11.

SCHETTINI, C.A.F.; ALMEIDA, D.C. ; SIEGLE, E.; ALENCAR, A.C.B. 2010. A snapshot of suspended sediments and fluid mud distributions in the Tijucas Bay (Brazil): a mixed-energy environment. **Geo-Marine Letters**, 30:47-62.

SCHETTINI, C.A.F., PEREIRA, M.D., SIEGLE, E., MIRANDA, L.B., SILVA, M.P., (2013). Residual fluxes of suspended sediment in a tidally dominated tropical estuary. C**ont. Shelf Res**. 70 (2013), 27–35.

SCHETTINI, C.A.F., VALLE-LEVINSON, A., TRUCCOLO, E.C., (2016). The circulation of the lower Capibaribe Estuary (Brazil) and its implications in the transport of scalars. **Braz. J. Oceanogr.** 64 (3), 263–276.

SCHETTINI, C. A.F.; VALLE-LEVINSON, A.; TRUCCOLO, E. C. (2017). Circulation and transport in short, low-inflow estuaries under anthropogenic stresses**. Regional Studies in Marine Science.** S. L., p. 52-64.

SCHETTINI, C.A.F., ASP, N.E., OGSTON, A.S., GOMES, V.J.C., MCLACHLAN, R.L., FERNANDES, M.E.B., NITTROUER, C.A., TRUCCOLO, E.C., GARDUNHO, D.C.L. (2020) Circulation and fine-sediment dynamics in the Amazon Macrotidal Mangrove Coast. **Earth Surface Processes and Landforms**, doi.org/10.1002/esp.4756.

SCHUBEL, J.R.; KENNEDY,V.S. (1984). The Estuary As A Filter: An Introduction, In he Estuary As a Filter, **Academic Press, 1984**, Pages 1-11, ISBN 9780124050709, https://doi.org/10.1016/B978-0-12-405070-9.50007-4.

SIEGLE, E.; SCHETTINI, C. A. F., KLEIN, A. H. F., TOLDO JR., E. E. Hydrodinamics and Suspended Sediment Transport in the Camboriú Estuary Brazil: Pre- Jetty Condition. **Braz. J. Oceanogr.,** V. 57, N. 2, P. 123- 135, 2009.

SILVA, M.H., PASSAVANTE, J.Z.O., SILVA-CUNHA, M.G.G., VIEIRA, D.A.N., GREGO, C.K.S., MUNIZ, K., (2004) Distribuição espacial e sazonal da biomassa fitoplanctônica e dos parâmetros hidrológicos no estuário do rio Formoso (Rio formoso, Pernambuco, Brasil). **Tropical Oceanography, 3**2(1): 89-106.

SCHUBEL, J. R.; CARTER, H. H. The estuary as a filter for fine-grained suspended sediment. *In*: **The estuary as a filter**. [s.l.] Elsevier, 1984. p. 81–105.

SCULLY, M. E.; GEYER, W. R.; LERCZAK, J. A. The influence of lateral advection on the residual estuarine circulation: A numerical modeling study of the Hudson River estuary. **Journal of Physical Oceanography**, v. 39, n. 1, p. 107–124, 2009.

SMITH, N. E. D. P.; PIERCE, F. Tidal and Low-frequency Net Displacement in a Coastal Lagoon **t. v. 6, n. 3, p. 1**80–189, 1983.

SOUSA, S.H.M., AMARAL, P.G.C., MARTINS, V., FIGUEIRA, R.C.L., SIEGLE, E., FERREIRA, P.A.L., SILVA, I.S., SHINAGAWA, E., SALAROLI, A., SCHETTINI, C.A.F., SANTA-CRUZ, J., MAHIQUES, M.M., (2014) Environmental evolution of the Caravelas Estuary (Northeastern Brazilian coast, 17° S, 39° W) based on multiple proxies in a sedimentary record of the last century. **Journal of Coastal Researc**h, 30(3):474-486.

SRH-PE. (2010) Secretaria de Recursos Hídricos do Estado dePernambuco. Plano hidroambiental da bacia hidrográfica do Rio Capibaribe: T**omo I - diagnóstico hidroambiental. Recife:SRH-PE - Projetos Técnicos**,. 389 p.

SWEET, D.C. (1971). The economic and social importance of estuaries. [Washington] : Environmental Protection Agency, Water Quality Office, Technical Support Division; [for sale by the Supt. of Docs., U.S. Govt. Print. Off.

VALLE-LEVINSON, A. Residual Exchange Flows in Subtropical Estuaries. n. May 2014, 2008. **Estuaries and Coasts** (2009) 32:54–67

VALLE-LEVINSON, A. *et al.* Residual exchange flows in subtropical estuaries. **Estuaries and Coasts**, v. 32, n. 1, p. 54–67, 2009.

___. **Contemporary issues in estuarine physics**. [s.l.] Cambridge University Press, 2010.

VALLE-LEVINSON, A.; SCHETTINI, C. A. F. Fortnightly switching of residual flow drivers in a tropical semiarid estuary. **Estuarine, Coastal and Shelf Science**, v. 169, p. 46–55, 2016.

VALLE-LEVINSON, A. (2010). Contemporary Issues in Estuarine Physics, Edited by A. Valle-Levinson, C**ambridge University Press, Cambridge**, UK, 2010, 326 pp.

VALLE-LEVINSON, A.; SCHETTINI, C.A.F., (2016). Fortnightly switching of residual flow drivers in a tropical semiarid estuary. **Estuarine Coastal and Shelf Science v**. 169, p. 46-55, 2016.

VELASCO, G. G. DE; WINANT, C. D. Wind- and density-driven circulation in a well-mixed inverse estuary. **Journal of Physical Oceanography**, v. 34, n. 5, p. 1103–1116, 2004.

VICTOR, S. *et al.* Fine sediment trapping in two mangrove-fringed estuaries exposed to contrasting land-use intensity, Palau, Micronesia. **Wetlands Ecology and Management**, v. 12, n. 4, p. 277–283, 2004.

WALSH, J. J. DOC storage in Arctic Seas: the role of continental shelves. **Coastal and Estuarine Studies**, p. 203, 1995.

WATERHOUSE, A. F.; VALLE-LEVINSON, A.; WINANT, C. D. Tides in a system of connected estuaries. **Journal of Physical Oceanography**, v. 41, n. 5, p. 946–959, 2011.

WILLMOTT, C. J.; ROBESON, S. M.; MATSUURA, K. A refined index of model performance. **International Journal of Climatology**, v. 32, n. 13, p. 2088–2094, 2012.

WILLEMSEN, P.W.J.M., HORSTMAN, E.M., BORSJE, B.W., FRIESS, D.A., DOHMEN-JANSSEN, C.M., (2016) Sensitivity of the sediment trapping capacity of an estuarine mangrove forest. **Geomorphology**, 273:189-201.

WINTERWERP, J.C. AND VAN KESTEREN, W.G.M. 2004. Introduction to the physics of cohesive sediment dynamics in the marine environment. **New York, Elsevier**, 576p.

WOLANSKI, E.; MAZDA, Y.; RIDD, P. (1992) Mangrove Hydrodynamics, in Tropical Mangrove Ecosystems (eds A.I. Robertson and D.M. Alongi), **American Geophysical Union,** Washington, D. C.. doi:10.1029/CE041p0043

WOLANSKI, E. *et al.* Mangrove hydrodynamics. **Tropical mangrove ecosystems. coastal and estuarine studies**, v. 41, 1992.

WOLANSKI, E.; NHAN, N. H.; SPAGNOL, S. Sediment dynamics during low flow conditions in the Mekong River estuary, Vietnam. **Journal of Coastal Research**, v. 14, n. 2, p. 472–482, 1998.

WOLANSKI, E.; RIDD, P. Mixing and trapping in Australian tropical coastal waters. *In*: **Residual currents and long-term transport**. [s.l.] Springer, 1990. p. 165–183.

UNCLES, R.J. (2002). Estuarine physical processes research: Some recent studies and progress. ***Estuarine Coastal and Shelf Science***, 55, 829–856.

ZALESKI, A. R.; SCHETTINI, C. A. F. Procedimentos para calibração de perfiladores acústicos de corrente por Efeito Doppler para a determinação da concentração de material particulado em suspensão na água. **Revista Brasileira de Recursos H{\'i}dricos**, v. 11, n. 3, p. 191–200, 2006.

APÊNDICE A - OBSERVATIONS OF LOCAL AND LATERAL FLOW IN HIGHLY ENERGETIC, BAR-BUILT ESTUARY

Oliveira Fo, J.C.[1*]., Valle-Levinson, A.[2], Schettini, C.A.F.[3]

RUNNING TITLE: OBSERVATIONS OF FLOW IN A BAR-BUILT ESTUARY

Author 1*: José Cavalcante de Oliveira Filho

Geosciences Department. Federal University of Pernambuco– Docean/UFPE. Av. Prof. Moraes Rego, 1235, Recife-PE, CEP: 50.670-901. e-mail: josefilho77@gmail.com*. Orcid: 0000-0002-4785-2986

* Corresponding Author

Author 2: Arnoldo Valle-Levinson

Civil and Coastal Engineering Department ,365. Weil Hall. PO Box: 116580. Gainesville, FL, USA: 32611. e-mail: arnoldo@ufl.edu. Orcid: 0000-0002-3852-0971

Author 3: Carlos Augusto França Schettini

Institute of Oceanography, Federal University of Rio Grande. Av. Itália, km 8, Rio Grande. RS, Brazil. CEP 96000-000. e-mail: guto.schettini@gmail.com . Orcid: 0000-0003-4286-3691

I, José Cavalcante de Oliveira Filho, in behalf of the author and co-authors, declare no conflict of interest.

ABSTRACT

The present study aims to analyze the spatio-time variability of tidal currents and salinity in a shallow and tropical estuary (bar-built type) under moderate tidal influence. Tidal current data were acquired by an ADCP (Acoustic Doppler Current Profiler) moored in the main estuarine channel. Also, a boat-towed ADCP acquired lateral variability of flow over the cross section. A CTD sensor, in the tidal channel, acquired hydrographic data during one semidiurnal tidal cycle. Through the collected dataset was possible to observe that the vertical estuarine structure is vertically homogeneous and well mixed or 1a following Hansen & Rattray's classification diagram. The maximum velocities observed during ebb tide (80 $cm.s^{-1}$) were greater

than the maximum observed in flood tide (60 $cm.s^{-1}$). Salinity distribution showed lower values (2 $g.kg^{-}$) during the low tide and maximum values (35 $g.kg^{-}$) in the high tide. The Richardson number (Ri) showed the strong tidal influence in mixing the tidal column under influence of vertical velocity gradient, which keeps the environment with laterally and vertically homogeneous.

INTRODUCTION

The time scale of the hydrodynamic processes in estuarine waters span from seconds to years, from micro-turbulent eddies to intra Annual River discharge variation for example. The strong longitudinal gradients in estuaries allow one to distinguish three sectors in these environments: a) the lower estuary, where marine processes prevail and water are mostly marine; b) the middle estuary, where occur the interactions among the marine and freshwater; and c) the upper estuary, where marine wateris not observed, but there is still effects of tides (Dionne, 1963).

Pritchard (1955) described the different circulation patterns observed in estuaries, ranging from those - which show highly stratified vertical structure - dominated by freshwater inflow and buoyancy flux, to those vertically homogeneous, dominated by tidal mixing and dispersion. The dominant transport processes in each one are fluvial advection and macro-turbulent dispersion, respectively. This dynamical structure is greatly affected by the basin morphology, where the river and marine waters interact. The understanding of the temporal and spatial variability of these forces and the resulting processes is a challenging task (Kjerfve et al., 1982;1989), especially when one takes to account the rich diversity of estuaries abroad (e.g. Fairbridge, 1980).

Moreover, the importance of understanding estuarine circulation relies on the fact that estuaries play an important role in the global ecology, since most of the matter originated from the continental weathering reaches the costal margins (e.g. Schettini, 2002). Thus, a small number of estuaries have been investigated regarding its dynamical processes to the point the information could provide basis for decision makers and sustainable development. The present study focuses on the circulation of a tropical, narrow and shallow estuary, which has never been observed before and also publications are scarce. Lessa (1996) investigated a shallow tropical estuary in Australia, which was characterized as an indentation of the coastline with relative

small freshwater inflow. The inlet is constituted by mobile sand bars and presents a large number of intertidal areas, where there is an extensive mangrove area. Also, the circulation is mainly forced by the tides. This investigation aims to provide a comprehensive description of the dynamical processes in the Barra de Jangadas estuary, Pernambuco State, Brazil, which is an estuary that presents similar characteristics with the one studied by Lessa (1996), although it receives a relatively larger freshwater inflow.

STUDY AREA

The Barra de Jangadas Estuary – BJE (Figure 1) - (8º15'00", 8º12'00" S and 34º56'00", 34º57'00" W) is formed by the convergence of Jaboatão and Pirapama rivers. It is situated in the Recife Metropolitan Area, nearly 20 km South of Recife City, and its banks are moderately urbanized. The estuary has 15 km^2 of area, and depth ranges from 1 to 4 m, with an average width of 150 m. The Jaboatão and Pirapama rivers are part of a group of small rivers that drains the coastal area of Pernambuco State, and the overall drainage area is of 1025 km^2, with mean river discharge of 16 m^3s^{-1} (CPRH, 2001). The river discharge is directly driven by the annual precipitation seasonality, where the rains are concentrated between April and August.

Because of its strategic position, the Jaboatão River is considered the second most polluted river of Pernambuco State. It receives direct sewage discharge with no treatment from seven small-urbanized cities. Similarly, Pirapama River receives domestic and industrial sewage and also drains a large area of sugar cane crops. The convergence of these two rivers creates the Barra de Jangadas Estuary, which is responsible for acting as a filter between continent and ocean fluxes.

Although under impact of urbanization, BJE system plays a crucial role in the local economy, once that the local community lives based on fisheries. Also, it is responsible to furnish a part of the sediment amount to sustain the adjacent coastal zone against marine erosion.

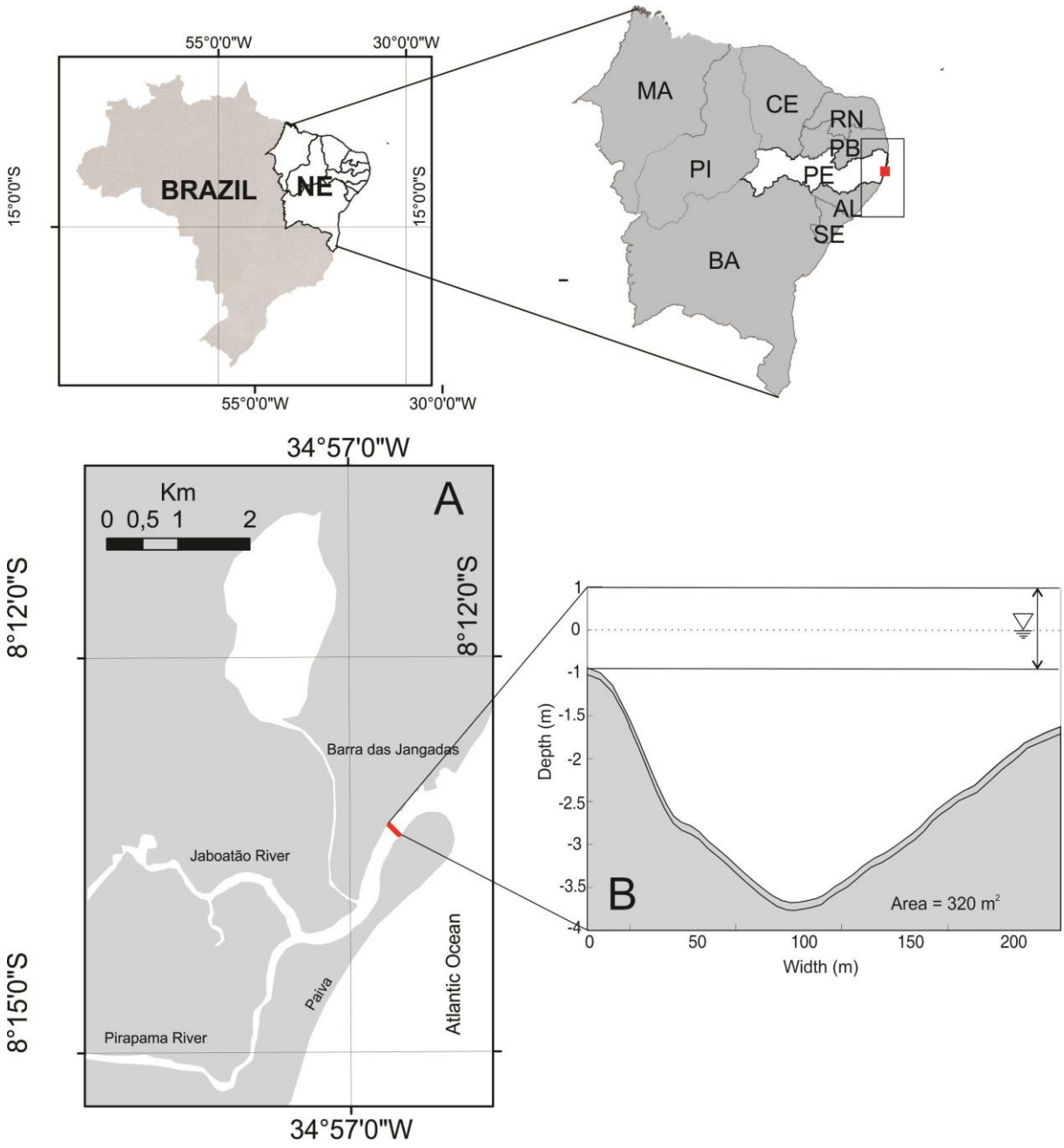

Figure 1. Barra de Jangadas estuary in South America context. The “A” panel shows the study área with the cross section. The “B” panel shows the studied cross section.

The Figure 2 shows the annual variation of the monthly river discharge of the Pirapama River from the historical records of the #39200000 fluviometric station (National Water Agency of Brazil), which drains a watershed of 572 km^2. The BJE mean discharge varies from 5 m^3.s^{-1} in the dry season to 35 m^3.s^{-1} in the rainy season with maximum values reaching 87m^3.s^{-1}.

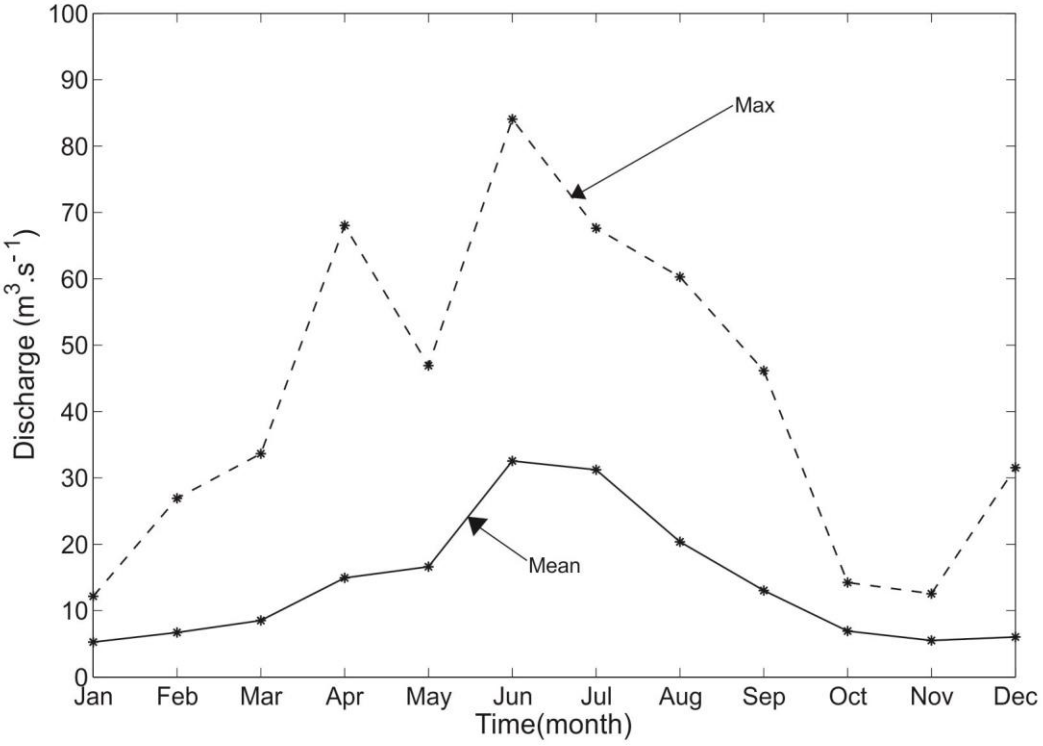

Figure2: Annual monthly mean and maximum (dashed line) river discharge of the Pirapama River, based on 20 years data set.

The regional tides are semi-diurnal with mean range of about 1.3 and 1.8 m at neap and spring tide, respectively (Araújo et al., 1999). The climate is tropical with mean annual temperature of about 25 ^{o}C, and annual precipitation rate higher than 2000 mm.yr^{-1}, with well-defined wet and dry periods. The dry period under normal conditions is from September to February, when the evaporation rate usually is higher than the precipitation. Yet, the wet period extends from March to august.

MATERIAL AND METHODS

Field data acquisition

A field experiment was carried out in order to record oceanographic data in the Barra de Jangadas estuary at September 10th, 2011. The campaign was carried out under mean tidal range period (between spring and neap tide), and during the dry season. Data of water level, currents, cross-sectional discharge, salinity and temperature were recorded during a full semi-diurnal tidal cycle, starting at 7:30 and

finishing at 20:30, in a cross section, nearly 500 m upstream from the estuarine mouth (figure 1).

Water level and tidal currents were recorded with an Acoustic Doppler Current Profiler (ADCP) by Nortek A/S model Aquadopp Profiler of 1000 kHz moored in the estuarine main channel. The ADCP was setup to solve the currents at 0.35 m of cell size, averaging 180 s at 10 minutes sampling interval. Water level was obtained from instrument pressure transducer.

Cross sectional discharge was recorded with an ADCP by RDI-Teledyne model Workhorse of 1200 kHz with bottom track, towed in a small catamaran, operating at Mode-12. This ADCP was configured to record vertical profiles at 2.5 s of sampling rate with 0.5 m of vertical resolution. The cross-sections were performed several times (4-6 times) at every 30 minutes.

Vertical profiles of salinity and temperature were recorded with a conductivity-temperature-depth probe (CTD) by SeaBird Electronics-SBE model SBE 19plus. The vertical profiles were performed as close as possible from the moored ADCP at 30 minutes intervals. The data of the CTD was reduced in order to synchronize in time and space with the moored ADCP.

Estuarine Circulation Analysis

The estuary was classified using the circulation-stratification diagram of Hansen and Rattray (1966). This diagram is based on a simplified numerical model considering some assumptions like lateral homogeneity. In spite of its simplicity, the application of this diagram has been successfully applied in many different types of estuaries and still is a straightforward way to classify estuaries (Miranda et al., 2002).The circulation and stratification parameters are calculated based on vertical profiles time-averaged over one or more complete tidal cycles. The circulation parameter is obtained by the ratio of the surface current $\boldsymbol{U_S}$ to the depth averaged current $\overline{\boldsymbol{U}}$, or $< \boldsymbol{U_S} > / < \overline{\boldsymbol{U}} >$, where the brackets denotes the time average and the over bar denotes the depth average The stratification parameter is obtained by the ration of the salinity difference between the bottom,$\boldsymbol{S_B}$, and surface, $\boldsymbol{S_S}$, to the depth averaged salinity$\overline{\boldsymbol{S}}$, or $(< \boldsymbol{S_B} > - < \boldsymbol{S_S} >) / < \overline{\boldsymbol{S}} >$. From the Hansen & Rattray's

diagram is also possible to extract the value of parameter $\boldsymbol{\nu}$, which is an indicator of the main characteristic of the salt transport, advection or dispersion.

The nature of flow was described in terms of Richardson number (Ri), which is the ratio of the water column stability (stratification) and the water column mixing (vertical shear), or:

$$Ri = -\frac{\frac{g\partial\rho}{\rho\partial z}}{\left(\frac{\partial u}{\partial z}\right)^2} \quad (1)$$

where$g$ is the acceleration of gravity (~9.8 ms^{-2}),ρ is the water density ($kg.m^{-3}$) , z is the vertical length (m) and u is velocity (ms^{-1}). Based on laboratory results, values of Ri> 0.25 indicates the water column stability, while Ri< 0.25 indicates that the vertical shear dominates (Dyer, 1997; Miranda et al., 2002).

Additionally, the flow ratio ($F_R = R/P$) is the relationship of the freshwater inflow during the tidal cycle and the tidal prism. The volume of freshwater inflow is obtained by integrating the river discharge Q_R over one tidal cycle as:

$$R = \int_{t_1}^{t_2} Q_R \, \partial t \quad (2)$$

and the tidal prism P is obtained by the averaged volume of the integrated volume transportQ_T during the ebb and flood phases as:

$$P = \int_{t_1}^{t_2} Q_T \, \partial t \quad (3)$$

In terms of circulation, the estuarine vertical momentum can be hypothesized as a balance between the longitudinal pressure gradient and friction (Cameron and Pritchard, 1963; Hansen and Rattray, 1965; 1966). The solution of this analytical profile of velocity$u\,(z)$, with boundary conditions at surface the wind stress and at the bottom the bed friction, is given by

$$u(z) = \underbrace{\frac{gGH^3}{48\rho A_z}\left[9\left(1-\frac{z^2}{H^2}\right)-8\left(1+\frac{z^3}{H^3}\right)\right]}_{\text{Density induced}} + \underbrace{\frac{3}{2}\frac{R}{H}\left[1-\frac{z^2}{H^2}\right]}_{\text{River induced}} + \underbrace{\frac{1}{4}\frac{\tau H}{\rho A_z}\left[4\left(1+\frac{z}{H}\right)-3\left(1-\frac{z^2}{H^2}\right)\right]}_{\textit{WindInduced}}$$

(4)

Where G is the longitudinal density gradient, H is the depth, A_Z is the eddy viscosity, R_F is the river discharge by unity of width, and τ is the wind stress. The three terms of the right side of Eq. 4 furnishes the separated effects of the longitudinal baroclinic gradient, river discharge, and the wind stress, respectively. Preceding the best fit of the observed residual velocity profile with the theoretical one is possible to depict the dominant forcing of the momentum balance. The eddy viscosity is usually unknown, and also is used as a tuning parameter (e.g. Miranda et al. 2002).

Hydrological Data

Ancillary data of river discharge were obtained with the Brazilian Water Agency (ANA: *AgênciaNacional de Águas*) through the database portal Hidroweb ((http://hidroweb.ana.gov.br). River discharge data of the PirapamaRiver was recovered for the period of 1986 to 2006 for the fluviometric station #39200000. This station drains 372 km^2, which account 62% of the total drainage basin. The data was analyzed in terms of annual variability, and the mean value of the river discharge of September was used as a reference for the discharge during the experiment. Since there was no rain during the previous weeks, this value is a reasonably proxy for the effective discharge.

RESULTS AND DISCUSSION

This section presents spatial and temporal distributions of the longitudinal flow and salinity for the period of observation. Figure 3, A and B, shows the vertical-temporal distribution of u velocity component and vertical salinity, respectively. The highest values of u occurred during the ebb tide (0.8 m.s^{-1}) and reached -0.4 m.s^{-1} in the flood tide. Also, figure 3(B) shows the tidal variation of the vertical salinity profile in the main estuarine channel. Maximum values of salinity occurred in the high tide (30 PSU) and minimum values (5 PSU) occurred in the ebb tide under influence of river discharge. The surface mean salinity is 18 PSU and the bottom mean salinity is 20 PSU over one tidal cycle.

The estuarine circulation dynamics can be simplified as a balance between buoyance effects which is generated by the river discharge, and the shear effects as a response to the turbulence and stirring of tidal currents (Dyer, 1997). Taking in consideration that the Barra de Jangadas Estuary (BJE) is a shallow estuary (< 4m depth), which is also under influence of relatively strong tidal currents and weak river discharge, one can hypothesize that this system becomes vertically homogeneous, in normal conditions, because of the strong tidal mixing. The theoretical vertical profile of u velocity component was modulated to the BJE system and compared with the observed values in order to find the main estuarine forces acting in this system through the residual profiles over one tidal cycle.

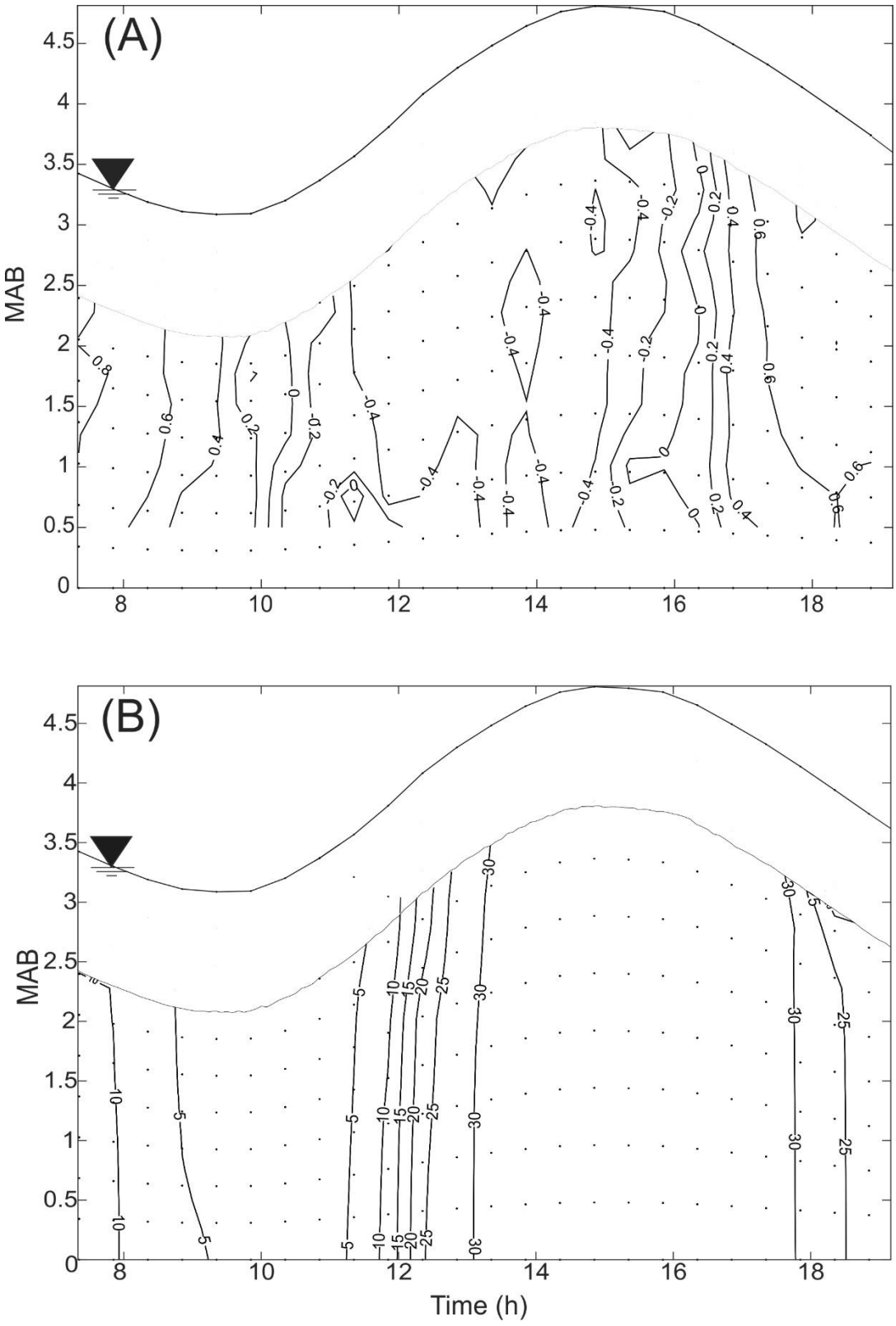

Figure 3. (A) Vertical distribution of the longitudinal (u) velocity component over one tidal cycle;(B) shows the vertical distribution of salinity over one semidiurnal tidal cycle. The dashed line represents the temporal variation of the water level. MAB – Meters Above Bottom (ADCP transducer). The black dots represent sample points.

In this context, figure 4 shows the mean vertical profile observed in the Barra de Jangadas estuary as well as the adjusted model. One can notice that residual flux is totally downstream and the maximum value reach 0,13 $m.s^{-1}$, near the surface, while the minimum value (0,04 $m.s^{-1}$) occurred near bottom. The adjusted model (Fig. 4 – dashed line) showed vertically unidirectional flux downstream which suggests river discharge and tidal currents as being the main driving components of the residual circulation once that wind effectwas removed.

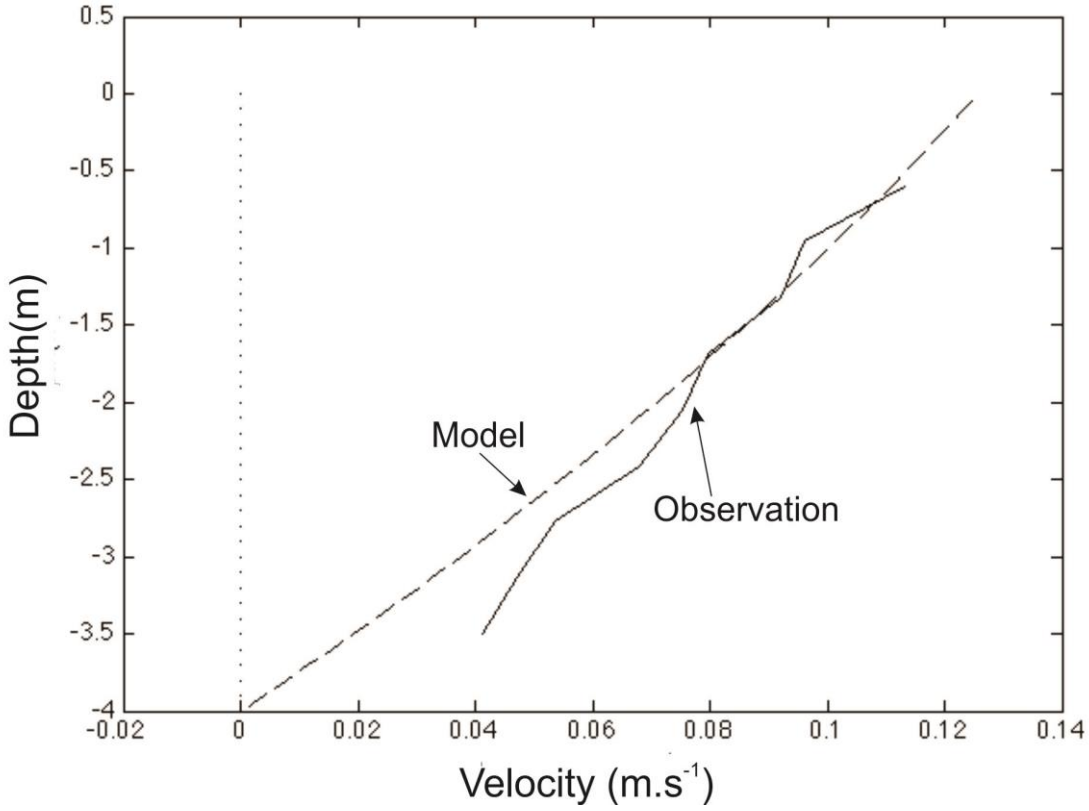

Figure 4. Vertical mean profile of adjusted theoretical model (dashed line) and the vertical residual mean of the longitudinal velocity component (u).

Also, the observed residual profile ranged from 0.04 $m.s^{-1}$, near bottom to 0.12 $m.s^{-1}$ in the free surface. This range of values was expected since bottom friction acts slowing down currents. The balance among wind, river and tidal influences produces a competition between mixing and buoyance effects and this relation may be a good proxy for BJE estuarine energetic dynamics, which was analyzed in this manuscript by the using of non-dimensional Richardson Number (Ri – Figure 5).

Figure 5. Temporal and vertical variation of Richardson Number (Ri). The x-axis represents the time variation (hours) and the y-axis shows meters above bottom (MAB). The continuous line is tidal variation of water level and the black dots are the sampling points.

Vertical and temporal variation of Rito the BJE system followed water level variability. During the flood tide, the BJE estuarine flow was in supercritical state (Ri> .25),which shows that the flow tends to be stable. On the other hand, along the high tide and the ebb tide, the BJE estuarine flow was in a subcritical state with the shear effects causing vertical mixing and turbulence predominance. The competition between vertical stratification and mixing caused by shear stress plays an important role in fluid dynamics, in particular, in the estuarine dynamics. Thus, if the vertical gradient of salinity is in the opposite direction of turbulent momentum exchanges, an extra velocity shear is necessary to the vertical mixing (Dyer, 1997).

In this context, the BJE system shows a time-space dependence of Ri with the flow changing from a laminar, along flood tide, to a turbulent flow in the ebb tide. In practice, a laminar flow reflects on stratification, which, in turn, is better for the exchange between the estuary and the adjacent sea. In a different manner, the turbulent flow cause vertical mixing and enhance material trapping upwards estuary. This analysis was made in the thalweg estuarine channel; however, many authors argue that circulation and stratification as well as Ri changes with intratidal lateral variability of flow. In this context, the lateral variability of longitudinal flow is investigated in the next subsection of this paper.

Lateral variability of the longitudinal flow

This section presents the lateral variability of the longitudinal flow in the BJE, along one complete tidal cycle. Figure 6 (A, B and C) show waterlevel, intratidal variability of longitudinal flow in the estuarine cross section, and the longitudinal velocity anomaly, respectively. The distance between BJE margins follow water level variation and presents homogeneity along tidal cycle. At the start until the end of the flood tide, there is lateral variation of the longitudinal flow in late flood tide (-10 $cm.s^{-1}$) on the right margin of BJE looking towards Atlantic Ocean. The maximum velocity

observed was 63 cm.s^{-1} in the ebb tide. On the contrary, the maximum velocity observed in flood tide was -57cm.s^{-1}. The panel “C” of figure 6 shows a lateral gradient of flow which is caused by irregular mixing and cross-sectional depth variation (Valle-Levinson & Atkinson, 1999).

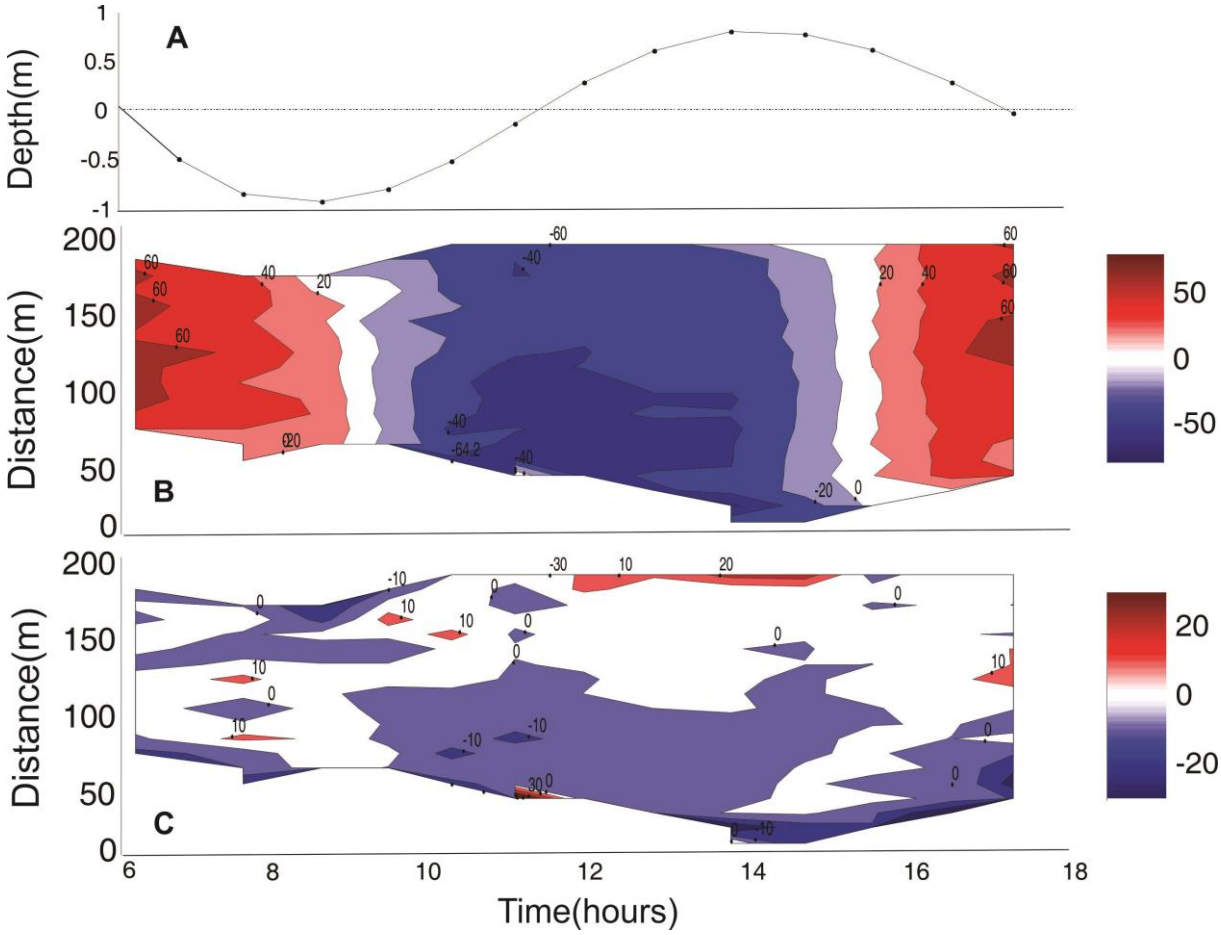

Figure 6. (A) Temporal variation of water level (meters);(B) lateral variability of longitudinal mean velocity component (Hov-Moller diagram) and; (C) shows lateral distribution of longitudinal velocity anomaly over one tidal cycle.

Estuarine Classification

In order to put BJE system in a global context of estuaries, two classification schemes were analyzed. Figure 7 shows volume transport variability over one tidal cycle. Maximum values reached 257.8 m^3.s^{-1} in the ebb tide and reached 196 m^3.s^{-1} in the flood tide. After the ebb tide period, the water volume that entered towards the estuarine head was integrated in the time interval of flood tide that gave us the BJE

tidal prism (2.83 x 10^6 m^3). The first approach taken was to calculate the flow rate (F_R) and to balance the tidal prism and mean historical freshwater inflow of the Pirapama River over one tidal cycle.

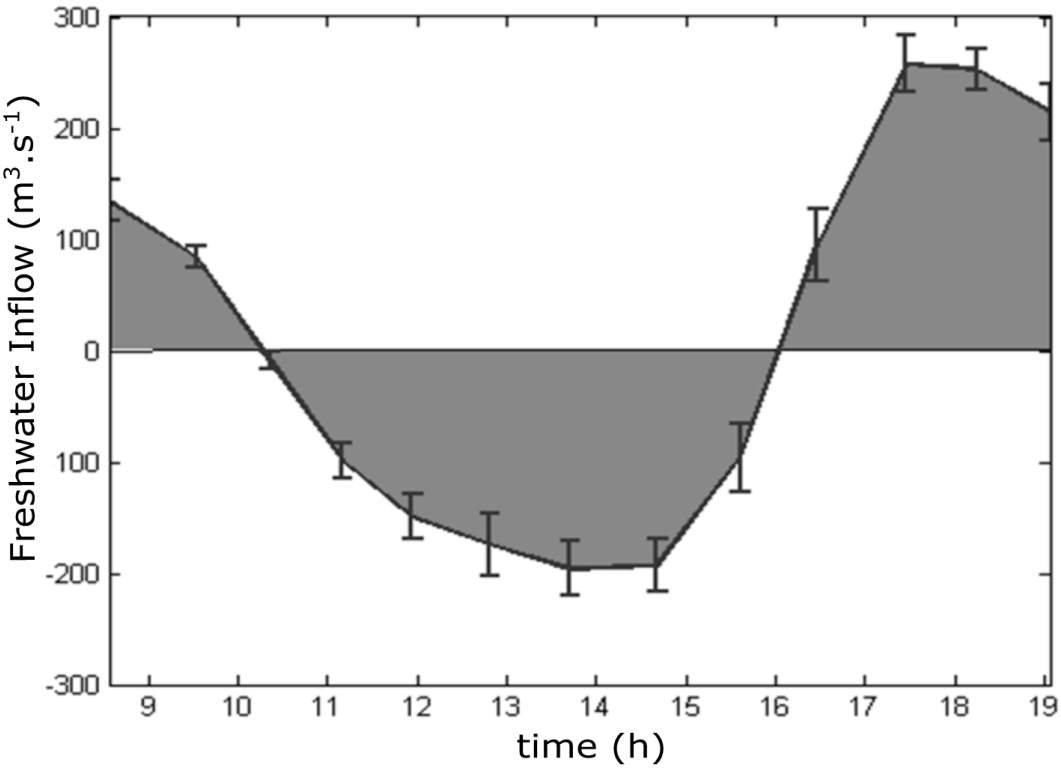

Figura 7.Temporal variability of water discharge in the Barra de Jangadas Estuary - the vertical bars represent standard deviation of values.

The F_R was first introduced as a control parameter to indicate changes in vertical density stratification caused by tidal or fluvial influence. With foundation on empirical studies and experimental analysis (Miranda *et al.,* 2002), we have three types of estuary: highly stratified, when $F_R \geq 1$; well mixed, when $F_R \leq 0.1$; and partially mixed, when $F_R \approx 0.25$.The value of F_R calculated to BJE is 0.26, which suggests that this estuary is partially mixed. However, these criteria used to determinate the F_R are very general once that bathymetric variation can modify turbulent mixing.

Furthermore, we have taken a second approach to compare BJE system with other estuaries from different regions. The Hansen & Rattray's diagram gives us a classification scheme based on the estuarine hydrodynamics. Also, the HR diagram shows the nature of salt transport that predominates in the estuary. The figure 8

shows the HR diagram applied to the BJE system. The circulation parameter found is 1.37, while the stratification parameter is 0.12. These results put BJE system as being 1a (well mixed) estuary, where there is no gravitational circulation and no vertical stratification. Furthermore, the $\mu = 0.99$ calculated to BJE system suggests that salt transport is mainly by diffusive processes.

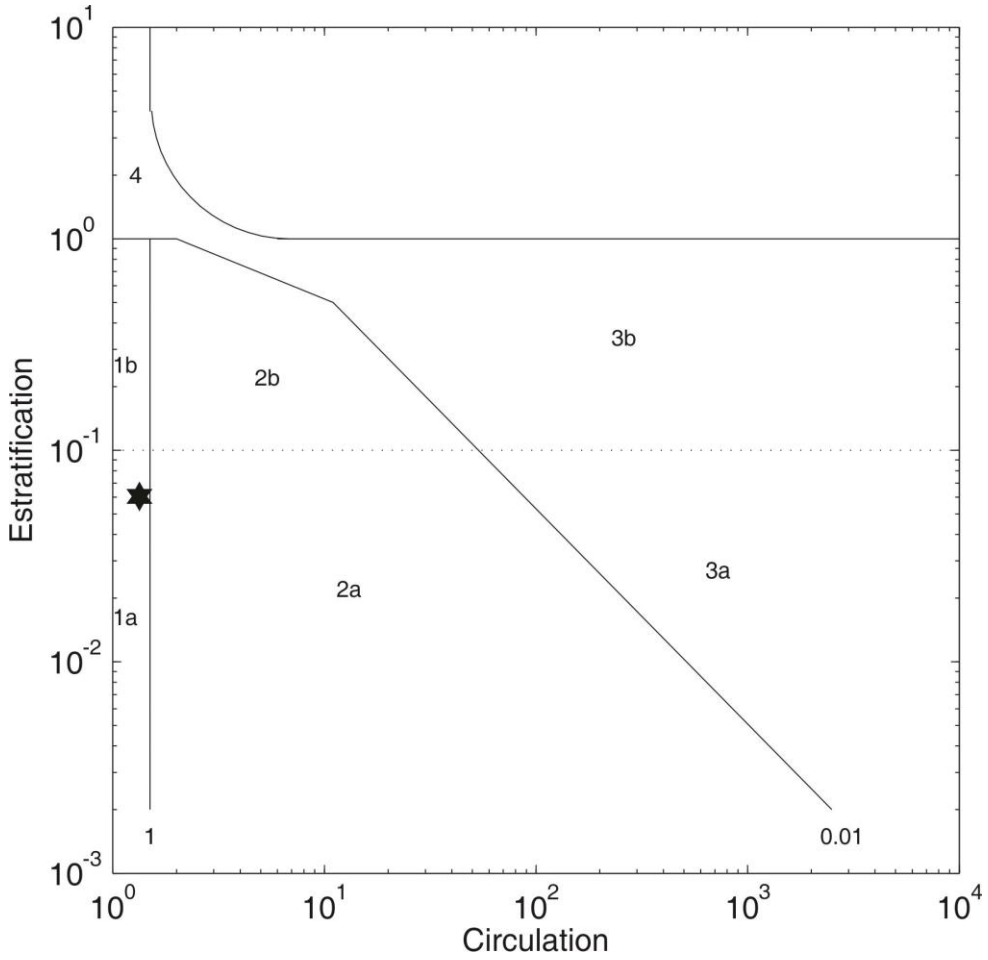

Figure 8. Hansen & Rattray's (1966) classification diagram using data observationin the Barra de Jangadas Estuary.

In estuaries with low freshwater inflow, the vertical residual velocity is similar to the surface velocity (i.e. river discharge), thus the circulation parameter is > 10 (Valle-Levinson, 2010). In general, gravitational circulation is as much as the circulation parameter. Similarly, the stratification parameter reflects in the vertical stratification and also in the exchange fluxes with the costal sea (Valle-Levinson, 2010). BJE system shows both HR diagram parameters near to 1, which is similar to the results observed in the Caravelas Estuary (Pereira et *al.,* 2010).

CONCLUSIONS

The main discoveries of this study on the hydrodynamics of BJE estuary, a shallow and tropical system, may be summarized as follows:

(I) The Barra de Jangadas Estuary did not showed vertical salinity and temperature variability, thus this environment is vertically homogeneous. Also, the vertical residual mean profile observed to BJE showed vertically unidirectional flux seawards;

(II) The Richardson number calculated to the BJE showed that vertical salinity distribution put the water in a subcritical state of mixing. However, when is in high tide, vertical shear change the water column to the supercritical state with Ri< 0.25 in the whole water level;

(III) There is no significant lateral variation of the longitudinal flow and the velocity anomaly indicated that there is a negative anomaly in the right margin of estuary along flooding tide.

(IV) Flux Rate (F_R) indicated that tides are three times bigger than river discharge in terms of the amount of volume that entered in the estuarine basin in each tidal cycle; Also, the HR diagram indicated that tides are more important in the estuarine dynamics and can be classified as 1a or vertically homogeneous and the salt transport is mainly controlled by diffusive processes.

REFERENCES

Araujo, M., Medeiros, C., Ribeiro, C. (1999).Energy balance and time-scales of mixing and stratification in the jaboatão estuary, Brazil.*Brazilian Journal of Oceanography*, 47(2):145-154.

Cameron, W. M., Pritchard, D. W. (1963). Estuaries. in: hill, m. n.ed. the sea, v. 2. new york, john wiley& sons, 306-324.

CPRH. (2001). Planilhas de controle industrial do estado. CompanhiaPernambucana de Controle da Poluição e RecursosHídricos, recife.

Dionne, J.C. (1963). Towards a more adequate definition of the st.lawrence estuary. zeitschr. f. geomorph., v.7(1):36-44.

Dyer, K.R. (1997). Estuaries: a physical introduction. 2a ed. *john wiley and sons*, 195p.

Fairbridge, R.W. (1980). The estuary its definition and geodynamic cycle.in: *olausson, e. &cato, i.* (eds.) chemistry and biogeochemistry of estuaries. wiley, new york. 1-35pp.

Hansen, D. V., RattrayJr, M. (1966). New dimensions on estuarine classification.*limnologyandoceanography*, v.11:319-326.

Hansen, D.V., Rattray, Jr.M. (1965).Gravitational circulation in straits and estuaries.*journal of marine research*,23:104–122.

Kjerfve, B. (1989) Estuarine geomorphology and physical oceanography.in: *estuarine ecology.* johnwiley& sons, 47-78.

Kjerfve B, Proehl J.A., Schwing F.B., Seim, H.E., Marozas, M. (1982). Temporal and spatial considerations in measuring estuarine water fluxes in: kennedyvs (ed.). *estuarine comparisons*. new york, academicpress, p. 37–51.

Kjerfve, B. (1986) Circulation and salt flux in a well mixed estuary. in: van de kreek j. (ed.). physics of shallow estuaries and bays. berlin: springer-verlag. p. 22-29.

Lessa, G. (1996) Tidal dynamics and sediment transport in a shallowmacrotidal estuary pp. 338-360.

Miranda, L.B., Castro, B.M., Kjerfve, B. (2002) Princípios de oceanografia de estuários. 2ª ed. sãopaulo: usp, 411p.

Pereira, M.D., Siegle, E. Miranda, L.B., Schettini, C.A.F.(2010). Hidrodinâmica e transporte de material paticuladoem suspensão sazonal em um estuário dominad opo rmaré: estuário de Caravelas, BA, Brasil. RevistaBrasileira de Geofísica. 28(3):427-444.

Pritchard, D.W.(1955).Estuarine circulation patterns.*proc.am.soc.civil*eng. new york v. 81,p.1–11.

Pritchard, D.W. Estuarine hydrography.(1952).*Advances in geophysics*.cambridge v.1, p. 243–280.1952.

Schettini, C.A.F. (2002). Caracterizaçãofísica do estuário do rioItajaı-acu. *rev.bras.rec.hídricos*., 7(1): 123–142.

Valle-levinson, A. (2010).Contemporary issues in estuarine physics.cambridge. 1ª ed. *cambridge university press*, 327p.

Valle-Levinson,A.,Atkinson,L.P.,(1999).Spatial gradientes intheflow overanestuarinechannel.EstuariesandCoasts. 22(1), 79–193.